





Doc n°: IA-RP-2000-4252-CNE
Issue: 1.0
Date: 2017-09-27
Sheet: 1 Of: 67

IASI QUARTERLY PERFORMANCE REPORT

FROM 2015/09/01 TO 2015/11/30



BY IASI TEC (TECHNICAL EXPERTISE CENTER)

FOR IASI PFM-R ON METOP B

		Doc n°: IA-RP-2000-4252-CNE Issue: 1.0 Date: 2017-09-27 Sheet: 2 Of: 67
--	---	--

<p align="center">ANALYSE DOCUMENTAIRE</p> <p align="center">Bordereau d'indexation</p>

Classe (Confidentialité) : NC		Code Consultation :	
Mots clés d'auteur : IASI TEC quarterly synthesis report			
OBJET : IASI TEC periodic report			
TITRE : IASI quarterly performance report			
Auteur(s) : Claire Maraldi, Elsa Jacquette et Denis Jouglet (CNES) avec le support de J-C Calvel (AKKA Technologies, marché ACIS 128780)			
RESUME : Quarterly report issued by the IASI TEC team to show trends and layout from the "long term synthesis" TEC function for flags and observables quality indicators			
Document(s) rattaché(s) : Ce document vit seul		Localisation physique du document : Salle IASI TEC	
Volume : 1	Nombre de pages total : 67 dont - liminaires : 7 annexes : 0	Nombre d'annexes : 0	LANGUE : English
Document géré en Configuration : Non		A DATER DU :	RESPONSABLE :
Contrat : Néant			
SYSTEME HOTE : (logiciel + référence fichier) : OpenOffice Writer 3.2			

		Doc n°: IA-RP-2000-4252-CNE Issue: 1.0 Date: 2017-09-27 Sheet: 3 Of: 67
--	---	--

DIFFUSION

On CNES web site : <https://iasi.cnes.fr>
Instrument characteristics / In-orbit performances monitoring

DOCUMENT MODEL CHANGE RECORD

Version	Date	Paragraphs	Description
1.0	05/03/11		Creation of the model
2.0	01/01/15	4.3.2.5 4.8	Cube corner Speed Quality (CSQ) monitoring IASI-B inter-calibration with IASI-A, CRIS and AIRS

DOCUMENT CHANGE RECORD

Version	Date	Paragraphs	Description
1.0	15/12/15		Creation of the document





		Doc n°: IA-RP-2000-4252-CNE Issue: 1.0 Date: 2017-09-27 Sheet: 4 Of: 67
--	--	--

Table of contents

1 INTRODUCTION.....	9
2 RELATED DOCUMENTS.....	9
2.1 APPLICABLE DOCUMENTS.....	9
2.2 REFERENCE DOCUMENTS.....	9
3 SIGNIFICANT EVENTS.....	10
3.1 EXTERNAL CALIBRATION.....	10
3.2 ON BOARD CONFIGURATION.....	11
3.3 GROUND CONFIGURATIONS UPDATES FOR LEVEL 1 PROCESSING.....	11
3.4 DATA BASES UPDATE FOR THE USERS.....	12
3.5 ON GROUND HW/SW EVOLUTION.....	12
3.6 DECONTAMINATION.....	13
3.7 INSTRUMENT.....	13
3.7.1 External events.....	13
3.7.2 Operation leading to mission outage.....	13
3.7.3 Anomaly leading to mission outage.....	14
4 PERFORMANCE MONITORING.....	15
4.1 PERFORMANCE MONITORING.....	15
4.2 PERFORMANCE SYNOPSIS.....	16
4.3 LEVEL 0 DATA QUALITY (L0).....	17
4.3.1 Overall quality.....	17
4.3.2 Main flag and quality indicator parameters.....	19
4.3.3 Second level flags and quality indicators.....	28
4.3.4 Conclusion.....	28
4.4 LEVEL 1 DATA QUALITY (L1).....	28
4.4.1 Overall quality.....	28
4.4.2 Main flag and quality indicator parameters.....	29
4.4.3 Conclusion.....	32
4.5 SOUNDER RADIOMETRIC PERFORMANCES.....	33
4.5.1 Radiometric Noise.....	33
4.5.2 Radiometric Calibration.....	33
4.5.3 Delay of Detection Chains.....	38
4.5.4 Optical Transmission.....	39
4.5.5 Interferometric Contrast.....	41
4.5.6 Interferogram Baseline.....	42
4.5.7 Detection Chain.....	43
4.5.8 Conclusion.....	43
4.6 SOUNDER SPECTRAL PERFORMANCES.....	44
4.6.1 Monitoring of the ISRF inputs.....	44
4.6.2 Spectral calibration assessment.....	46
4.6.3 Ghost evolution monitoring.....	48
4.6.4 Conclusion.....	50
4.7 GEOMETRIC PERFORMANCES.....	51
4.7.1 Sounder / IIS co-registration monitoring.....	51
4.7.2 IIS / AVHRR co-registration.....	51

		Doc n°: IA-RP-2000-4252-CNE Issue: 1.0 Date: 2017-09-27 Sheet: 5 Of: 67
--	--	--

4.7.3 Conclusion.....	52
4.8 IASI-B INTER-CALIBRATION WITH IASI-A, CRIS AND AIRS.....	52
4.8.1 IASI-B inter-calibration with IASI-A.....	53
4.8.2 IASI-B inter-calibration with CRIS.....	56
4.8.3 IASI-B inter-calibration with AIRS.....	58
4.9 IIS RADIOMETRIC PERFORMANCES.....	60
4.9.1 IIS Radiometric Noise Monitoring.....	60
4.9.2 IIS Radiometric Calibration Monitoring.....	61
4.9.3 Conclusion.....	63
5 IASI TEC SOFTWARE AND INTERFACES.....	64
5.1 IASI TEC EVOLUTION.....	64
5.2 SIC EVOLUTION.....	64
5.3 EUMETCAST INTERFACE.....	65
5.4 FTP INTERFACE.....	66
6 CONCLUSION AND OPERATIONS FORESEEN.....	67
6.1 SUMMARY.....	67
6.2 SHORT-TERM EVENTS.....	67
6.3 OPERATIONS FORESEEN.....	67

Figures and tables

Table 1: External Calibration TEC Requests.....	9
Table 2: DPS and MAS configuration TEC Requests.....	9
Table 3: DPS and MAS previous configuration.....	9
Table 4: IASI L1 Auxiliary File Configuration on the Operational EPS Ground Segment.....	10
Table 5: IASI L1 auxiliary file previous configuration.....	10
Table 6: IASI Data Bases for the users.....	10
Table 7: previous IASI Data Bases.....	10
Table 8: IASI L1 PPF Configuration on the Operational EPS Ground Segment.....	11
Table 9: Previous IASI L1 PPF.....	11
Table 10: Decontamination TEC Requests.....	11
Table 11: Previous decontamination.....	11
Table 12: Overview of METOP manoeuvres in the reporting period.....	11
Table 13: PL-SOL.....	12
Table 14: Scheduled interruptions.....	12
Table 15: Major anomalies.....	12
Table 16: Minor anomalies.....	12
Table 17: Functional status legend	13
Table 18: IASI product components functional status	14
Figure 1 : IASI L0 data quality orbit average (per pixel and CCD).....	15
Figure 2 : IASI L0 data quality spatial distribution (per pixel).....	15
Figure 3 : Temporal evolution of spikes anomaly ratio in % for all pixels (orbit average).....	15
Figure 4 : Geographical distribution of spikes occurrences in % for band 3 and all pixels.....	15
Figure 5 : Temporal evolution of NZPD determination anomaly ratio in % for all pixels (orbit average).....	16
Figure 6 : IASI NZPD determination quality flag spatial distribution (per pixel).....	16
Figure 7 : NZPD inter-pixel for all pixels and CCD calculated with respect to pixel 1 (orbit average).....	16







		Doc n°: IA-RP-2000-4252-CNE Issue: 1.0 Date: 2017-09-27 Sheet: 6 Of: 67
--	--	--

Figure 8 : IASI L0 over/under-flows orbit average of all pixels.....	17
Figure 9 : IASI Overflows and Underflows spatial distribution (per pixel).....	17
Figure 10 : Max of NZPD quality index for all pixels and CCD - BB.....	17
Figure 11 : Max of NZPD quality index for all pixels and CCD - CS.....	17
Figure 12 : IASI L1 data quality orbit average (% of bad by PN at upper plot and % of good by PN and SB at lower plot).....	18
Figure 13 : IASI product overall quality spatial distribution (per pixel).....	18
Figure 14 : GQisQualIndex average (L1 data quality index for IASI sounder).....	18
Figure 15 : GQisQualIndexIIS average (L1 data quality index for IASI Integrated Imager).....	18
Figure 16 : GQisQualIndexSpect average (L1 data index for spectral calibration quality).....	18
Figure 17 : GQisQualIndexRad average (L1 data index for radiometric calibration quality).....	18
Figure 18 : GQisQualIndexLoc average (L1 data index for ground localisation quality).....	19
Figure 19 : MDptPixQual average (L1 quality index for IASI integrated imager, fraction of not dead pixels).....	19
Figure 20 : Instrument noise evolution between start and end of the period.....	19
Figure 21 : Scan mirror reflectivity evolution.....	19
Figure 22 : Radiometric calibration error due to scan mirror reflectivity dependency with viewing angle Maximum effect on SN1 for different scene temperature. Done with the period May / November.....	20
Figure 23 : Black Body Temperature.....	20
Figure 24 : Focal Plane Temperature.....	20
Figure 25 : Monitoring of detection chain maximum delays for all bands.....	20
Figure 26 : Ratio of calibration coefficient slopes as a function of wave number and time after the last decontamination.....	21
Figure 27 : Temporal evolution of calibration ratio coefficient slopes since the last decontamination. The curve was fitted with a decreasing exponential function to determine a rough date for the next decontamination (relative gain evolution of 0.8).....	21
Figure 28 : Monitoring of contrast for SB3.....	21
Figure 29 : Monitoring of detection chain margins.....	21
Figure 30 : GFaxAxeY average (Y filtered coordinates of sounder interferometric axis).....	23
Figure 31 : GFaxAxeZ average (Z filtered coordinates of sounder interferometric axis).....	23
Figure 32 : Cube Corner offset variation.....	23
Figure 33 : Optical bench Temperature.....	24
Figure 34 : Spectral shift error between L1C IASI and simulated L1C with A4/OP + ECMWF.....	24
Figure 35 : Inter pixel spectral shift error for L1C IASI.....	24
Figure 36 : Ghost amplitude as a function of wave number for different time (Top: pixel 2, bottom: pixel 4).....	25
Figure 37 : Column offset (black) guess vs. column offset averaged over all lines (LN) as a function of the scan position (SP=SN), and orbit number.....	26
Figure 38 : Line offset guess (black) vs. line offset averaged over all lines (LN) as a function of the scan position (SP=SN), and the orbit number.....	26
Figure 39 : Temporal evolution of the noise between start and end of the period.....	26
Figure 40 : Slope and offset coefficients matrix.....	26
Figure 41 : Relative evolution in % of average of slope (red curve) and offset (black curve) coefficients.....	26
Figure 42 : IIS Focal Plane Temperature.....	27
Table 19: IASI TEC at CNES Toulouse.....	28



		Doc n°: IA-RP-2000-4252-CNE Issue: 1.0 Date: 2017-09-27 Sheet: 7 Of: 67
--	---	--

LIST OF ACRONYMS

4A/OP	Automatized Atmospheric Absorptions Atlas/ Operational
APO	Other Parameters OPS
AR	Anomaly Report
ASE	Acquisition Start End
AVHRR	Advanced Very High Resolution Radiometer
BB	Black Body
BRD	BoaRD configuration
CCFD	Cube Corner Functional Device
CCD	Cube Corner Direction
CCM	Cube Corner Mechanism
CD	Cube corner Compensation Device
CHART	Component Health Assessment and Reporting Tool
CGS	Core Ground Segment at EUMETSAT
CNES	Centre National d'Etudes Spatiales
CS	Cold Space
DA	Applicable document
DPS	Data Processing Subsystem
ECMWF	European Centre for Medium Range Weather Forecasts
EM	Engineering Model
EPS	EUMETSAT Polar System
EUMETSAT	European organisation for exploitation of METeorological SATellites
FM2 / FM3	Flight Model n°2 or 3
FOV	Field Of View
GRD	GRound configuration
IASI	Infrared Atmospheric Sounding Interferometer
IIS	Integrated Imaging Subsystem
IPSF	Instrument Point Spread Function
ISRF	Instrument Spectral Response Function
LFD	Locking Filtering Device
LN	Line Number
LSB	Least Significant Bit
METOP	METeorological OPERational satellite
MPF	Mission Planning Facility
NedT	Noise equivalent difference Temperature
NDVI	Normalized Difference Vegetation Index
NZPD	Number of Zero Path Difference
ODB	Operational Data Base
OPS	Operational Software
PC	Principal Component
PDD	Position Data Diagnostic

		Doc n°: IA-RP-2000-4252-CNE Issue: 1.0 Date: 2017-09-27 Sheet: 8 Of: 67
--	---	--

PDU	Product Dissemination Unit
PL SOL	PayLoad Switch Off-Line
PN	Pixel Number
PTSI	Parameter Table Status Identifier
RMS	Root Mean Square
RD	Reference Document
SAA	South Atlantic Anomaly
SEU	Single Event Upset
TEC	IASI Technical Centre of Expertise (located in CNES, Toulouse)
TIGR	Thermodynamic Initial Guess Retrieval data set
VDS	Verification Data Selection
ZPD	Zero Path Difference

		Doc n°: IA-RP-2000-4252-CNE Issue: 1.0 Date: 2017-09-27 Sheet: 9 Of: 67
--	---	--

1 INTRODUCTION

The IASI TEC is based at CNES Toulouse and is responsible for the monitoring of the IASI system performances, covering both instrument and level 1 processing sub-system.

This document describes the activities and results obtained at the IASI TEC for instrument PFM-R on METOP-B during the following period:

- Start Time: 2015/09/01 Orbit: 15320
- End Time: 2015/11/30 Orbit: 16612
- Duration: 3 months

Note that IASI ended the Calibration / Validation (commissioning) phase on April 2013.



2 RELATED DOCUMENTS

2.1 *APPLICABLE DOCUMENTS*

N°	Reference	Titre
DA.1	IA-SP-0000-3242-CNE	Spécification de suivi de la performance en vol de IASI sur METOP-A
DA.2	IA-DF-0000-4195-CNES	Spécification de l'outil d'inter-étalonnage SIC

2.2 *REFERENCE DOCUMENTS*

N°	Reference	Titre
RD.1	EUM/OPS-EPS/REP/14/748544	Metop-B IASI annual in-flight performance report 2013
RD.2	EUM/OPS-EPS/REP/15/796329	Metop-B IASI annual in-flight performance report 2014

		Doc n°: IA-RP-2000-4252-CNE Issue: 1.0 Date: 2017-09-27 Sheet: 10 Of: 67
--	---	---

3 SIGNIFICANT EVENTS

The following tables present a timeline of the various requests sent by TEC and the external IASI activities.

Those events are typically the configuration changes, programming requests, software update, but also any external operation or activity such as mission interruption, manoeuvre, dissemination problem, ...

3.1 EXTERNAL CALIBRATION

Table 1 shows the External Calibration within the time period reported here. Note that the VDS files that come with each request are not described here.

Execution	TEC ref. ⁽¹⁾	Description	Activities
From 02/09/2015 5h18 to 03/09/2015 8h07 orb. 15336 to 15352	RL-10	Moon avoidance MPF ⁽²⁾ Targets: 1 st Deep Space	Monitoring of moon intrusion in CS1 FOV
24/09/2015 from 5h16 to 9h12 orb. 15649 to 15651	RM-31	Monthly_MPF ⁽²⁾ Targets: Earth 15, Blackbody, 2 nd Deep Space, Mirror Backside	For routine monitoring (IIS and IASI NeDT, scan mirror reflectivity, ghost,...)
From 01/10/2015 20h47 to 02/10/2015 0h37 orb. 15758 to 15760	RL-11	Moon avoidance MPF ⁽²⁾ Targets: 1 st Deep Space	Monitoring of moon intrusion in CS1 FOV
23/10/2015 from 5h16 to 9h12 orb. 16061 to 16063	RM-32	Monthly_MPF ⁽²⁾ Targets: Earth 15, Blackbody, 2 nd Deep Space, Mirror Backside	For routine monitoring (IIS and IASI NeDT, scan mirror reflectivity, ghost,...)
21/11/2015 from 5h16 to 9h12 orb. 16473 to 16475	RM-33		

Table 1: External Calibration TEC Requests



⁽¹⁾ TEC convention: R for Routine, M for Monthly and L for moon avoidance, followed by a chronological number

⁽²⁾ An external calibration could be the result of:

- a TEC request or
- a “MPF” uploaded directly by EUMETSAT in full accordance with TEC. The reference “Monthly_MPF” is based on the March 2008 TEC External Calibration request. The MPF for moon avoidance is based on the December 2008 TEC External Calibration request: “ICAL_OCF_xx_M02_20081216060000Z_20090616060000Z_20081209100934Z_IAS_EXTCALIBRA.dts”

Moon external calibration on September 2nd 5:18^Z to 3rd 8:07^Z (orbits 15336 to 15352) detail:

External Calibration		External Calibration	
from	to	from	to
2015/09/02 05:18:06	05:42:05	2015/09/02 21:03:10	21:53:17
2015/09/02 06:58:22	07:28:29	2015/09/02 22:44:30	23:40:13
2015/09/02 08:38:38	09:10:37	2015/09/03 00:51:10	01:25:01
2015/09/02 10:18:22	10:51:57	2015/09/03 02:32:30	03:08:45
2015/09/02 12:03:26	12:33:17	2015/09/03 04:15:10	04:48:13
2015/09/02 13:50:54	14:14:53	2015/09/03 06:01:18	06:27:41
2015/09/02 15:59:10	16:21:33	2015/09/03 07:45:18	08:07:41
2015/09/02 17:38:54	18:05:17		

		Doc n°: IA-RP-2000-4252-CNE Issue: 1.0 Date: 2017-09-27 Sheet: 11 Of: 67
--	--	---

Moon external calibration on October 1st 20:47^Z to 2nd 0:37^Z (orbits 15758 to 15760) detail:

External Calibration		External Calibration	
from	to	from	to
2015/10/01 20:47:05	21:09:45	2015/10/02 00:14:01	00:37:13
2015/10/01 22:30:17	22:53:29		

3.2 ON BOARD CONFIGURATION

Table 2 presents the on-board processing configuration updates that had been made within the time period reported here:

PTSI	IASI on board parameter files	Delivery by TEC	activated on	TEC ref.	affected parameters of a DPS TOP configuration update

Table 2: DPS and MAS configuration TEC Requests

For information, Table 3 shows the delivery applicable at the beginning of the period:

PTSI	IASI on board parameter files	Delivery by TEC	activated on	TEC ref.	affected parameters of a DPS TOP configuration update
11 1.0	IDPS_OBP_xx_M01_20150209000000Z_20150809000000Z_20150206092603Z_IASD_DPSPARAMOD.tar	06/02/2015	19/02/2015, orbit 12572	R_41	Update of reduced spectra

Table 3: DPS and MAS previous configuration

The associated ground configuration table (BRD file), necessary to handle coherent configuration at system level, is presented in the next section. These associated configuration table are necessary for L1 processing.

3.3 GROUND CONFIGURATIONS UPDATES FOR LEVEL 1 PROCESSING

Table 4 presents the on-ground processing configuration updates that had been made within the time period reported here:



IDef	IASI L1 auxiliary files	Delivery by TEC	Upload on GS1	Content

Table 4: IASI L1 Auxiliary File Configuration on the Operational EPS Ground Segment

For information, Table 5 shows the delivery applicable at the beginning of the period:

IDef	IASI L1 auxiliary files	Delivery by TEC	Upload on GS1	Content
41	IASI_BRD_xx_M01_20150209000000Z_XXXXXXXXXXXXXXZ_20150206092356Z_IASD_0000000011	06/02/2015	BRD and GRD activated on 19/02/2015 14:50, orbit 12572	Update of the IIS/AVHRR offset
20	IASI_GRD_xx_M01_20150202000000Z_XXXXXXXXXXXXXXZ_20150130134220Z_IASD_0000000020	30/01/2015		Update of Scan Mirror Reflectivity Update of the Dead Pixel Table
12	IASI_ODB_xx_M01_20130417100000Z_XXXXXXXXXXXXXXZ_20130417082506Z_IASD_0000000012	17/04/13	ODB activated on 14/05/13 12:05 orbit 3393	

Table 5: IASI L1 auxiliary file previous configuration

		Doc n°: IA-RP-2000-4252-CNE Issue: 1.0 Date: 2017-09-27 Sheet: 12 Of: 67
--	---	---

3.4 DATA BASES UPDATE FOR THE USERS

The Noise Covariance Matrix (NCM) and Spectral data base (SDB) are specific data bases for the users. They are updated according to the main ground level 1 evolutions.

Table 6 presents the updates of the NCM and SDB that had been made within the time period reported here:

IDef	Users Data-Base	Delivery by TEC	TEC ref.	Comments

Table 6: IASI Data Bases for the users

For information, Table 7 shows the delivery applicable at the beginning of the period:

IDef	Users Data-Base	Delivery by TEC	TEC ref.	Comments
2	IASI_NCM_xx_M01_20130522081244Z_20130522081244Z_20130522081245Z_IA ST_SPECTRESPO	22/05/13	CVA_COV_2	Update of NCM
12	IASI_SDB_xx_M01_20130923150000Z_20130923150000Z_20130923132439Z_IAS T_IASISPECDB	25/09/13	R_33	User database associated to ODB IDefSDB 12

Table 7: previous IASI Data Bases

3.5 ON GROUND HW/SW EVOLUTION

Table 8 presents the updates of PPF L1 software within the time period reported here:



IASI L1 PPF software version	Delivery by TEC	Date introduced on GS1	Comments
7.3	08/2015	29/09/2015 for sensing time 12:47 ^{UTC} Orbit 15725	CSQ impact on IIS

Table 8: IASI L1 PPF Configuration on the Operational EPS Ground Segment

For information, Table 9 shows the software version applicable at the beginning of the period:

IASI L1 PPF software version	Delivery by TEC	Date introduced on GS1	Comments
7.2	04/2015	27/05/2015 for sensing time 12:32 ^{UTC} Orbit 13949	

Table 9: Previous IASI L1 PPF

		Doc n°: IA-RP-2000-4252-CNE Issue: 1.0 Date: 2017-09-27 Sheet: 13 Of: 67
--	---	---

3.6 DECONTAMINATION

Table 10 presents decontaminations that have been made or requested within the time period reported here:

Last due date	Date of decontamination	Description
End of 2015	25-30 November 2015	Decontamination 200K

Table 10: Decontamination TEC Requests

For information, Table 11 shows the previous decontamination:

Last due date	Date of decontamination	Description
March 2014	10-14 March 2014	

Table 11: Previous decontamination

3.7 INSTRUMENT

3.7.1 External events

This category is for those activities/events that are external to IASI but still have an impact. It is broken down into classes of *PL-SOL* and *OOP* manoeuvre.

3.7.1.1 Manoeuvres

Date	Type ^(*)	Description	IP flag	OoP mission Outage

Table 12: Overview of METOP manoeuvres in the reporting period

(^{*}): IP for In-Plane manoeuvres (IASI stays in NOP) and OoP for Out of plane manoeuvres (IASI is put in Heater 2)

3.7.1.2 PL-SOL

Table 13 presents the PL-SOL events that have occurred within the time period reported here:

Dates	Orbits	Description



Table 13: PL-SOL

3.7.2 Operation leading to mission outage

This chapter presents the intervention on IASI needing routine interruption that have occurred within the time period reported here.

Dates	Orbits	type	IASI mode	Description
07/10/2015	15839			CD stop operations
14/10/2015	15938			IIS equalization
25/11/2015 08:00 30/11/2015 12:32	16531 to 16605			Decontamination 200K

Table 14: Scheduled interruptions

		Doc n°: IA-RP-2000-4252-CNE Issue: 1.0 Date: 2017-09-27 Sheet: 14 Of: 67
--	--	---

3.7.3 Anomaly leading to mission outage

Table 15 and Table 16 present the major and minor anomalies internal to IASI that have occurred within the time period reported here.

Note that, in this section minor anomalies are all identified and without any impact on the mission, and major anomalies only affect IASI instrument, and no other sub-systems of the spacecraft.



Dates	Orbits	Anomaly type (*)	IASI mode	Description
11/11/2015 20:22 12/11/2015 14:42	16340 to 16351	SEU	Heater Refuse	SEU in the DPS

Table 15: Major anomalies

(*): SEU (LAS, CCM or DPS) anomalies or SET anomalies

Day	Orbits	error n°	Severity	Anomaly type	LN	SN	Description

Table 16: Minor anomalies

		Doc n°: IA-RP-2000-4252-CNE Issue: 1.0 Date: 2017-09-27 Sheet: 15 Of: 67
--	---	---

4 PERFORMANCE MONITORING

4.1 *PERFORMANCE MONITORING*

In order to ensure that the IASI system is permanently running in good conditions, the CNES (IASI TEC) and EUMETSAT (CGS) are monitoring products at various temporal levels : at line, PDUs and DUMP (full orbit).

The on-board and ground processing performance algorithms issue more than one hundred quality indicators, called flags and simple parameters. Those are alarms for any bad functioning or local performance degradation.

According to the results, the TEC is also in charge of delivering new on-board or ground parameters to EUMETSAT when it is necessary. EUMETSAT is then in charge of uploading them on-board or as an input of the level 1 processing chain. During the whole instrument life, these parameter adjustments are necessary in order to take into account instrument evolution in the processing and finally to maintain a good data quality.

The Table 17 is the colour code used for the status report.

Status Colour	Meaning
GREEN	$\geq 95\%$ of good spectra
YELLOW	$< 95\%$ of good spectra
RED	Production interrupted
BLANK	No Status Reported



Table 17: Functional status legend

4.2 PERFORMANCE SYNOPSIS

Table 18 provides a synthetic view of all the indicators evaluated for L0/L1 data and their current status.

Section	Component	Description	Status	Comments
4.3	L0	Level-0 Data Quality <ul style="list-style-type: none"> Overall quality Main flag and quality indicator parameters Spikes monitoring ZPD monitoring Overflows/Underflows monitoring Reduced Spectra monitoring Second level flag and quality indicators 	GREEN	On-board processing
4.4	L1	Level-1 Data Quality <ul style="list-style-type: none"> Overall quality Main flag and quality indicator parameters 	GREEN	On ground processing
4.5	L1	Sounder radiometric performances <ul style="list-style-type: none"> Radiometric noise Radiometric calibration Acquisition chain delay Optical transmission <ul style="list-style-type: none"> Ice Prediction of decontamination date Interferometric contrast Interferogram Baseline Detection chain 	GREEN	
4.6	L1	Sounder spectral performances <ul style="list-style-type: none"> Dimensional stability <ul style="list-style-type: none"> Position of axis Cube Corner constant offset Cube Corner velocity Optical bench temperature Spectral calibration Ghost evolution 	GREEN	
4.7	L1	Geometric performances <ul style="list-style-type: none"> Sounder/IIS co-registration IIS/AVHRR co registration 	GREEN	
4.8	L1	IASI-B inter-calibration <ul style="list-style-type: none"> IASI-B inter-calibration with IASI-A IASI-B inter-calibration with CRIS IASI-B inter-calibration with AIRS 	GREEN	
4.9	L1	IIS radiometric performances <ul style="list-style-type: none"> IIS radiometric noise monitoring IIS radiometric calibration monitoring 	GREEN	

Table 18: IASI product components functional status

		Doc n°: IA-RP-2000-4252-CNE Issue: 1.0 Date: 2017-09-27 Sheet: 17 Of: 67
--	---	---

4.3 LEVEL 0 DATA QUALITY (L0)

4.3.1 Overall quality

The IASI L0 data quality (orbit average) through IASI engineering products is shown in Figure 1.

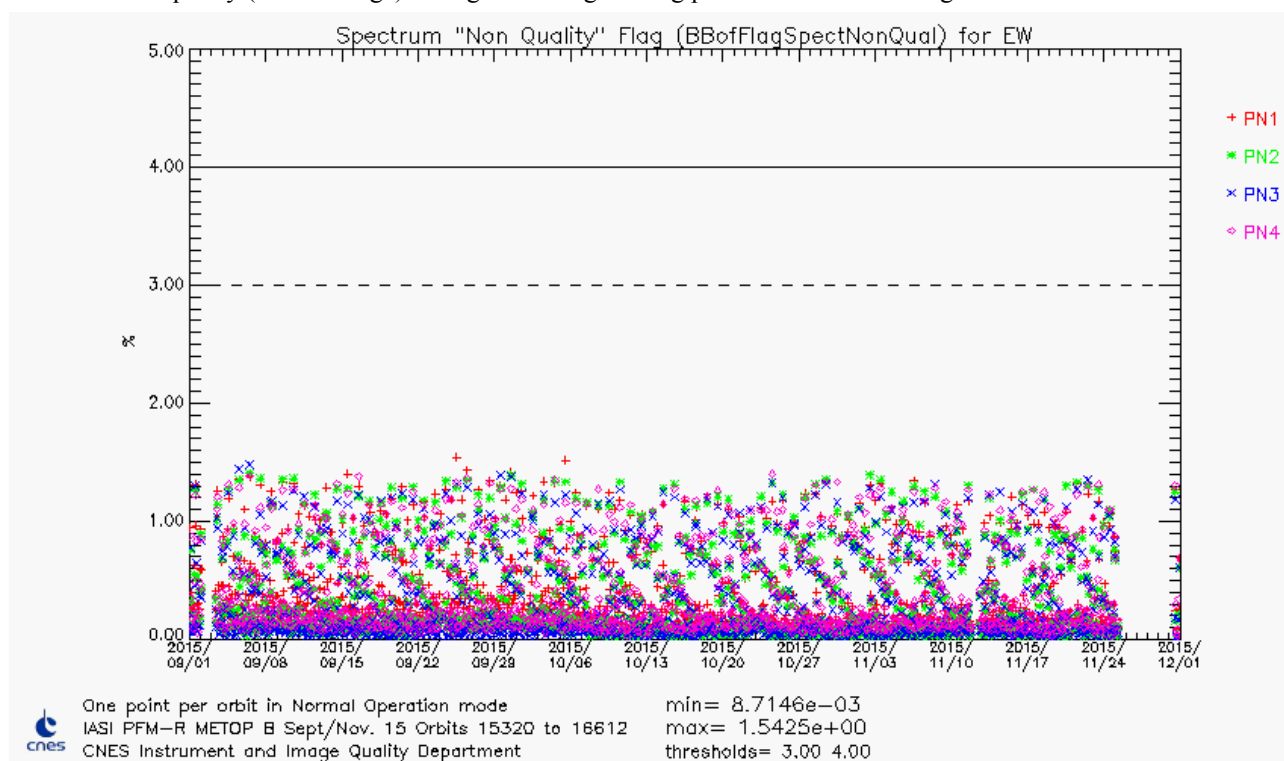


Figure 1 : IASI L0 data quality orbit average (per pixel and CCD)

The geographical distribution of the overall L0 (board) quality flag for the 4 pixels is shown in Figure 2.



Doc n°: IA-RP-2000-4252-CNE

Issue: 1.0

Date: 2017-09-27

Sheet: 18 Of: 67

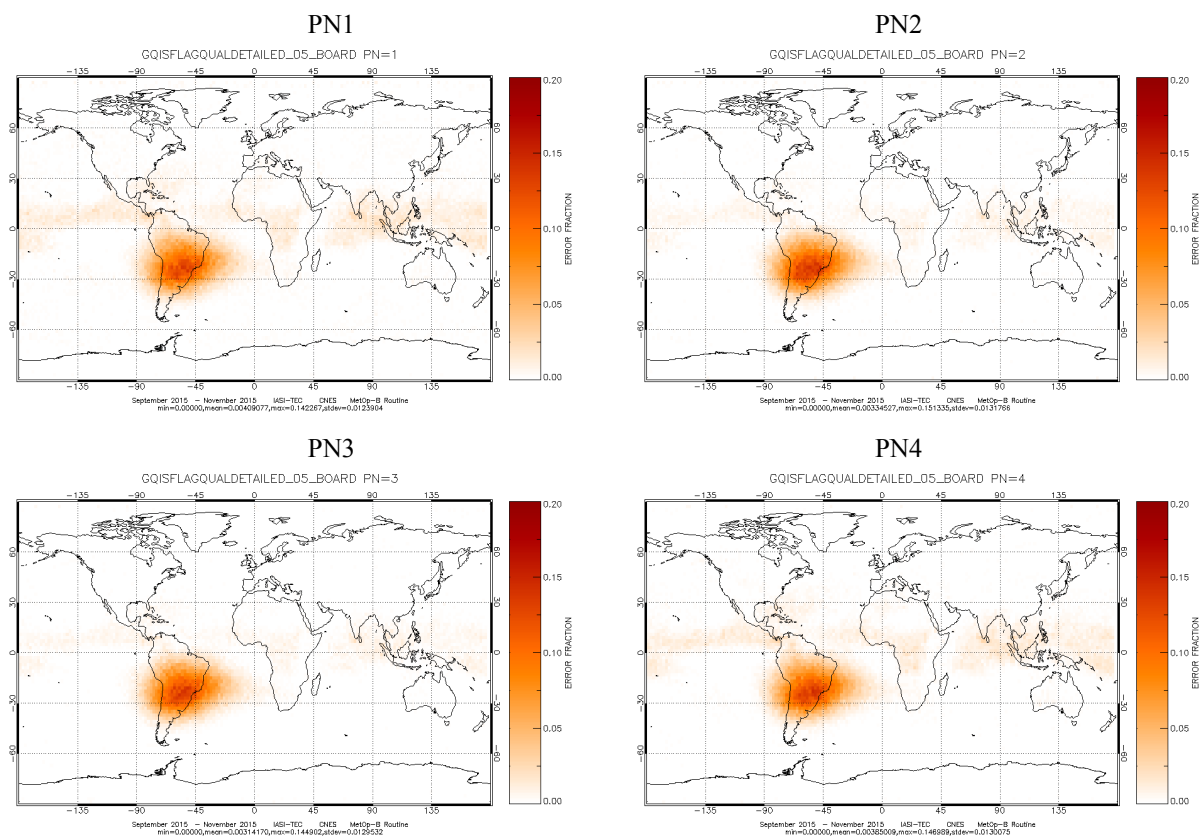




Figure 2 : IASI L0 data quality spatial distribution (per pixel)

The IASI L0 quality and on-board processing are nominal.

		Doc n°: IA-RP-2000-4252-CNE Issue: 1.0 Date: 2017-09-27 Sheet: 19 Of: 67
--	--	---

4.3.2 Main flag and quality indicator parameters

The main contributors to the rejected spectra by on-board processing are: spikes (proton interaction on detectors), failure of NZPD algorithm determination and over/underflows (measured data exceeding on-board coding tables capacity). They are analysed in details hereafter.

4.3.2.1 Spikes monitoring

Spikes occur when a proton hits a detector. This very high energetic particle disrupts the measure of the interferogram and then corrupts the spectrum.

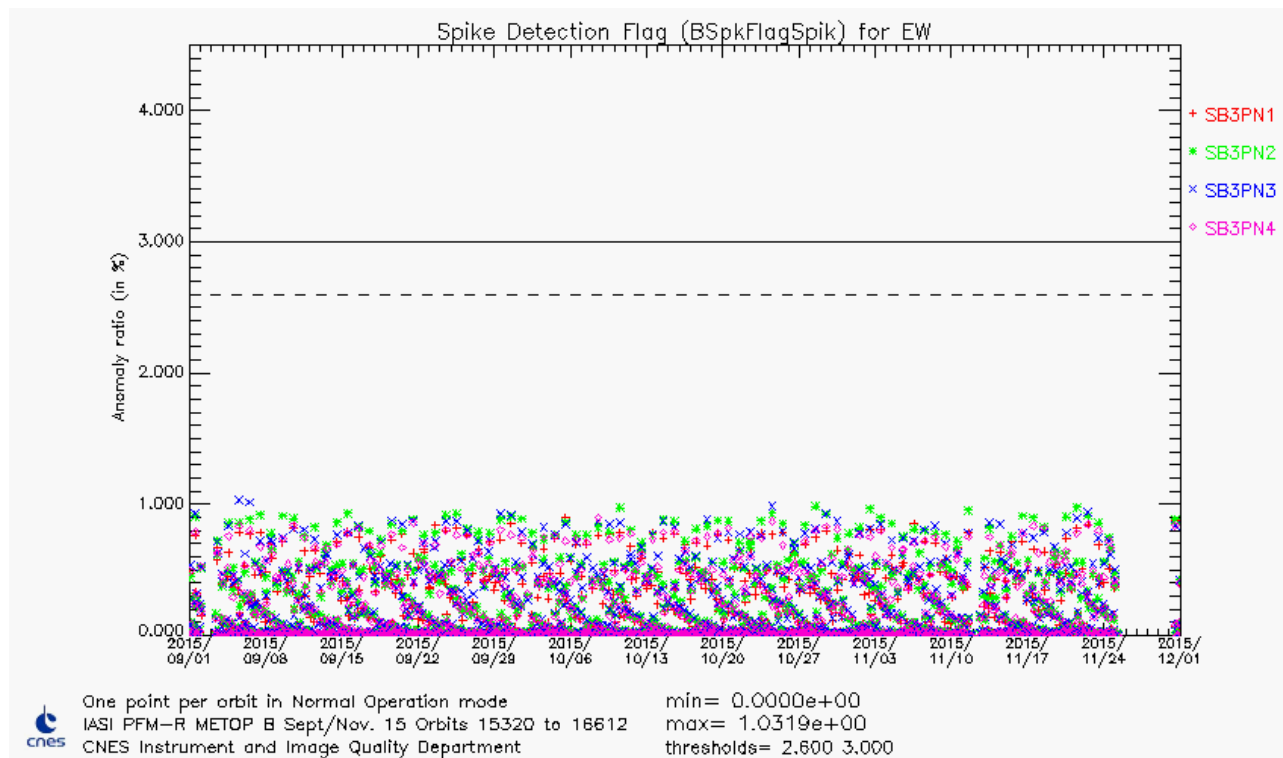


Figure 3 : Temporal evolution of spikes anomaly ratio in % for all pixels (orbit average)

An example of the geographical distribution of spikes occurrences on band 3 for the 4 pixels is shown in Figure 4.



Doc n°: IA-RP-2000-4252-CNE

Issue: 1.0

Date: 2017-09-27

Sheet: 20 Of: 67

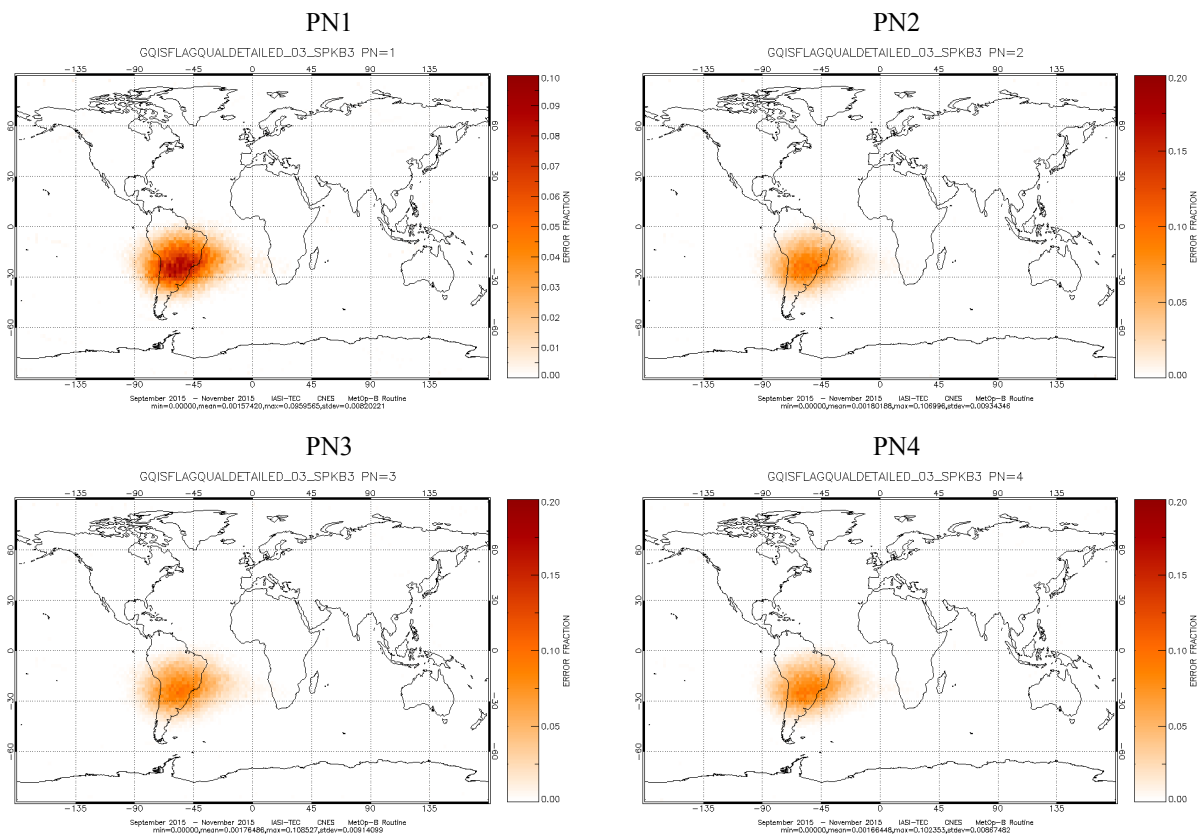




Figure 4 : Geographical distribution of spikes occurrences in % for band 3 and all pixels

Spikes are mainly located in the regions of Earth where the magnetic field doesn't protect the satellite from the energetic particles: the poles and the SAA (South Atlantic anomaly).

Spike anomaly ratio is nominal for the reported period.

		Doc n°: IA-RP-2000-4252-CNE Issue: 1.0 Date: 2017-09-27 Sheet: 21 Of: 67
--	--	---

4.3.2.2 ZPD monitoring

The ZPD (“Zero Path Difference”) is the position of the central fringe of the interferogram. The NZPD is the number of the sample detected as the ZPD. On IASI, it is determined by a software. This is a special feature of IASI in comparison to other instruments for which NZPD determination is done by hardware.

NZPD variations are governed by two phenomenons:

1. ASE fluctuations which have the same effect on each pixel and can produce NZPD variation of 30-40 samples over month. This is the first order phenomena.
2. Mechanical deformation of the interferometer or evolution of detection chain delays. These phenomenons affect the 4 pixels in different way. However this phenomenon has a second order effect in comparison to the first one.

We monitor both NZPD determination quality flag and interpixel homogeneity. We expect stability.

BZPDFlagNZPDNonQualEW: Temporal evolution of NZPD determination quality flag for earth view

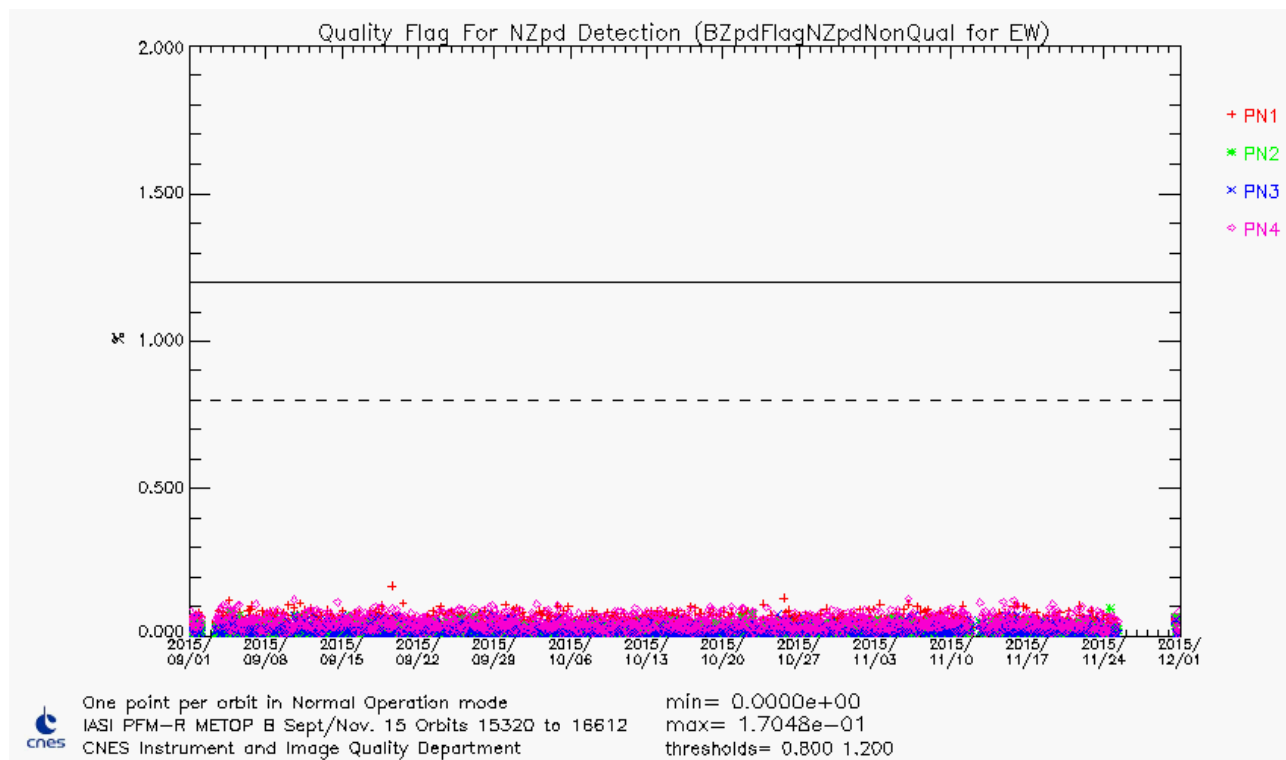


Figure 5 : Temporal evolution of NZPD determination anomaly ratio in % for all pixels (orbit average)

NZPD determination anomaly ratio is nominal for the reported period.

The geographical distribution of the NZPD determination quality flag for the 4 pixels is shown in Figure 6.

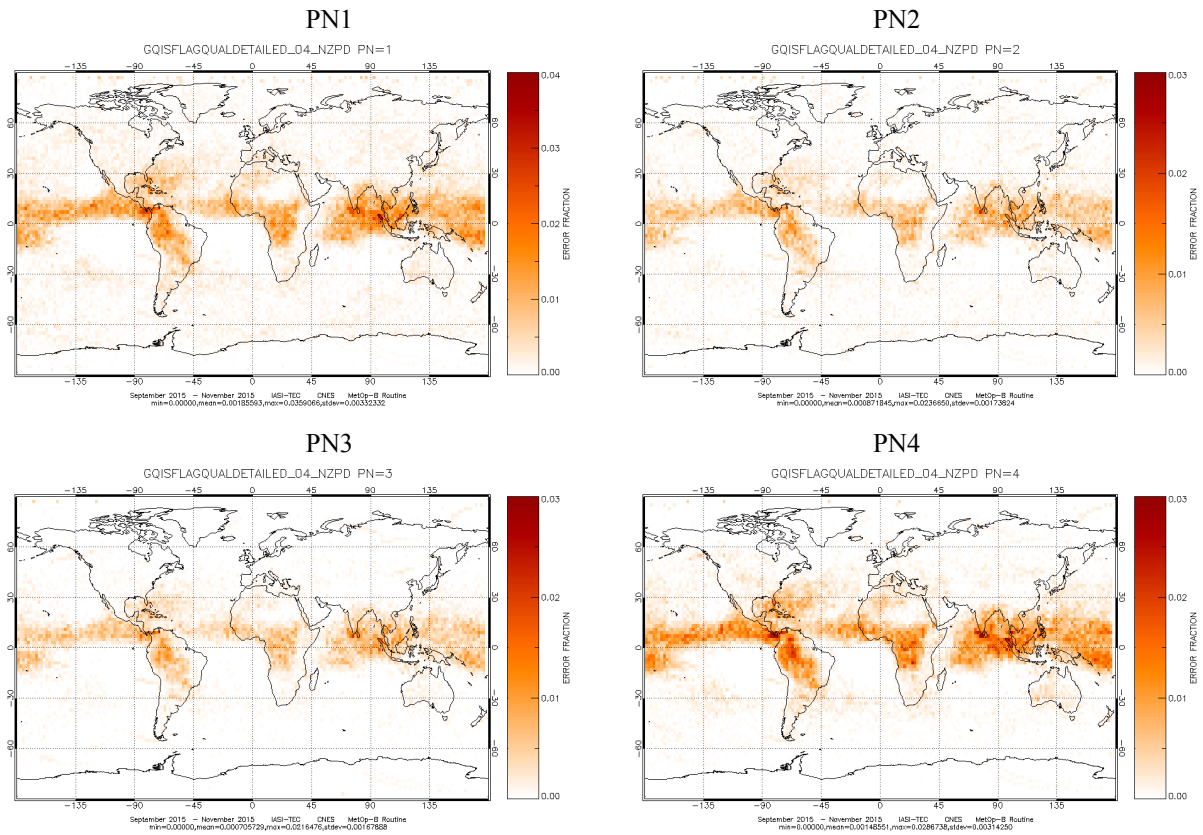


Figure 6 : IASI NZPD determination quality flag spatial distribution (per pixel)

The NZPD determination fails over some clouds that have a temperature that induces no energy in the central fringe of the interferogram.

NZPD inter-pixel homogeneity monitoring

This monitoring is necessary in order to follow potential deformation of the interferometer or evolution of detection chain delay.

The NZPD inter-pixel homogeneity is nominal over the reported period. Consequently, these parameters are perfectly stable and in-line with the specification.

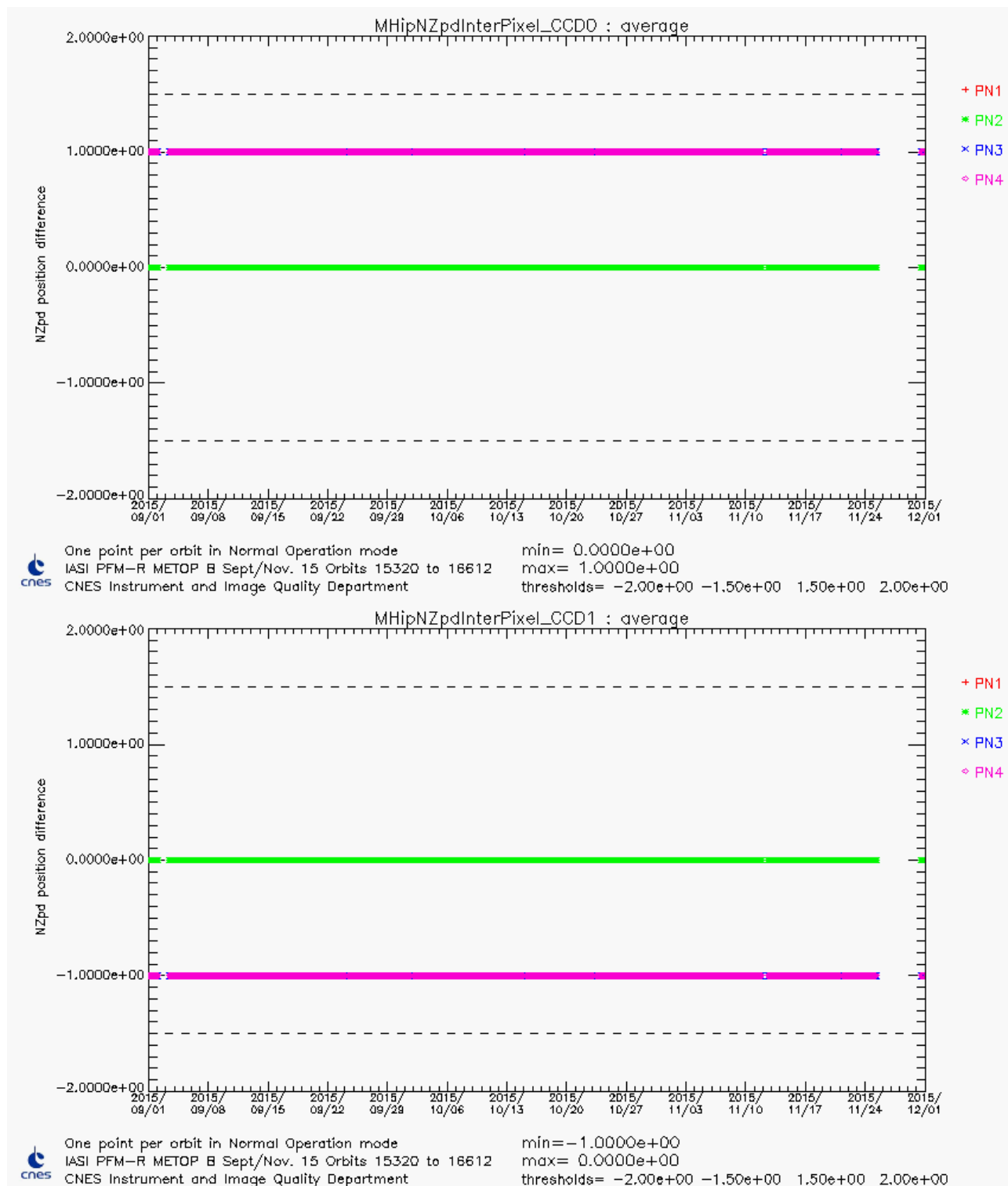




Figure 7 : NZPD inter-pixel for all pixels and CCD calculated with respect to pixel 1 (orbit average)

		Doc n°: IA-RP-2000-4252-CNE Issue: 1.0 Date: 2017-09-27 Sheet: 24 Of: 67
---	---	---

4.3.2.3 Overflows / Underflows monitoring

The total number of bits available for a spectrum to be transmitted to the ground is limited. For that reason, we have defined coding tables to encode each measured spectrum. These tables have been designed by using “extreme spectrum” corresponding to known drastic atmospheric conditions. The coding step is also set to not introduce additional noise into the spectrum. However for very extreme atmospheric conditions (sunglint in B3, very high stratospheric temperature...) a measurement can exceed on-board coding tables’ capacity and causes an over/underflow.

Over/underflows occurrences are monitored and stability is expected. As long as they remain to low levels, the coding table is not changed. Note that changing the coding tables requires compromises. Indeed, increasing the encoding capacity can be achieved by two different ways. A first solution consists in an increase of the coding step without changing the number of bits. However, that leads to an increase of the digitalization noise. Then, a second solution consists in keeping the coding step constant while increasing the number of bits available for a particular band. But, the total amount of bits available for the entire spectrum is limited and constant. So, that requires to decrease the encoding capacity in another spectral band.

Time series of Overflows and Underflows (orbit average) are shown in following figure for all pixels.

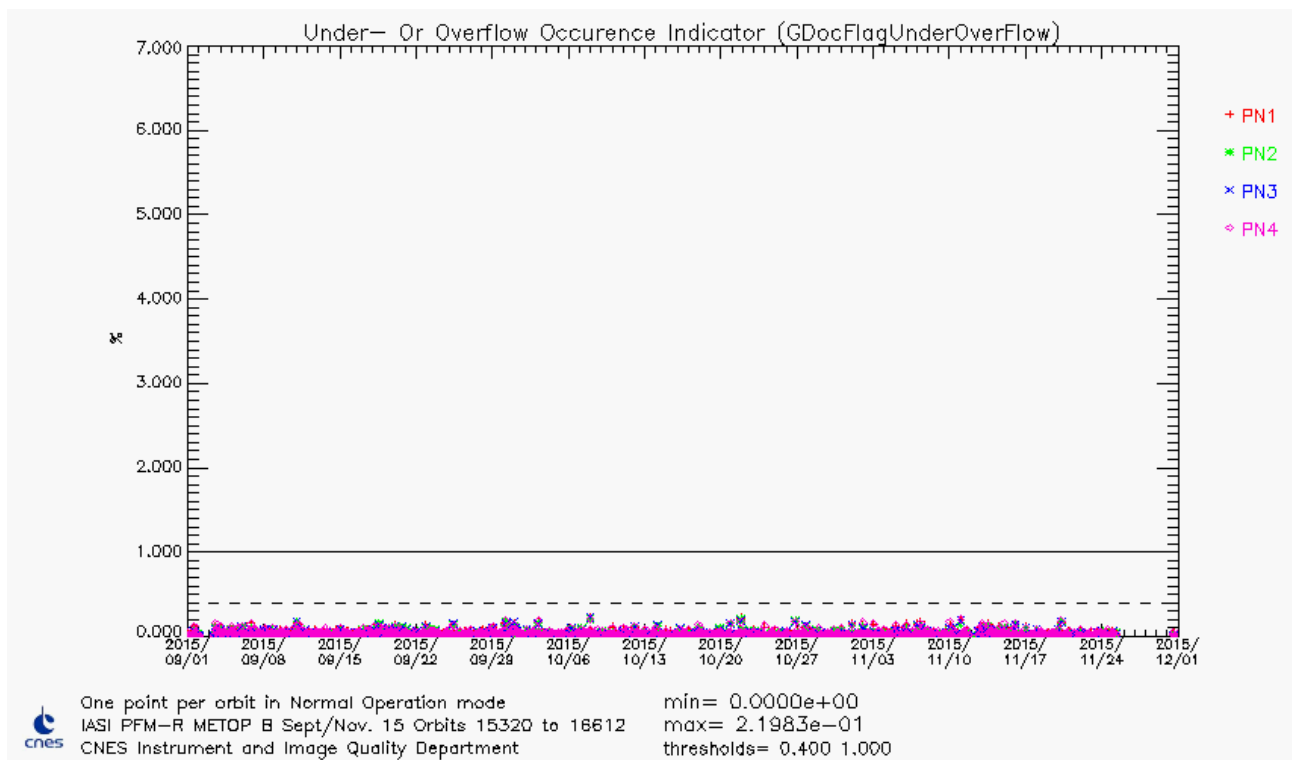




Figure 8 : IASI L0 over/under-flows orbit average of all pixels

Over/underflows ratio is nominal for the reported period.

The geographical distribution of the Overflows and Underflows for the 4 pixels is shown in Figure 9.

		Doc n°: IA-RP-2000-4252-CNE Issue: 1.0 Date: 2017-09-27 Sheet: 25 Of: 67
---	---	---

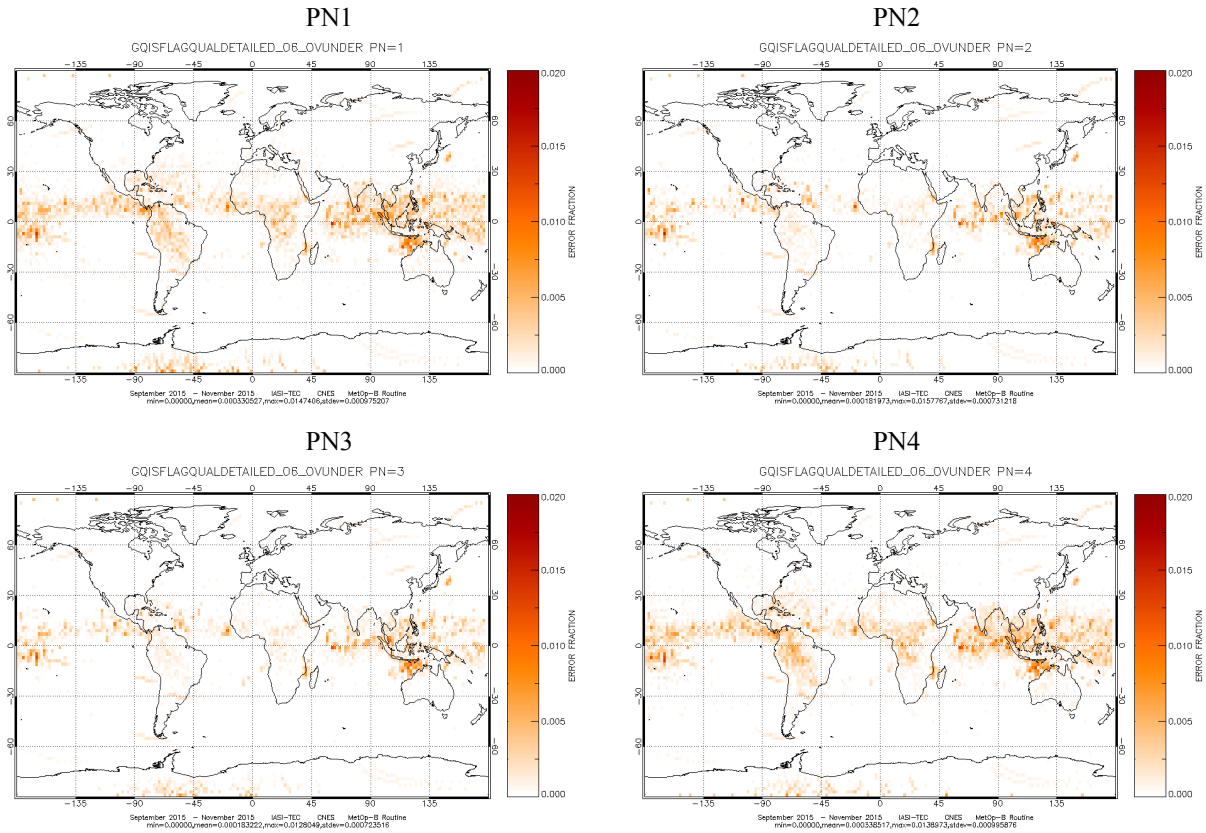


Figure 9 : IASI Overflows and Underflows spatial distribution (per pixel)

4.3.2.4 Reduced Spectra monitoring

On-board Reduced Spectra is one of the most important parameter to monitor. It ensures that on-board spectra still have a good radiometric calibration when on-board configuration reduced spectra are reloaded. This is the case, for instance, after an instrument mode change.

Reduced spectra are slightly evolving with respect to potential deformation of the interferometer (optical bench).

In order to prevent from a large difference between current and on-board configuration reduced spectra, we apply the DPS processing on the verification interferograms using the reduced spectra from the on-board configuration (TOP) instead of the filtered reduced spectra computed on-board with the current calibration views. These reduced spectra from the on-board configuration are used as initialisation each time there is mode change. If they are too far from the reality, no spectra can be computed on-board after a mode change. We monitor the evolution of ZPD determination quality index for calibration views (BZpdNzpdQualIndexBB and CS) obtained by this DPS processing at TEC, results of this monitoring are given hereafter.

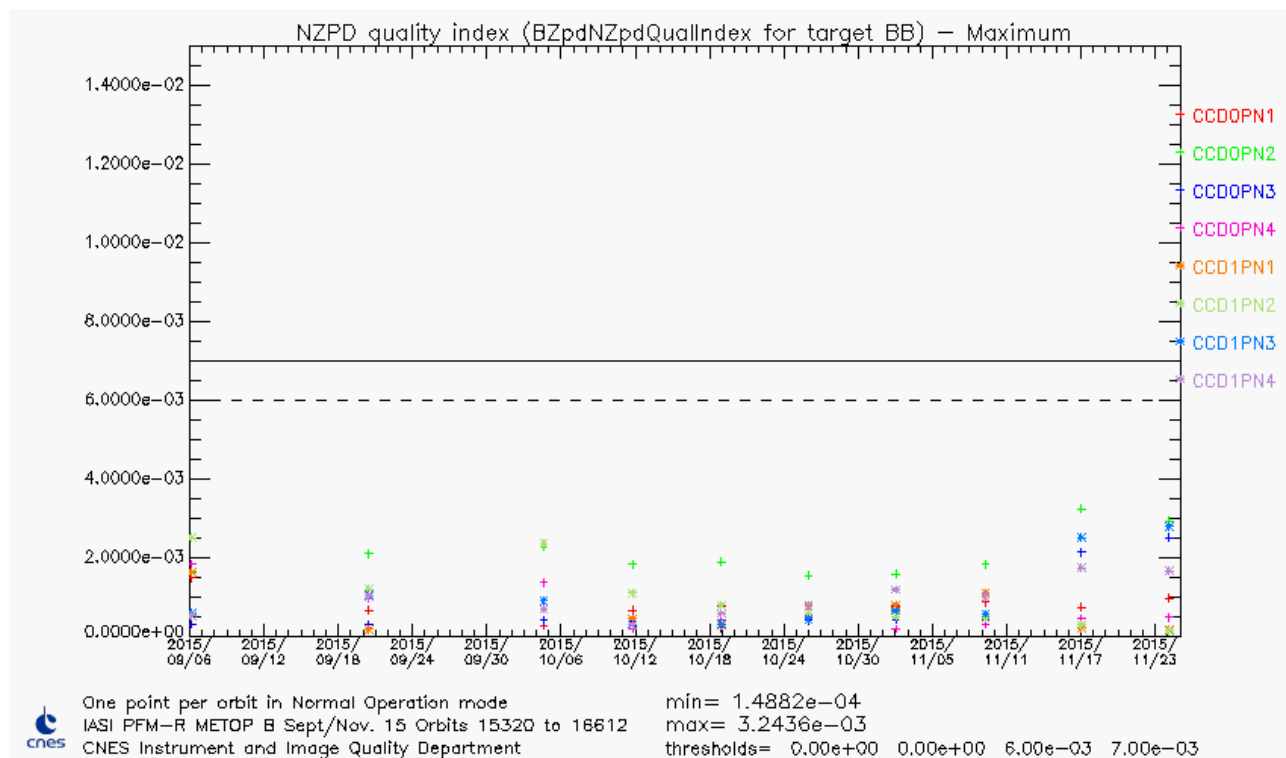


Figure 10 : Max of NZPD quality index for all pixels and CCD - BB

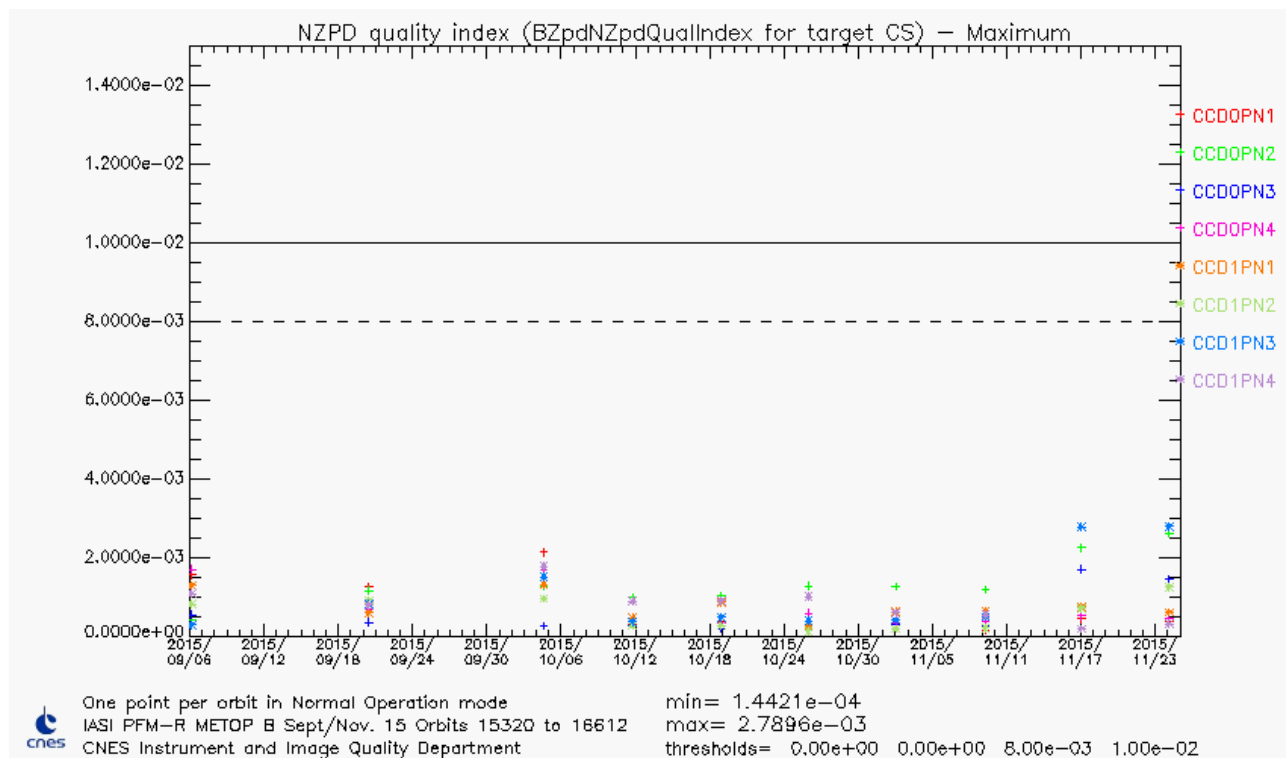




Figure 11 : Max of NZPD quality index for all pixels and CCD - CS

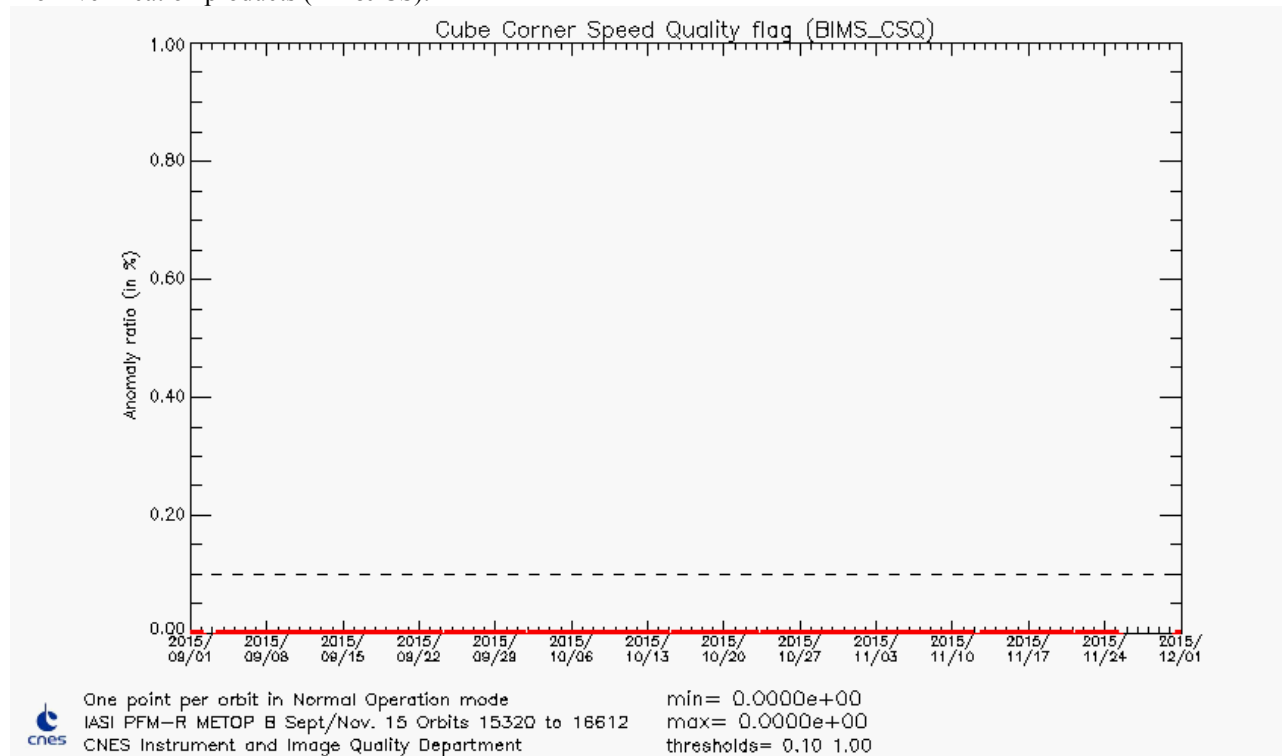
As soon as BZPDNZPDQualIndexBB and CS remain below 0.02 on-board reduced spectra are robust to an instrument mode change.

The reduced spectra quality is well within specification since the last update of the on-board reduced spectra performed in February 2015.

		Doc n°: IA-RP-2000-4252-CNE Issue: 1.0 Date: 2017-09-27 Sheet: 27 Of: 67
--	--	---

4.3.2.5 Cube corner Speed Quality (CSQ) monitoring

From verification products (BB & CS):



From engineering products (EW):

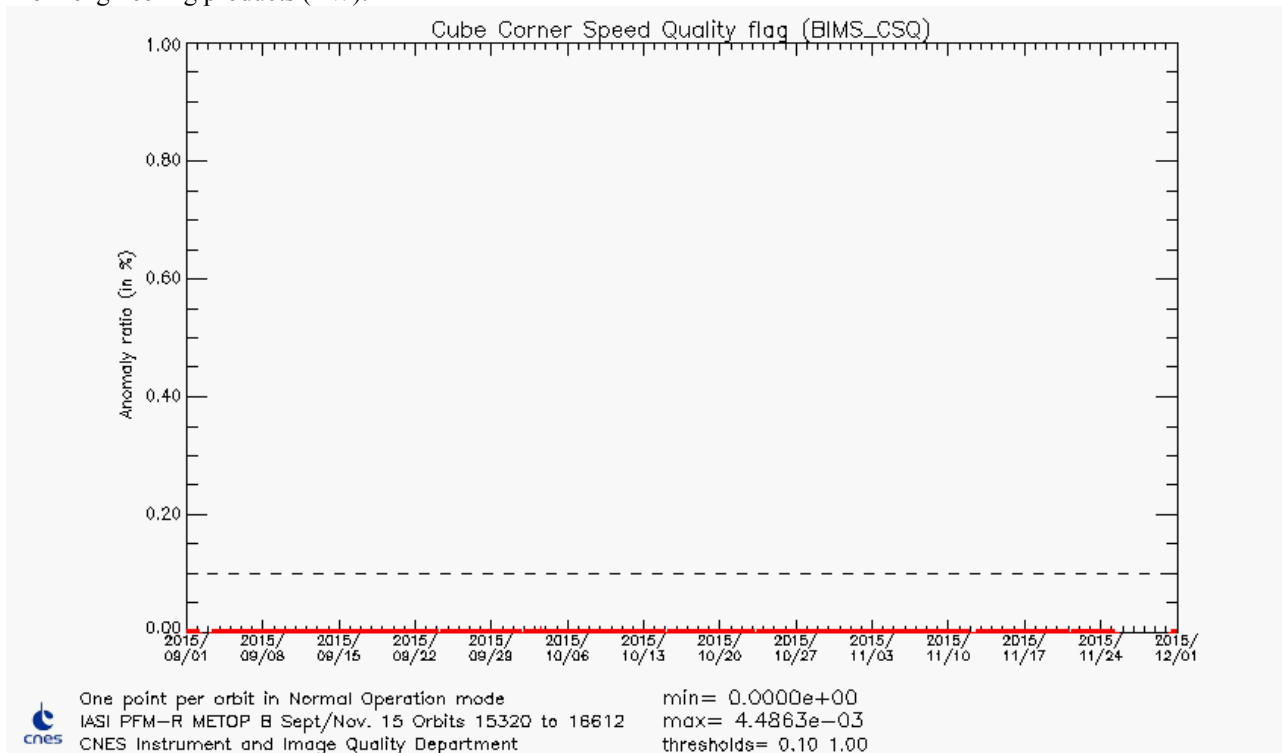




Figure 12 : Number of CSQ

		Doc n°: IA-RP-2000-4252-CNE Issue: 1.0 Date: 2017-09-27 Sheet: 28 Of: 67
--	--	---

4.3.3 Second level flags and quality indicators

All second level flags and indicators are stable and nominal.

4.3.4 Conclusion

L0 Flag and quality indicators are stable.

4.4 LEVEL 1 DATA QUALITY (L1)

4.4.1 Overall quality

The IASI overall quality is shown as the orbit averages of the quality indicator for the individual pixels in the next figure.

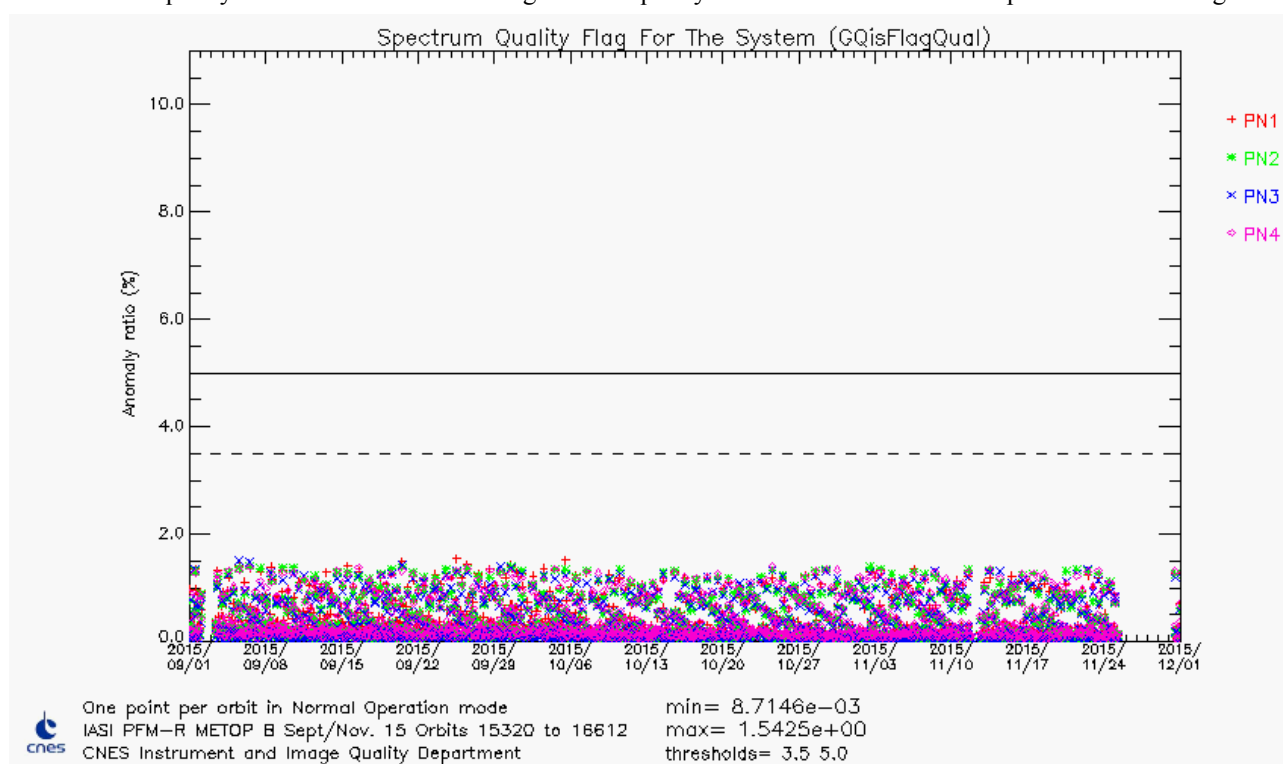




Figure 13 : IASI L1 data quality orbit average (% of bad by PN)

One should note that, over the period covered by the present document, the averaged data rejection ratio is less than 1%. We clearly see that data quality is better on the bands B1 and B2 in comparison to band B3 (which is the most affected by spikes).

The geographical distribution of the IASI product overall quality for the 4 pixels is shown in Figure 14.

		Doc n°: IA-RP-2000-4252-CNE Issue: 1.0 Date: 2017-09-27 Sheet: 29 Of: 67
---	---	---

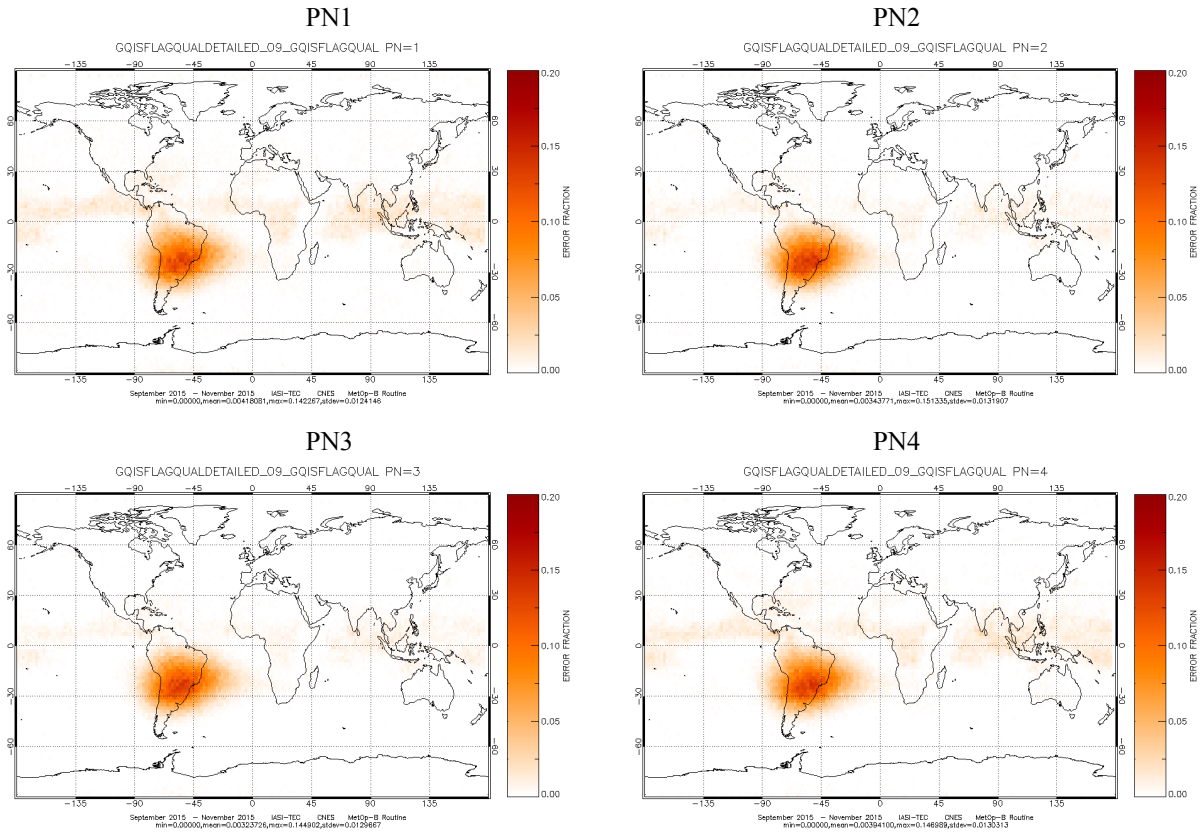


Figure 14 : IASI product overall quality spatial distribution (per pixel)

The main contributors are the spikes (mainly in band 3, which is the band the most sensitive to the spikes).

4.4.2 Main flag and quality indicator parameters

All the quality indexes that follow are general L1 quality indexes of sounder products.

GQisQualIndex – average – is the average general quality index of the sounder products.

GQisQualIndexIIS is the IASI integrated imager (IIS) images quality index.

GQisQualIndexSpect is the spectral quality index of the sounder products.

GQisQualIndexRad is the radiometric quality index of the sounder products.

GqisQualIndexLoc is the ground localisation quality index of the sounder products.

MDptPixQual is a quality index for IASI integrated imager (IIS) that represents a fraction of not dead pixels.

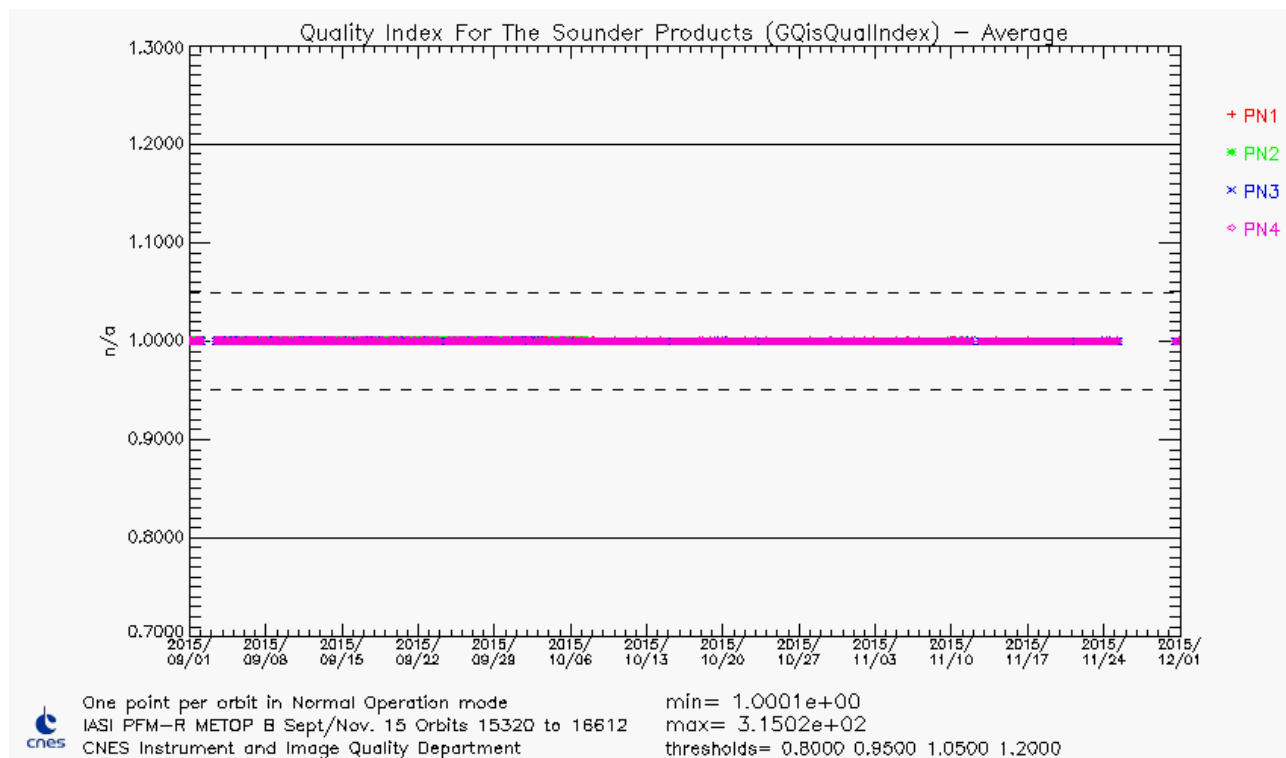


Figure 15 : GQisQualIndex average (L1 data quality index for IASI sounder)

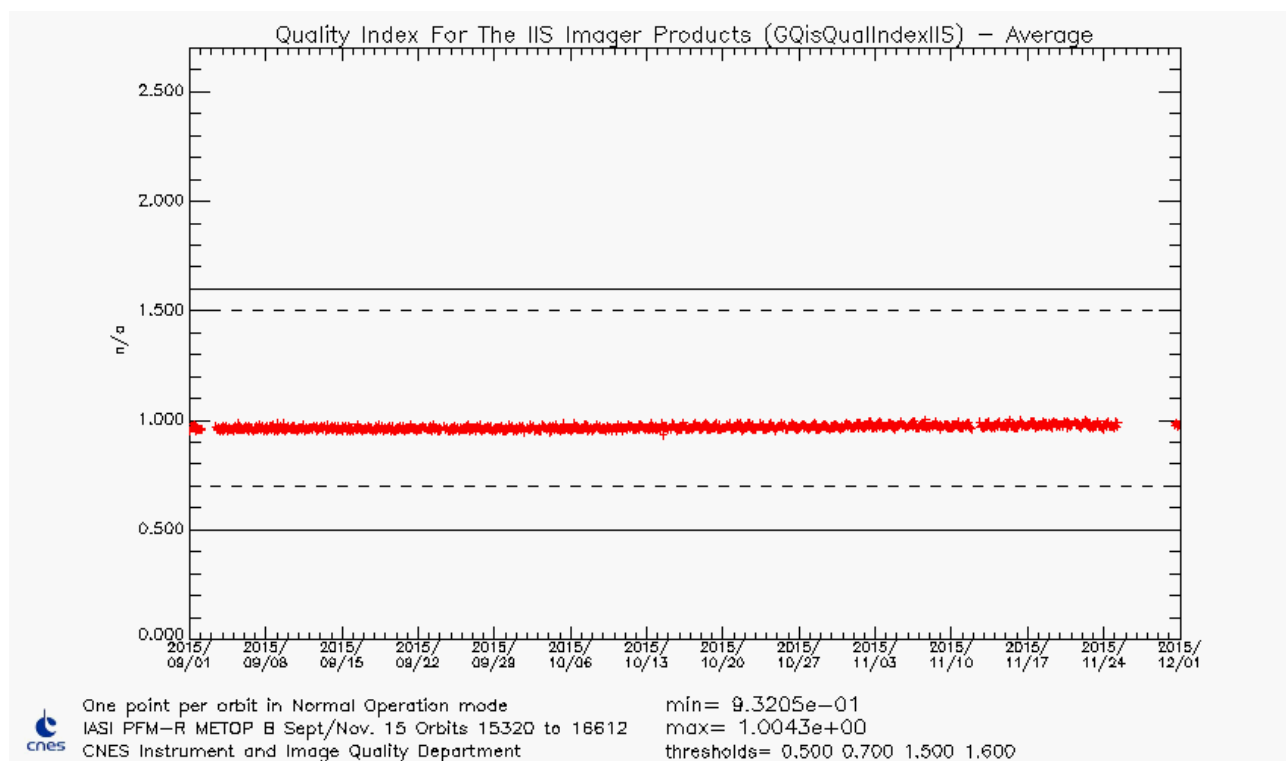


Figure 16 : GQisQualIndexIIS average (L1 data quality index for IASI Integrated Imager)

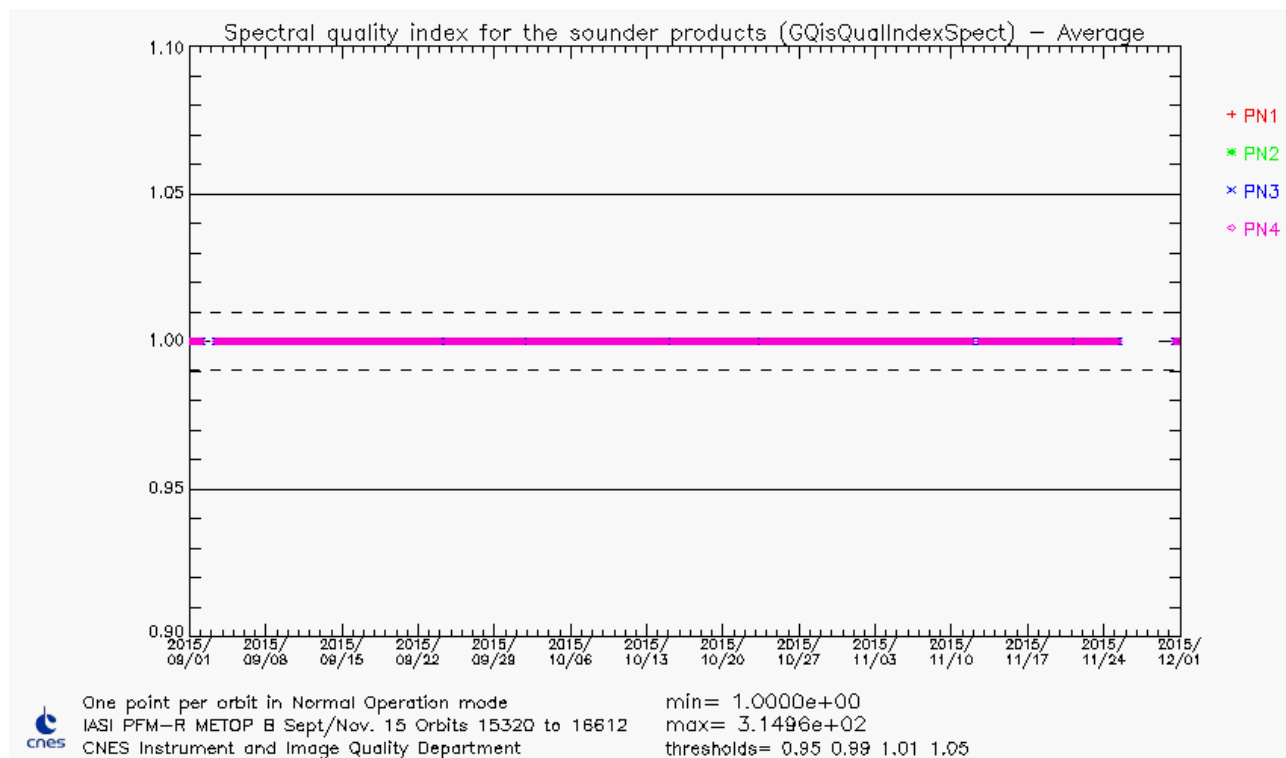


Figure 17 : GQisQualIndexSpect average (L1 data index for spectral calibration quality)

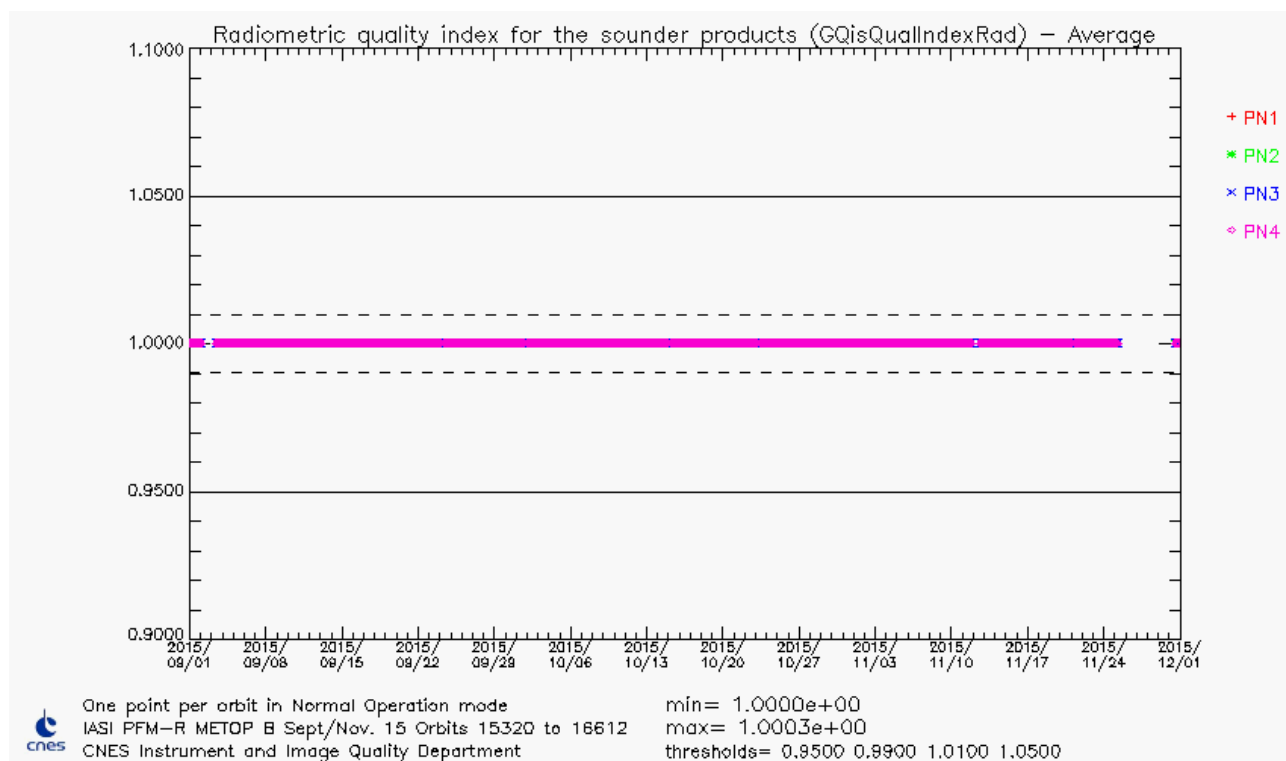




Figure 18 : GQisQualIndexRad average (L1 data index for radiometric calibration quality)

		Doc n°: IA-RP-2000-4252-CNE Issue: 1.0 Date: 2017-09-27 Sheet: 32 Of: 67
--	--	---

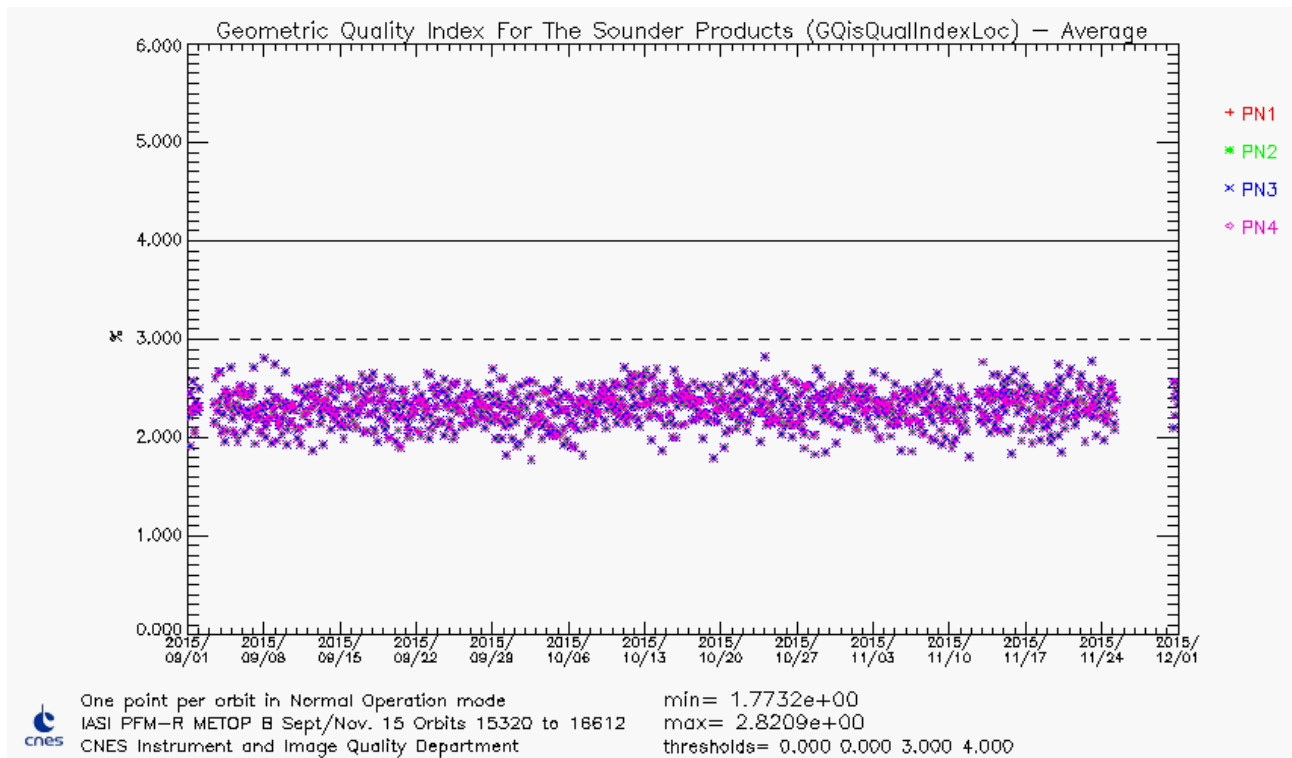


Figure 19 : *GQisQualIndexLoc* average (L1 data index for ground localisation quality)

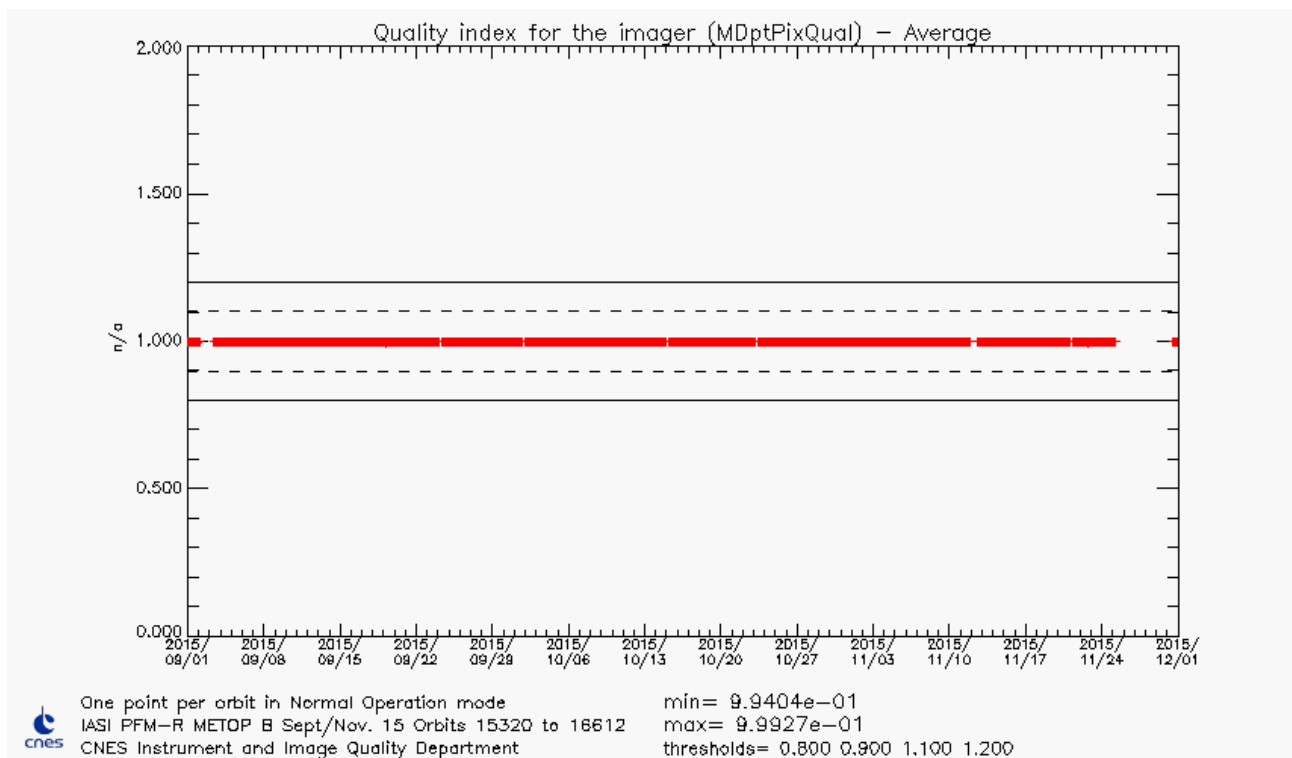


Figure 20 : *MDptPixQual* average (L1 quality index for IASI integrated imager; fraction of not dead pixels)

4.4.3 Conclusion

L1 Flag and quality indicators are stable and meet the specifications.

4.5 SOUNDER RADIOMETRIC PERFORMANCES

4.5.1 Radiometric Noise

Monitoring the radiometric noise allows to monitor the long term degradation of the instrument as well as to look for punctual anomaly of IASI or other component of METOP.

Monthly L0 noise estimation (CE)

This monthly estimation is performed during routine External Calibration on BB views.

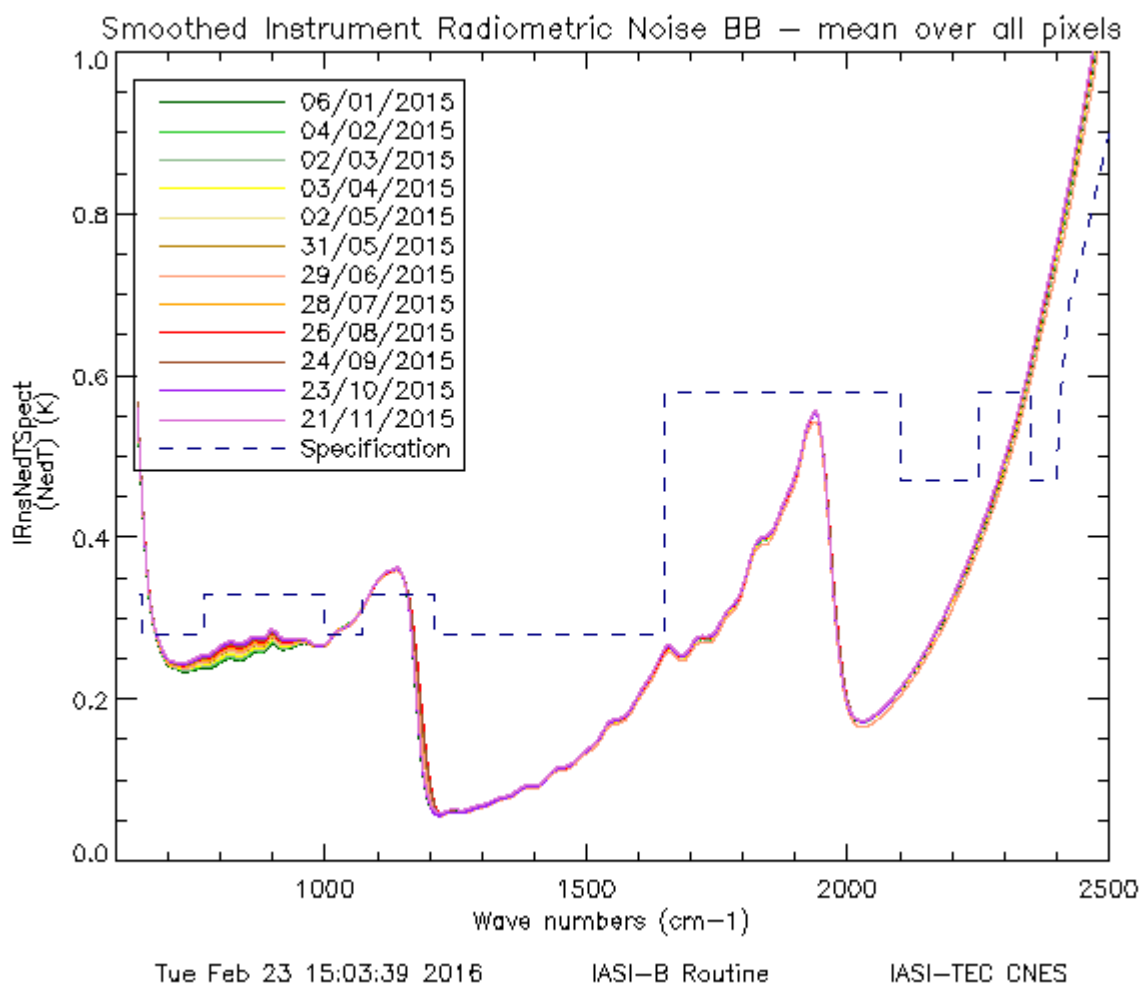


Figure 21 : Instrument noise evolution between start and end of the period

The instrument noise is very stable apart from ice effect between 700 and 1000 cm^{-1} . This point will be developed in section 4.5.4.1.

4.5.2 Radiometric Calibration

The radiometric calibration allows to convert an instrumental measurement into a physical value. The radiometric calibration is used to convert an interferogram into an absolute energy flux by taking into account instrument discrepancies. Even if the calibration has been studied on ground, it has to be continuously monitored in-flight in order to follow any potential degradation of the instrument (optics, detectors ...).

Approach: Radiometric fine characterization has been done during on-ground testing and Cal/Val. All parameters likely to cause a failure in radiometric calibration process have been identified and are continuously monitored. As long as they remain stable, there is no problem with radiometric calibration.

Evolution of scanning mirror reflectivity

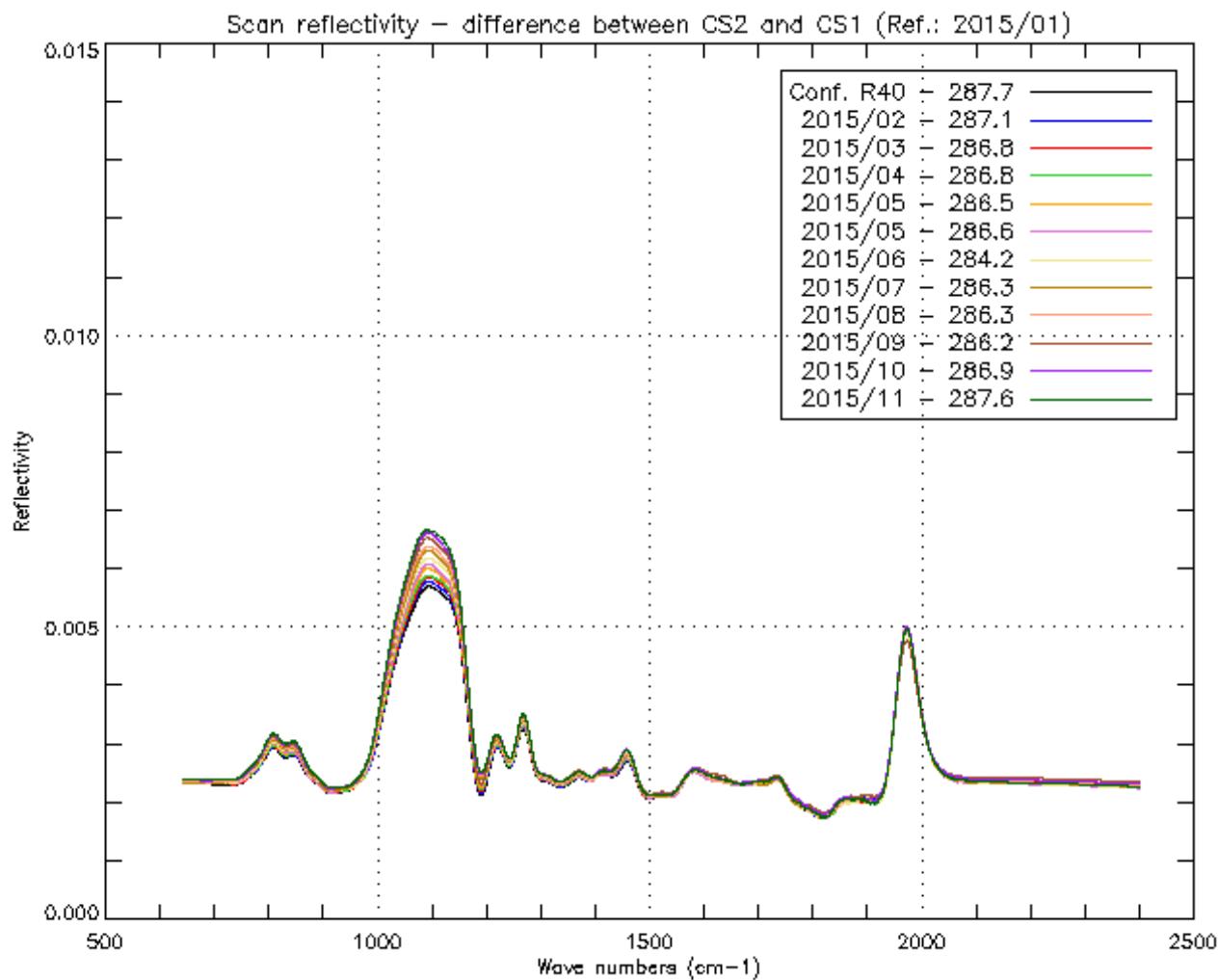
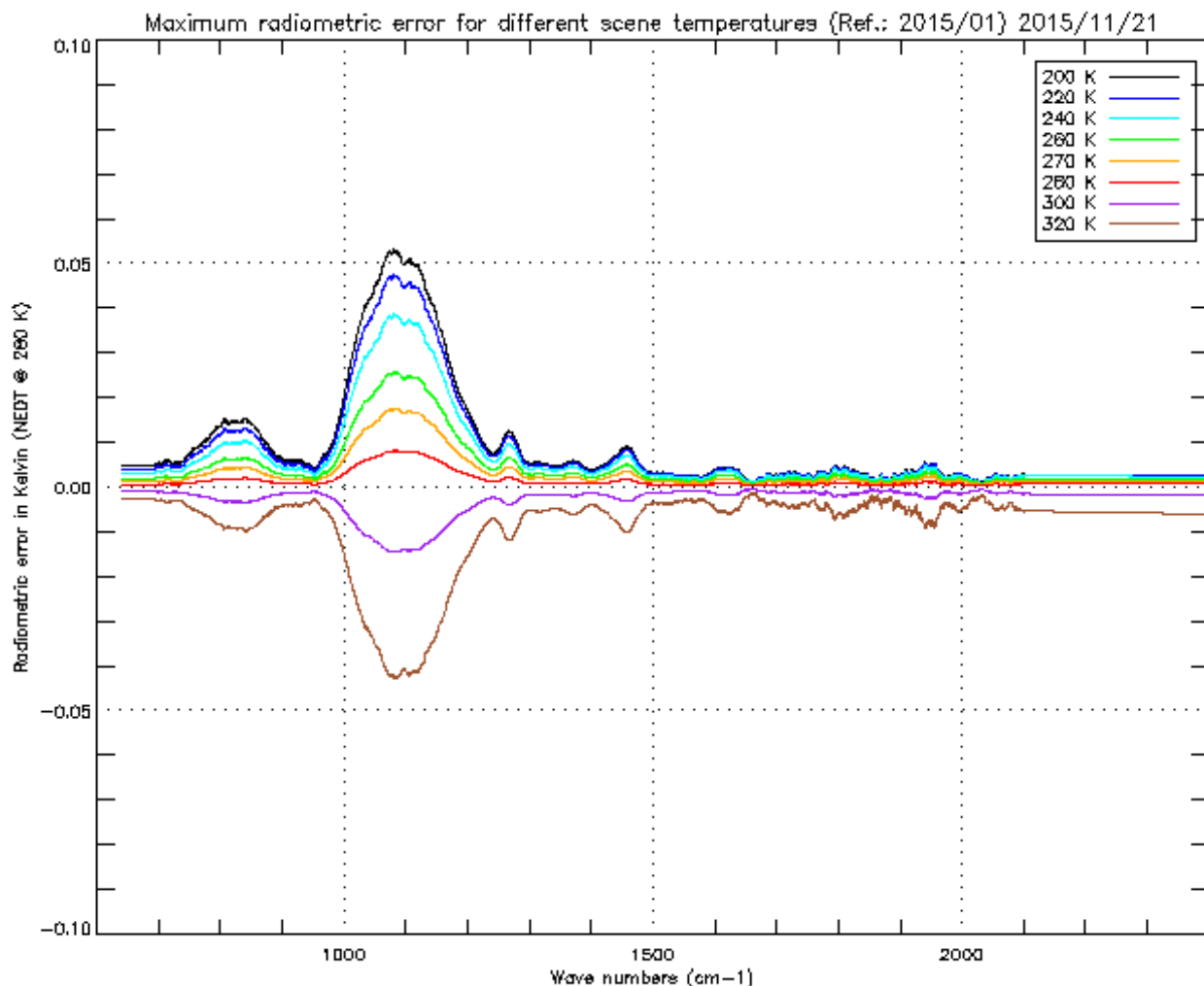


Figure 22 : Scan mirror reflectivity evolution



The reference reflexivity (in black) is the one computed on data from January 6th 2015. We see a slight evolution within [1000-1100 cm⁻¹] band. Values for wavenumbers greater than 2400 cm⁻¹ are not significant because of instrument noise.

The next figure shows the translation of scan mirror reflectivity in terms of maximum radiometric calibration error for different scene temperatures.



*Figure 23 : Radiometric calibration error due to scan mirror reflectivity dependency
with viewing angle Maximum effect on SN1 for different scene temperature.
Done with the period February / November*

In any cases radiometric calibration maximum error is lower than the specification (0.1K). The scan mirror reflectivity law (on ground configuration), prepared with January 6th routine External Calibration data, has been updated in the operational ground segment on February 19th 2015.

		Doc n°: IA-RP-2000-4252-CNE Issue: 1.0 Date: 2017-09-27 Sheet: 36 Of: 67
---	---	---

Internal black body

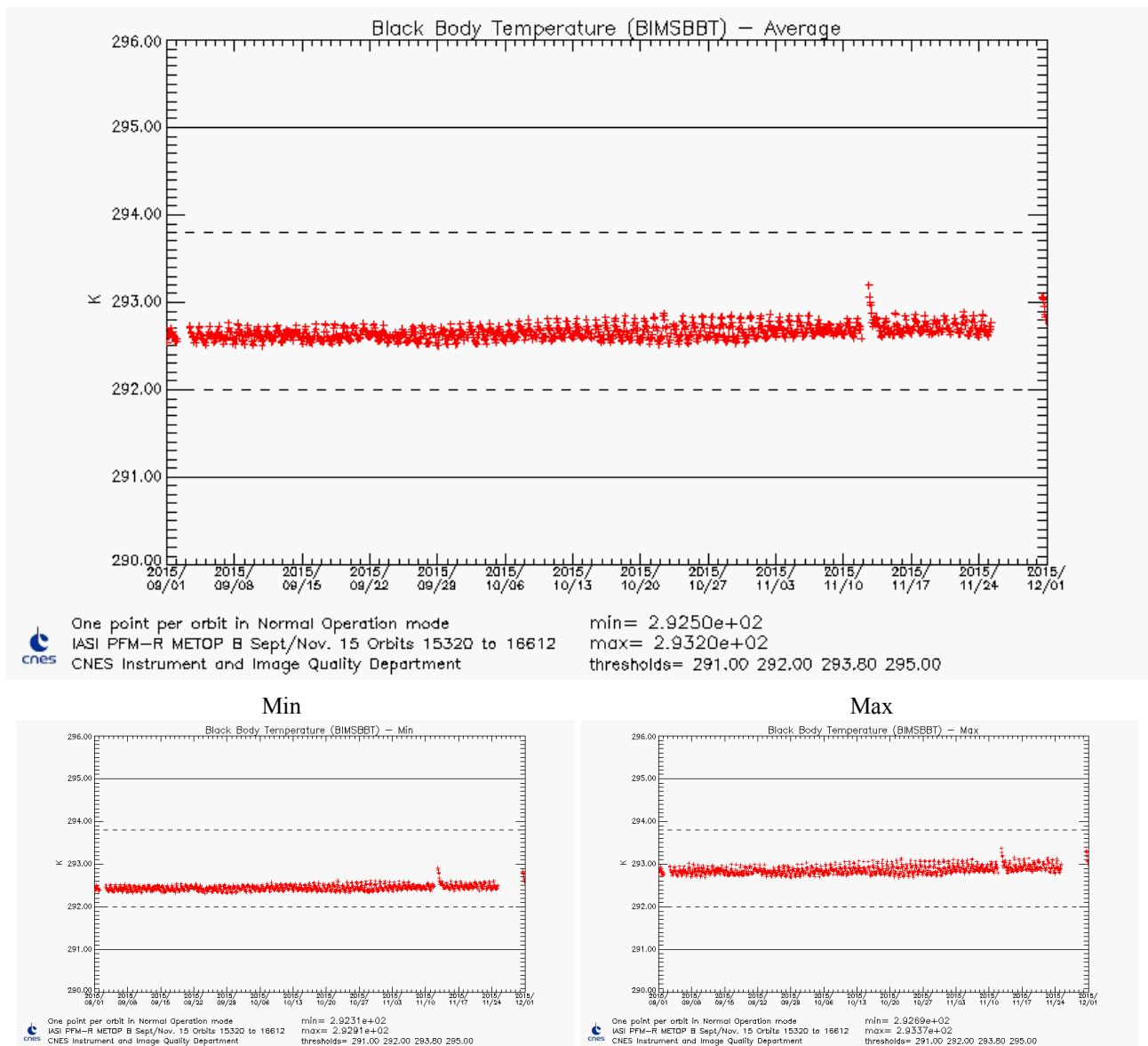




Figure 24 : Black Body Temperature

The black body temperature is stable. The highest values on the 11th November are due to the come back to normal operation after the SEU anomaly. There are also high values end of November after the decontamination.

		Doc n°: IA-RP-2000-4252-CNE Issue: 1.0 Date: 2017-09-27 Sheet: 37 Of: 67
--	--	---

Non linearity of the detection chains

Non-linearity tables of the detection chains are still nominal as long as sounder focal plane temperature variation amplitude is lower than 1K.

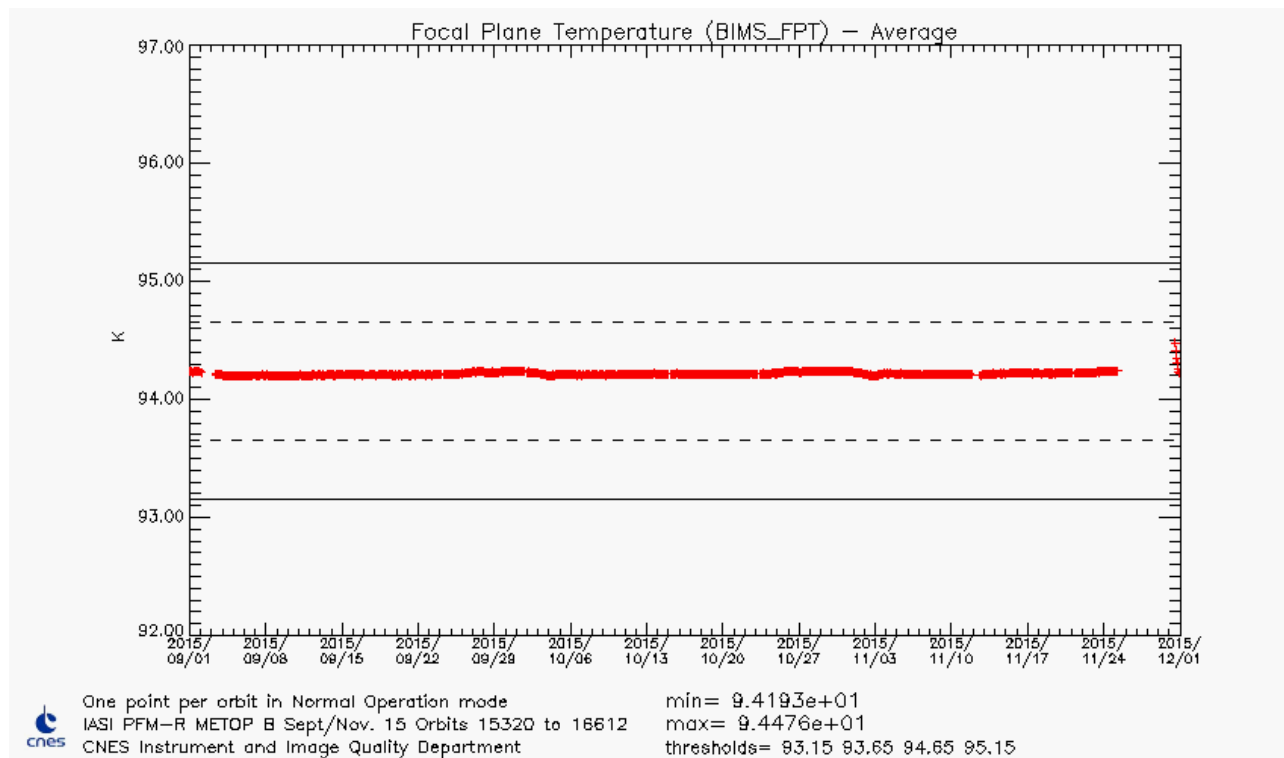




Figure 25 : Focal Plane Temperature

		Doc n°: IA-RP-2000-4252-CNE Issue: 1.0 Date: 2017-09-27 Sheet: 38 Of: 67
--	--	---

4.5.3 Delay of Detection Chains

Long term stability and values lower than 400 ns are required in order to properly take into account cube corner velocity fluctuations.

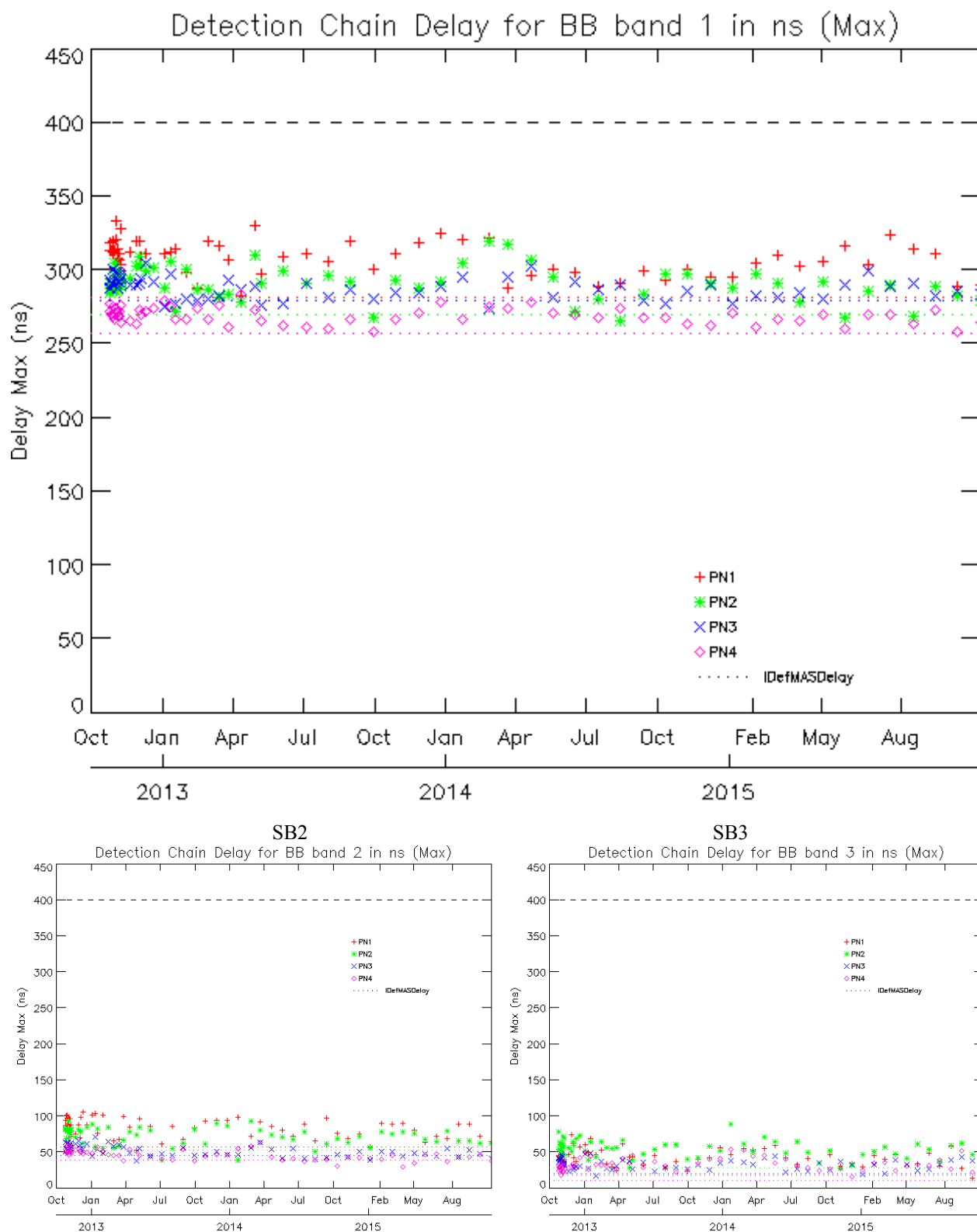


Figure 26 : Monitoring of detection chain maximum delays for all bands

4.5.4 Optical Transmission

4.5.4.1 Ice

The IASI interferometer and optical bench are regulated at 20°C temperature, while the cold box containing cold optics and detection subsystem is at about -180°C. Water desorption from the instrument causes ice formation on the field lens at the entrance of IASI cold box. This desorption phenomenon is particularly important at the beginning of the instrument in-orbit life. That's why one of the very first activities of IASI in-orbit commissioning was an outgassing phase consisting in heating the cold box up to 300 K during 20 days (from 22th September 2012 until 16th October 2012). This operation allows removing most of the initial contaminants coming from IASI and other MetOp instruments. A routine outgassing is then needed from time to time to remove ice contamination, but less and less frequently as the desorption process becomes slower.

The first routine outgassing procedure (shorter duration and at 200K) was done from 10th to 14th March 2014. The second one was done from 25th to 30th November 2015.

The maximum acceptable degradation of transmission is about 20% loss at 850 cm⁻¹ (which corresponds to an ice deposit thickness of about 0.5 µm).

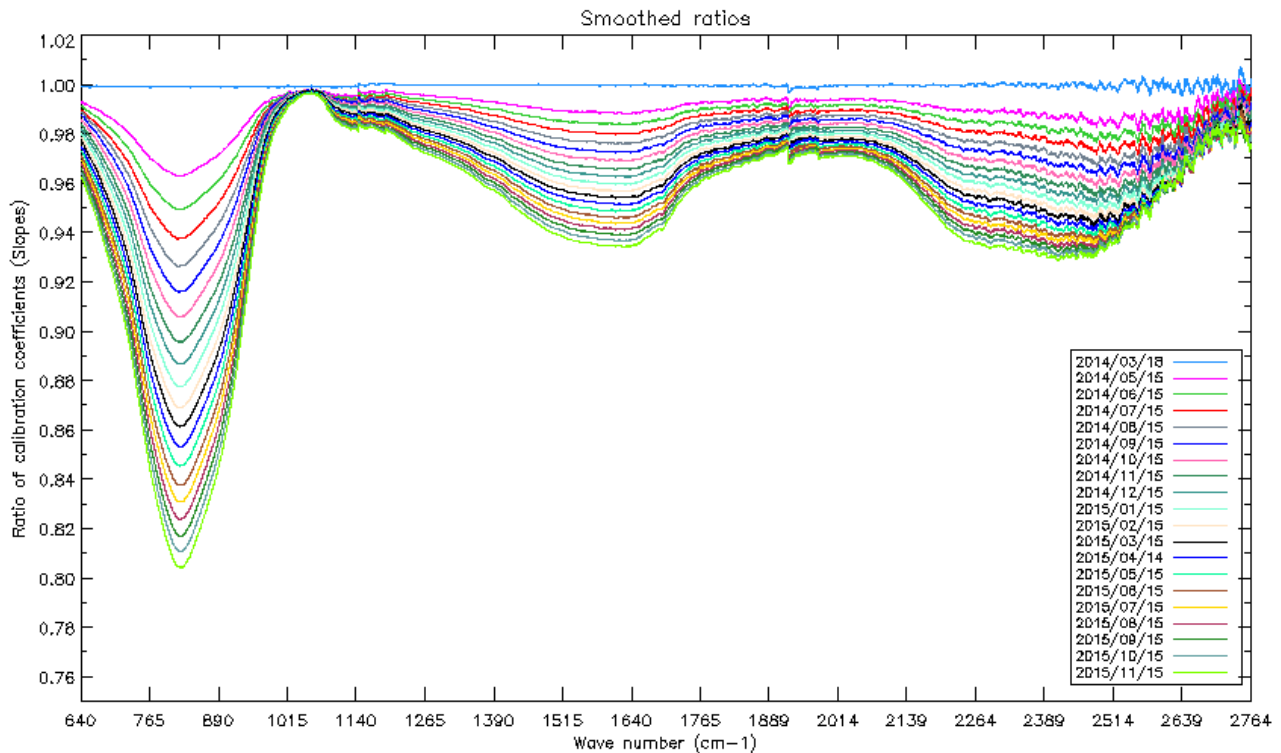




Figure 27 : Ratio of calibration coefficient slopes as a function of wave number and time after the last decontamination

		Doc n°: IA-RP-2000-4252-CNE Issue: 1.0 Date: 2017-09-27 Sheet: 40 Of: 67
--	---	---

4.5.4.2 Prediction of decontamination date

The transmission degradation rate is regularly monitored by CNES TEC through gain measurements given by calibration coefficients ratios.

The loss of instrument gain due to ice contamination is, as expected, decreasing over time. The next decontamination was scheduled at the end of the year and was performed end of November.

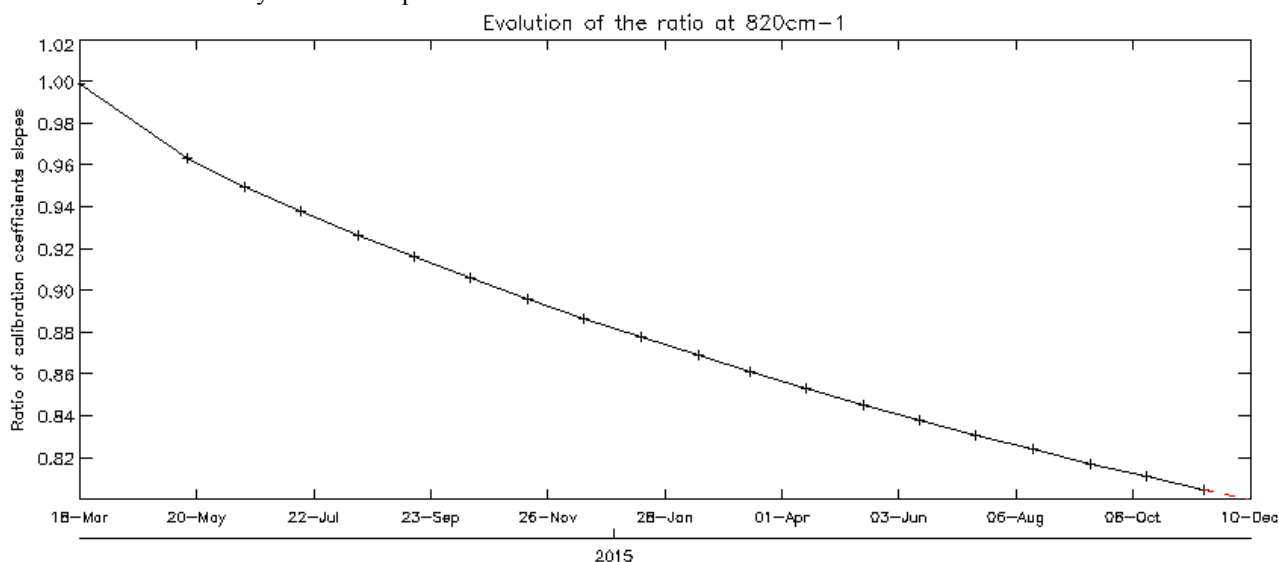


Figure 28 : Temporal evolution of calibration ratio coefficient slopes since the last decontamination. The curve was fitted with a decreasing exponential function to determine a rough date for the next decontamination (relative gain evolution of 0.8)

4.5.5 Interferometric Contrast

The interferometric contrast is defined as the interferogram fringe discrimination power. Figure 29 shows temporal evolution of instrument contrast since the beginning of IASI life in orbit for all pixels and all CCD.

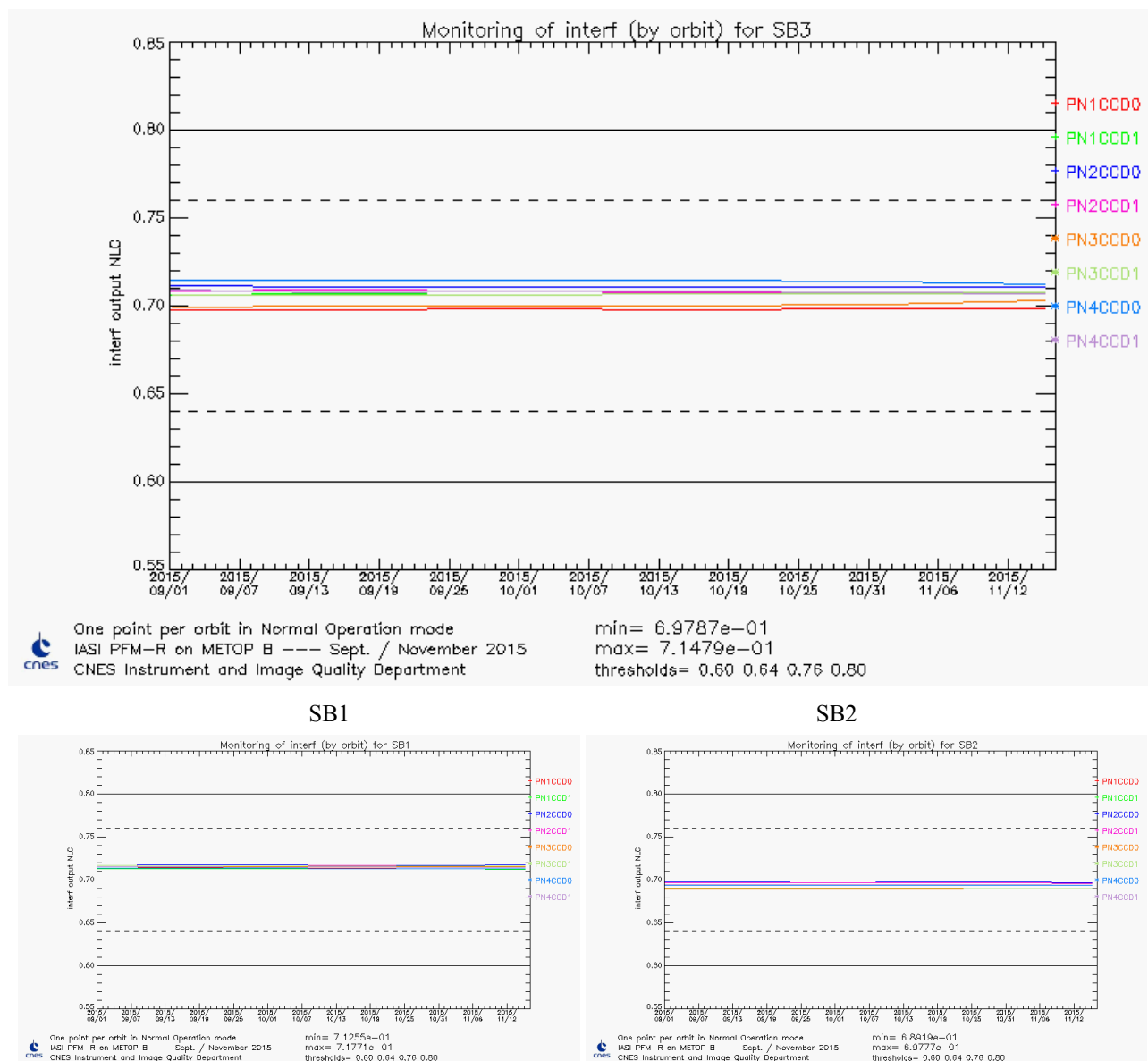


Figure 29 : Monitoring of contrast for SB3

4.5.6 Interferogram Baseline

The interferogram baseline is the mean value of the interferogram. Figure 30 shows temporal evolution of the baseline of the raw interferograms on calibration targets (BB and CS). The values are raw values, they are not physical, but the evolution is interesting: as the values are proportional to the energy received from a target and calibration targets are stable, the evolution can show the decrease of instrument transmission or events due to energetic particles.

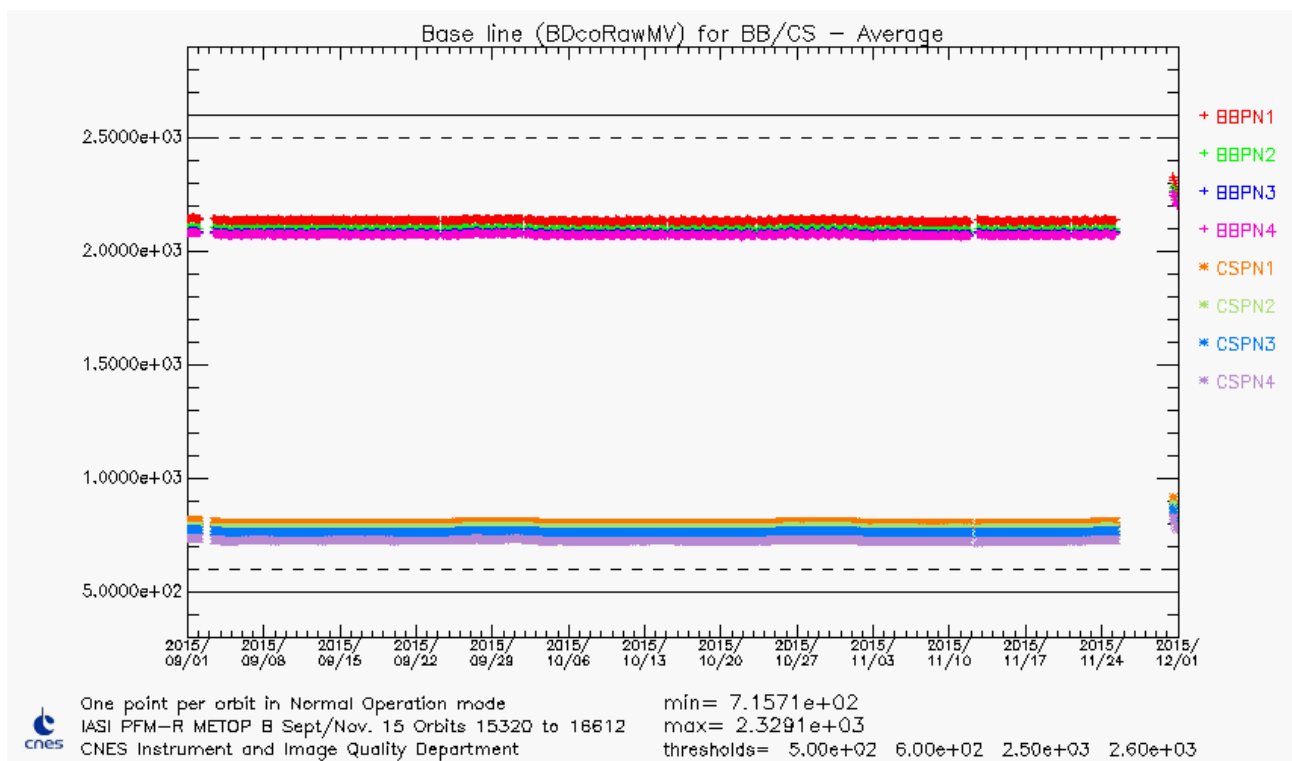




Figure 30 : Monitoring of interferogram baseline

The baseline of the interferograms after the decontamination in November has increased because the instrument transmission has increased (without the ice contamination), so more energy arrives on the detector.

		Doc n°: IA-RP-2000-4252-CNE Issue: 1.0 Date: 2017-09-27 Sheet: 43 Of: 67
--	--	---

4.5.7 Detection Chain

Detection chains are tuned in gain and offset via telecommand. The goal is to avoid saturation while conserving the maximum dynamic to limit digitalization noise.

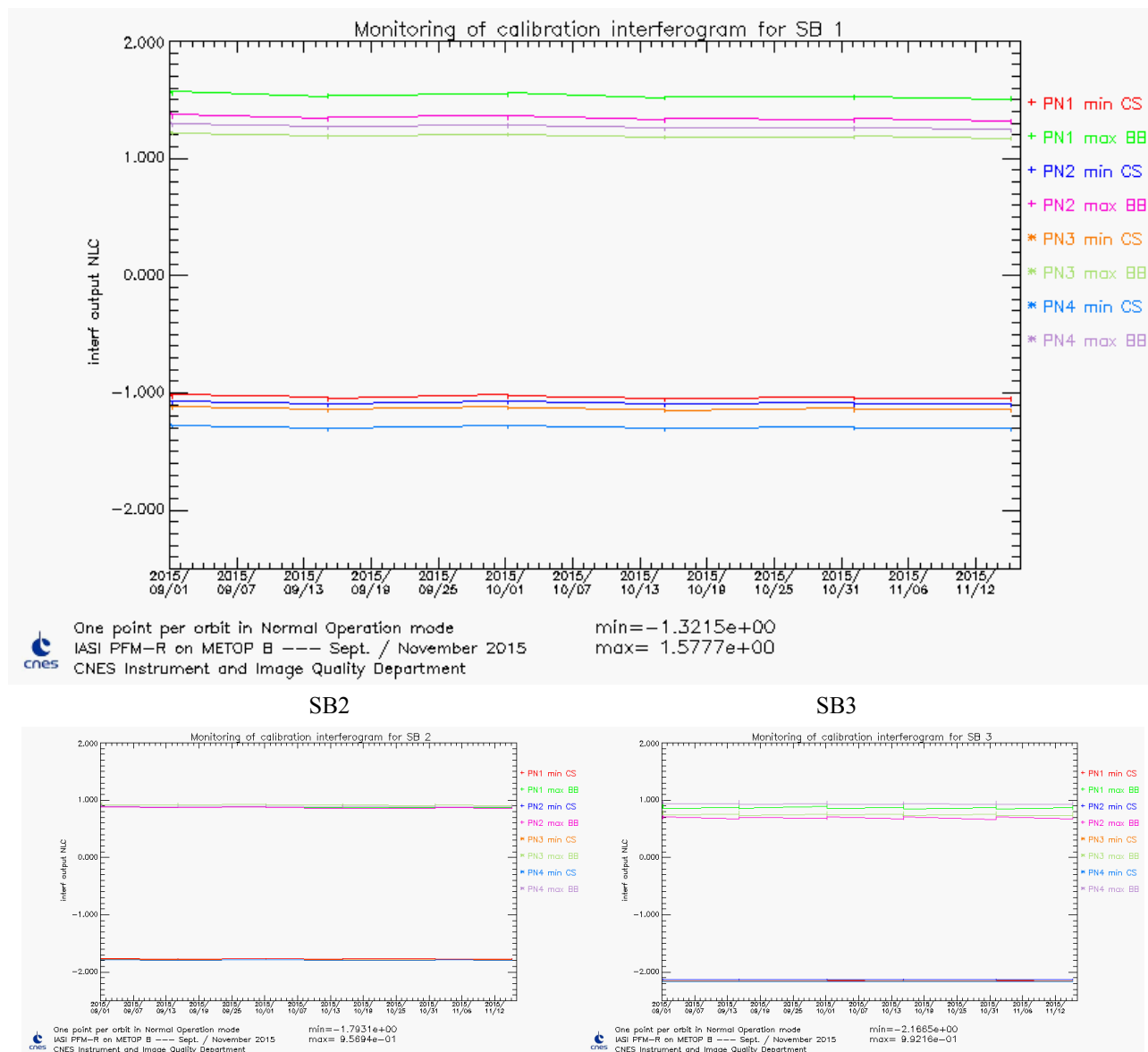




Figure 31 : Monitoring of detection chain margins

Margins are sufficient for the moment. The slight decreasing slope in SB1 (BB) for all pixels is linked to the instrument transmission evolution already mentioned in §4.5.4.1.

4.5.8 Conclusion

The radiometric performances of IASI are nominal and stable. A decontamination just occurred end of November so the next one is not expected before 2017. Scan mirror reflectivity was updated in February 2015. The next update is scheduled mid 2016.

		Doc n°: IA-RP-2000-4252-CNE Issue: 1.0 Date: 2017-09-27 Sheet: 44 Of: 67
--	--	---

4.6 SOUNDER SPECTRAL PERFORMANCES

The goal of the spectral calibration is to provide the best estimates of spectral position of the 8461 IASI channels.

The large sensitivity of infrared spectrum to spectral calibration errors has led to stringent specifications:

- A prior knowledge of spectral position better than of $2 \cdot 10^{-4}$ (design)
- A posterior maximum spectral calibration relative error of $2 \cdot 10^{-6}$ (after calibration by OPS)

In order to reach the specification of $2 \cdot 10^{-6}$, we need an accurate Instrument Spectral Response Function (ISRF) model. This model have been done and validated in the early time of IASI development.

For sake of operational time constrain, complete ISRF calculation is not done in real-time by OPS software but pre-calculated and stored in a database called “spectral database”. OPS processing determine on-line the most relevant instrument function to be used by OPS with respect to current values of a set of parameters (interferometric axis, cube corner offset...).

The approach to monitor IASI spectral performances is very similar to the one used for radiometric calibration. Spectral calibration fine characterization has been done during ground testing and Cal/Val. All parameters likely to cause a failure in spectral calibration process have been identified and are continuously monitored. As long as they remain stable, there is no problem with IASI spectral calibration.

In addition, a spectral calibration assessment is done over homogeneous scenes when IASI is in external calibration, nadir view.

4.6.1 Monitoring of the ISRF inputs

4.6.1.1 Position of the interferometric axis

The interferometric axis is the cube corner displacement direction. Its value has changed several times during CalVal due to the various configurations used. Since the end of CalVal, its value is now stable around ($Y = 1060 \mu\text{rad}$; $Z = 1210 \mu\text{rad}$). The central position used in the “spectral database” generation, are $1000 \mu\text{rad}$ and $1200 \mu\text{rad}$, respectively for Y and Z axis.

Since the drift of the interferometer axis is lower than $300 \mu\text{rad}$, there is no need to update the “spectral database”.

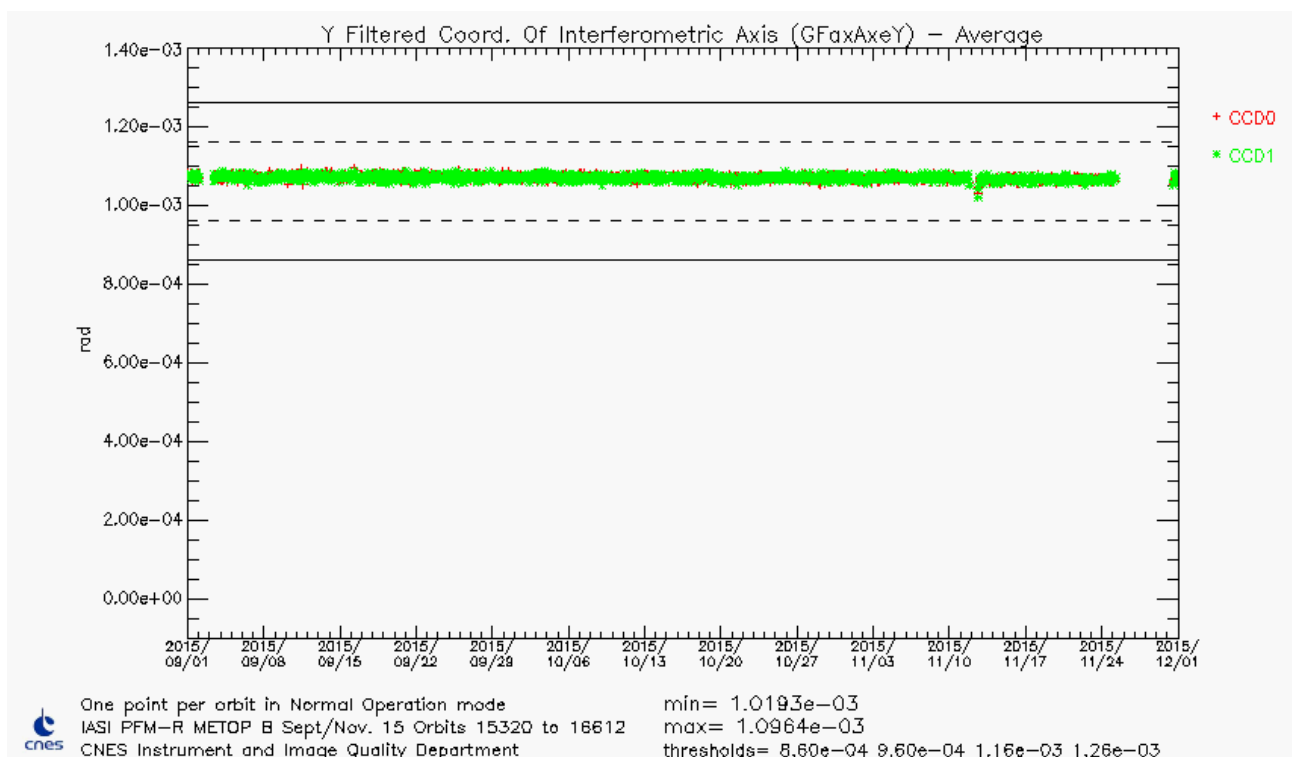
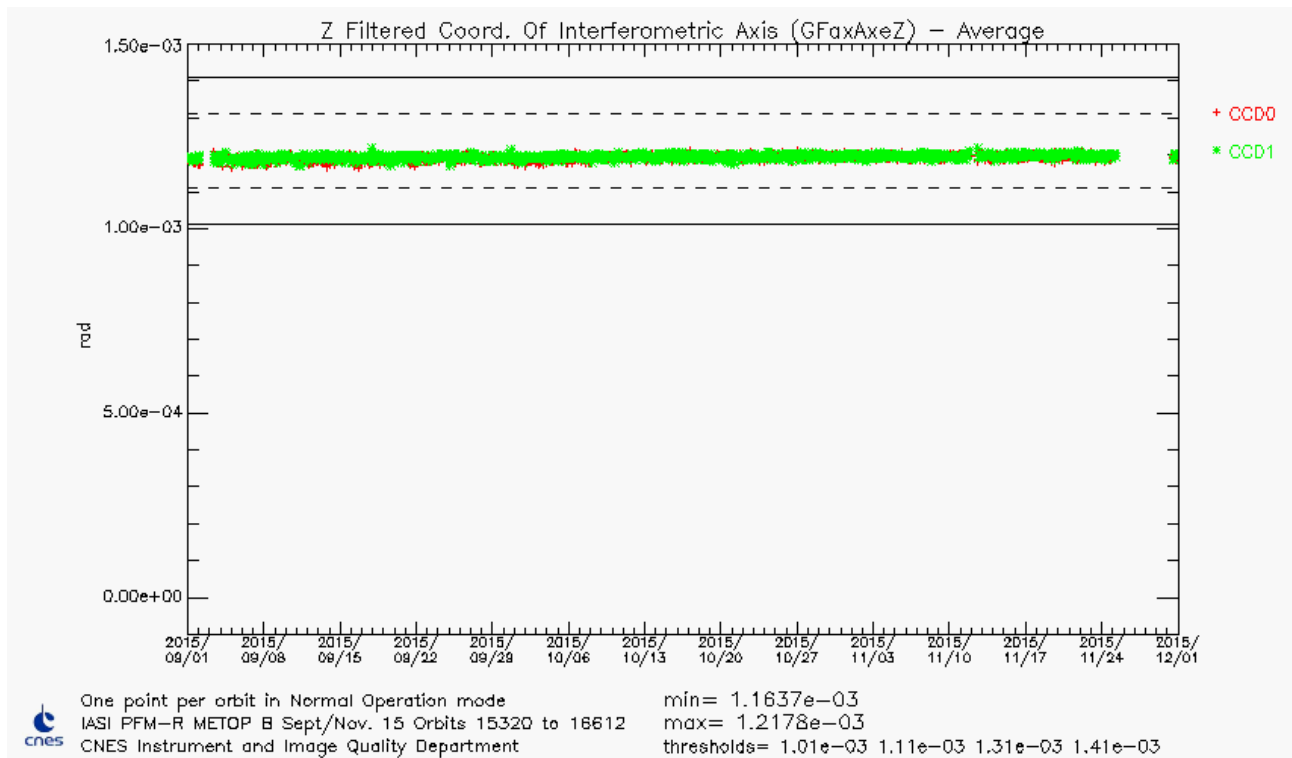
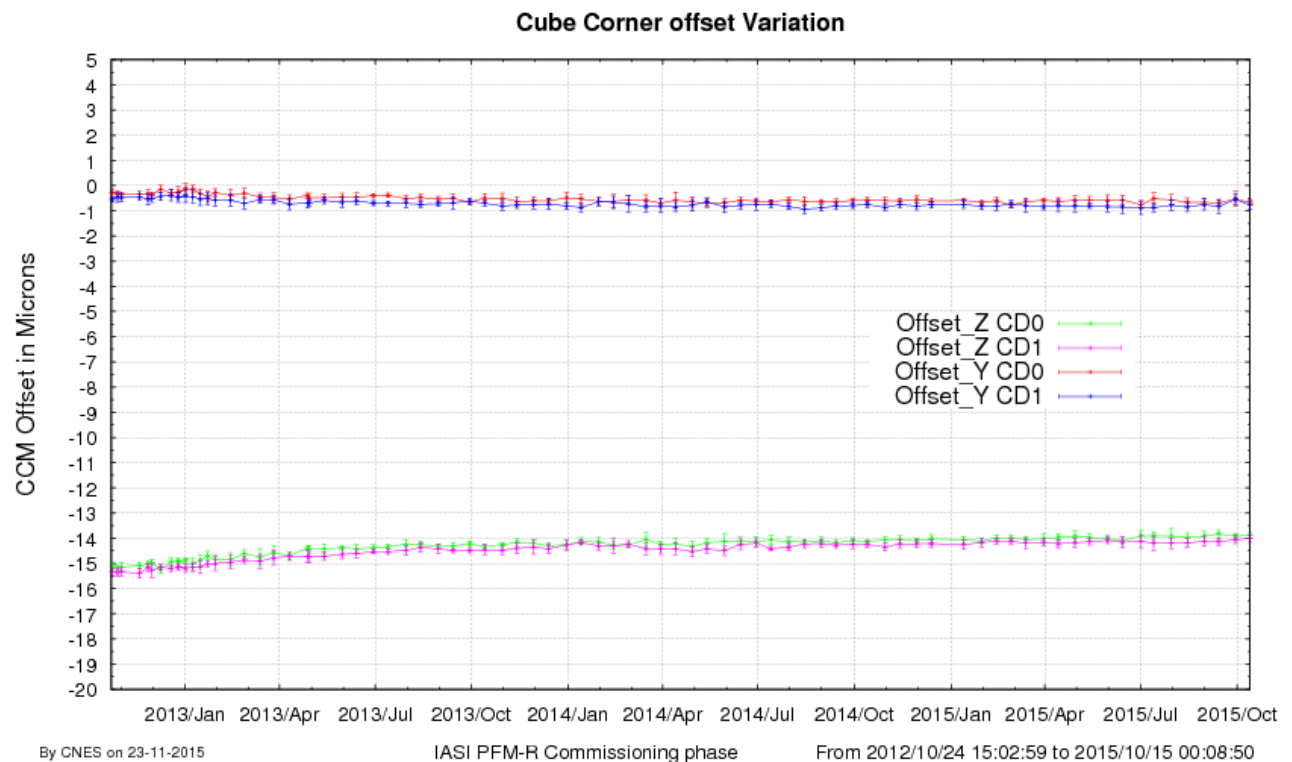




Figure 32 : GFaxAxeY average (Y filtered coordinates of sounder interferometric axis)



4.6.1.2 Cube Corner constant offset



		Doc n°: IA-RP-2000-4252-CNE Issue: 1.0 Date: 2017-09-27 Sheet: 46 Of: 67
---	---	---

Reference cube corner offsets, used in the spectral database of the period (ODB 12), are $-0.48\text{ }\mu\text{m}$, $-0.61\text{ }\mu\text{m}$, $-14.54\text{ }\mu\text{m}$ and $-14.64\text{ }\mu\text{m}$, respectively for Y CD0, Y CD1, Z CD0 and Z CD1. Since the drift of cube corner offset is lower than $4\text{ }\mu\text{m}$, there is no need to update the spectral database.

4.6.1.3 Cube corner velocity

Refer to REVEX, paragraph 5.5.

4.6.1.4 Interferometer optical bench temperature

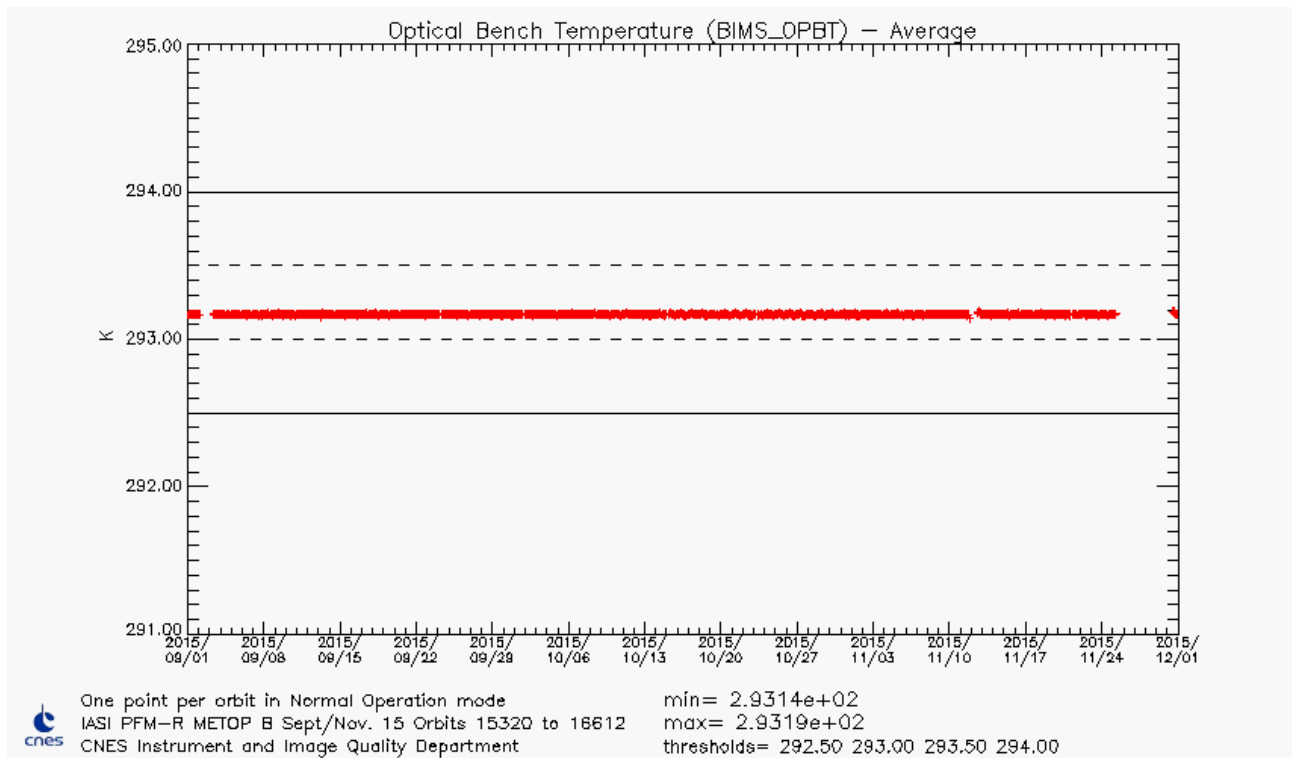


Figure 35 : Optical bench Temperature

4.6.2 Spectral calibration assessment

This assessment is performed during routine External Calibration on Earth views at nadir (SP 15).

4.6.2.1 Absolute spectral calibration assessment

IASI L1C spectra are compared with simulated spectra over homogeneous scenes, warm and clear.

The spectra are simulated with 4AOP radiative transfer model with collocated input profiles: temperature and water vapor profiles are extracted from meteorological analysis from ECMWF, the others gazes like CO_2 , O_3 , CO , N_2O and CH_4 profiles are extracted from a climatological data base.

The IASI spectra are selected using the pseudo channel Variance of the IIS radiance. The variance must be lower than 0.65 Kelvin, that is very close to the IIS noise level. This criterion insures a quasi-perfect homogeneity of the scenes (but not necessarily clear). The minimum of the pseudo channel IIS brightness temperature is 286K, which insures to have a hot scene, rejecting the areas where there is a lack of dynamic in the atmospheric spectral lines and rejecting the majority of cloudy scenes (which are not simulated). Then only contiguous selected scenes are kept (20 lines maximum, 1000 km).

The 4AOP spectra are simulated using the coordinates of the center of each sequence.

The comparison is done by using the correlation method in spectral windows (using the derivative of the spectrum). The position of the maximum of the correlation coefficient gives us the spectral shift. The result is expressed in terms of relative spectral shift error between L1C simulated and measured spectra for each pixel.

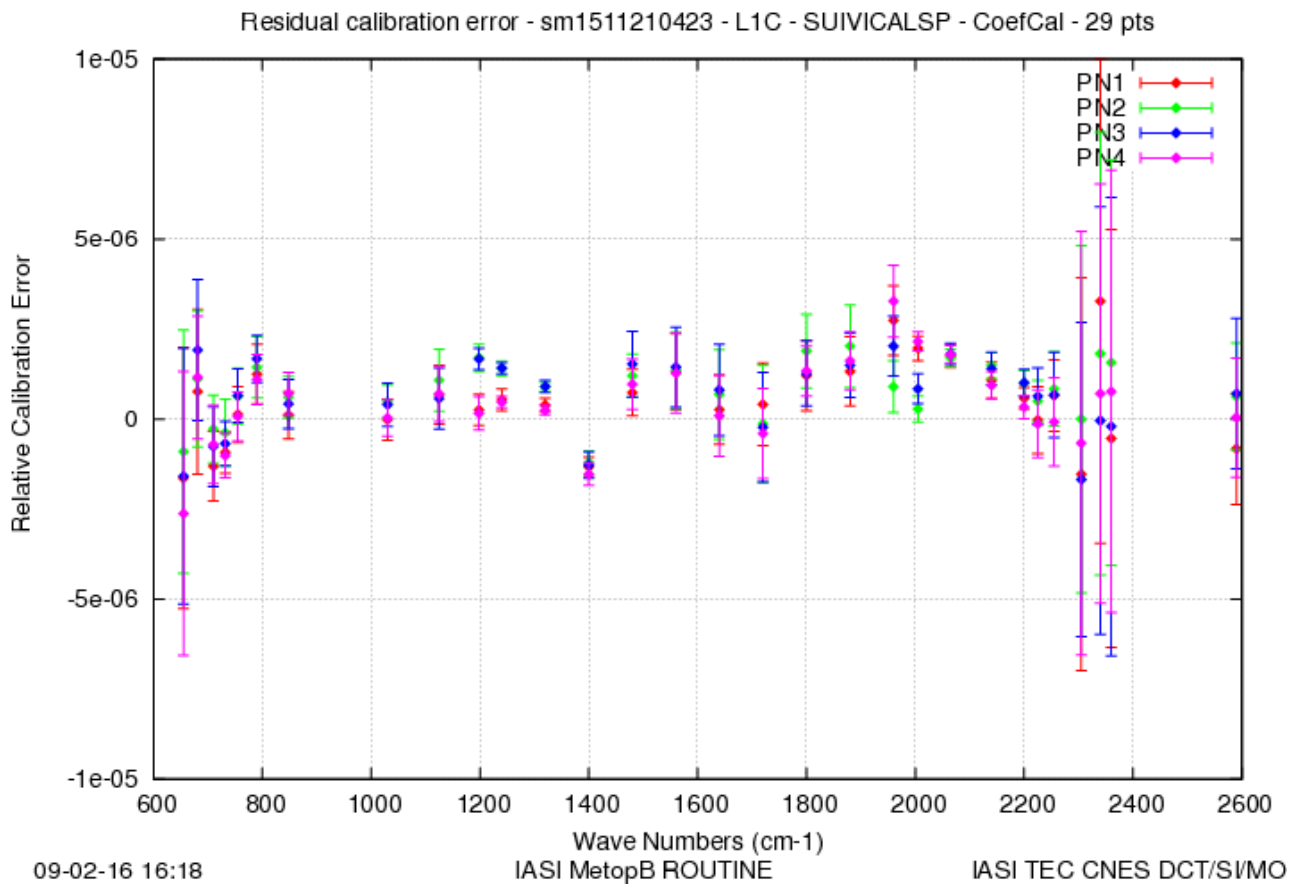


Figure 36 : Spectral shift error between L1C IASI and simulated L1C with A4/OP + ECMWF

The absolute spectral calibration assessment by comparison with a model is fully satisfactory on spectral bands that permits this exercise, the specification of 2.10^{-6} is reached.

We can note that the spectral shift in the inter-band is not good because of a sharp gradient of the spectral filters (transmission function) at the edge of spectral bands. So, the energy in a line is not the same in every channel included in the line, the barycenter of the line changes, that induces a spectral shift. For B1/B2, the inter-band limit is around 1169 cm^{-1} , and for B2/B3 it is around 1953 cm^{-1} .

The model has its limits : it is not true everywhere in the spectrum, because the geophysical conditions are not well known. For example, in B2 a bad knowledge of the water vapor content leads to a bad simulation and thus to a spectral shift in B2 only due to the variability of the water vapor. There are still improvements to make on spectroscopy and the radiative transfer models.

4.6.2.2 Interpixel spectral calibration assessment

Over the same homogeneous scenes used for absolute spectral calibration assessment, IASI L1C spectra of each pixel are compared with the average spectra of all pixels. The result is expressed in terms of interpixel relative spectral shift error.

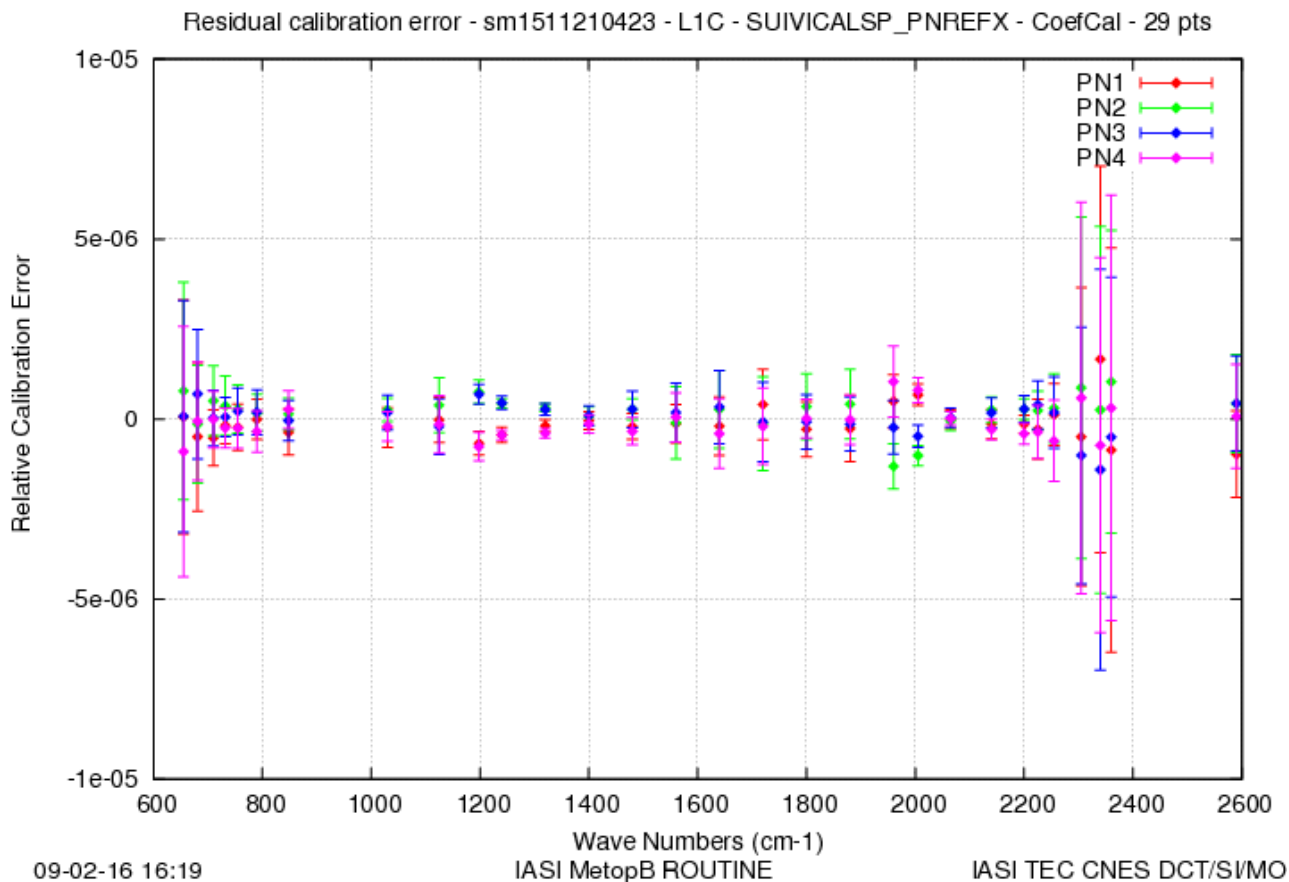


Figure 37 : Inter pixel spectral shift error for L1C IASI

The interpixel spectral calibration is better than 0.2ppm.

The results in the interband region are higher for the same reasons exposed in paragraph 4.6.2.1 . The error bars are high in B3 because of the noise that is higher at the end of B3.

In conclusion, the IASI pixels are spectrally independent.

4.6.3 Ghost evolution monitoring

On-ground test of the instrument has shown a perturbation in the ISRF mainly caused by micro-vibrations of the interferometer separator blade induced by the compensation device.

Ghost origin is understood to be due to micro-vibrations of the beam-splitter. It is therefore stronger for the FOVs which project onto the top part of the beam-splitter (which vibrates more), and weaker for the FOVs which project onto the bottom part of the beam-splitter as it is attached to the optical bench.

The micro-vibrations of the beam-splitter lead to a sampling jitter of the interferogram. The perturbed interferogram $I(t)$ is expressed as:

$$I(t) = \frac{I_0}{2} \cdot \cos(2 \cdot \pi \cdot \nu_0 (x_{nom} + \delta x(t)))$$

with $\delta x(t) = U_0 \cdot \cos(2 \cdot \pi \cdot f \cdot t + \psi)$ the part added by the ghost

The phase ψ is random, the frequency is $f = 380\text{Hz}$, and the amplitude is difficult to quantify in flight.

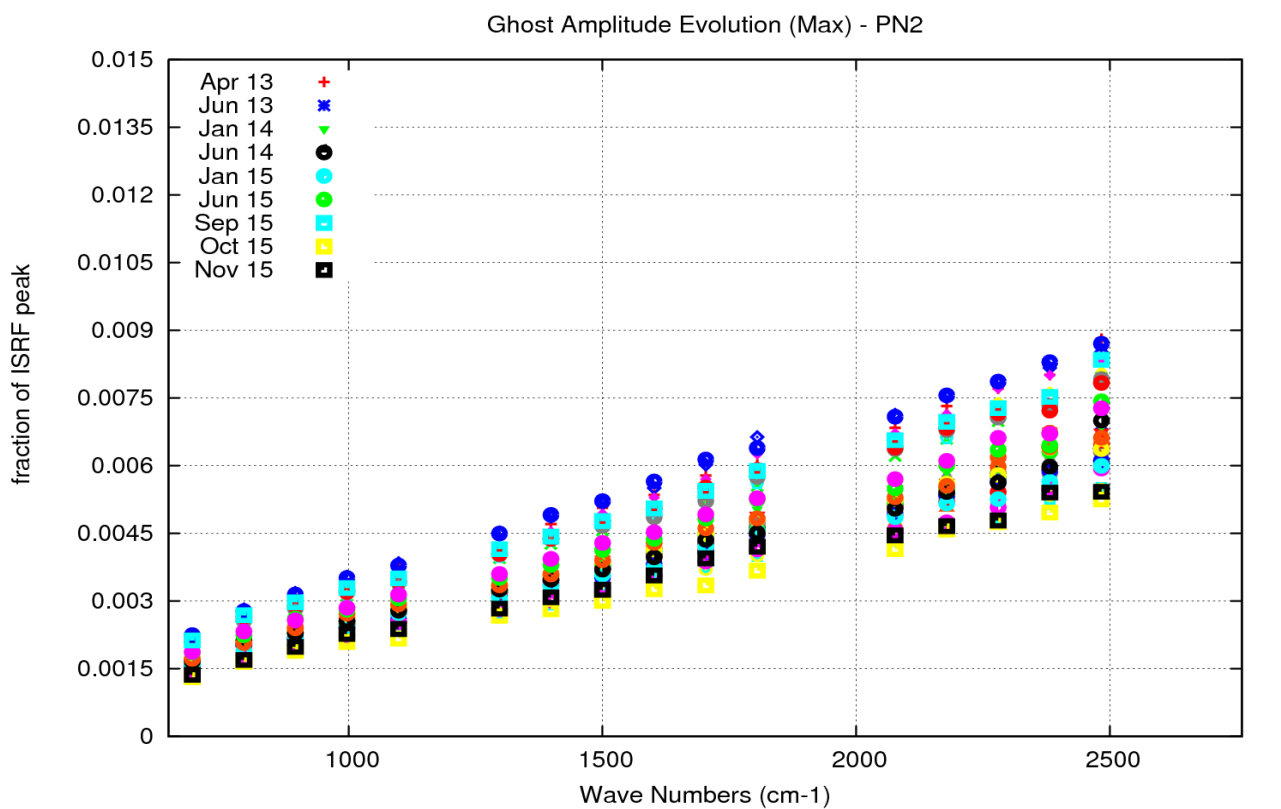
The ghost affects the ISRF by replicating it at about $\pm 14\text{cm}^{-1}$. The amplitude of these replications is very low with respect to ISRF maximum value. The amplitude and the central wave number of ISRF replications are function of: cube corner velocity, frequency and mechanical amplitude of the beam-splitter vibration and wave number.

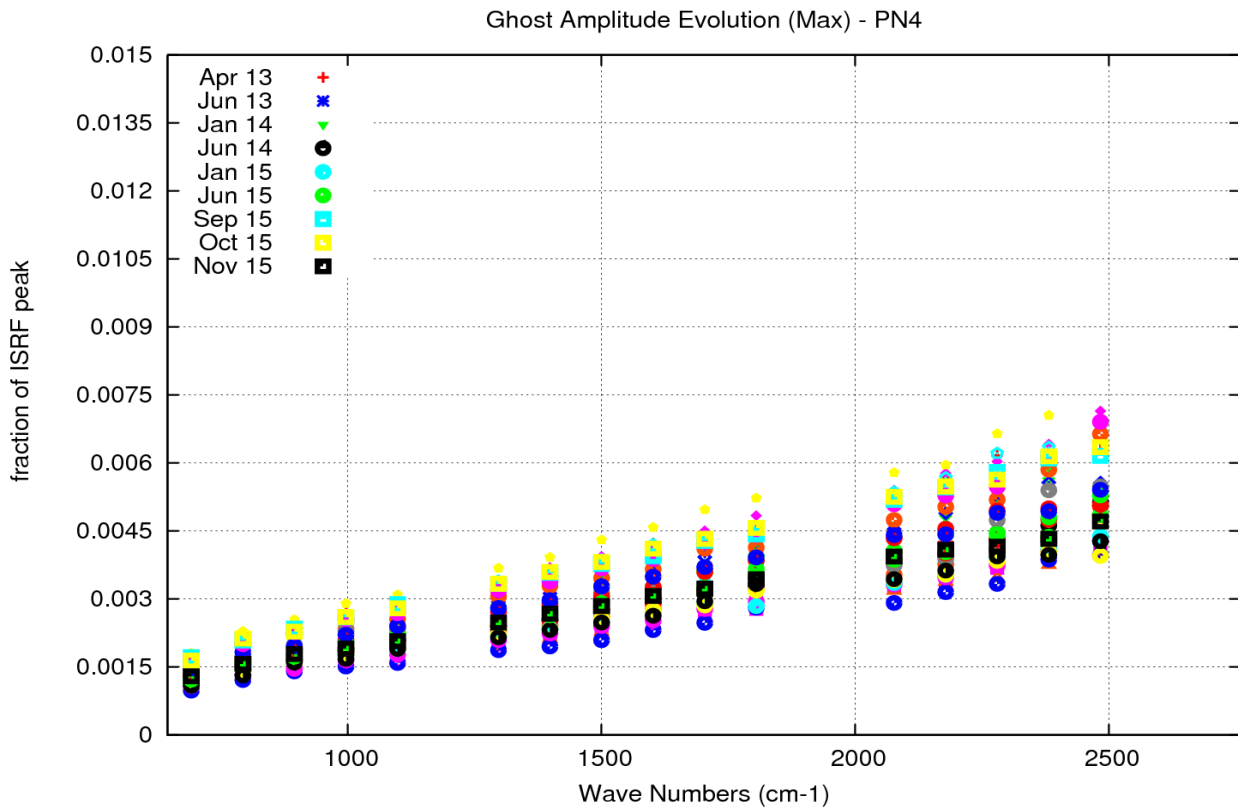
The ghost is monitored at TEC using monthly external calibration (BB views), by computing the ratio between the maximum of the residuals of the imaginary part of the spectrum after on board calibration and the Planck function at the black body temperature:

$$fractionISRF_{peak} = \frac{\max(BArcImagMean)}{Planck(T_{BB})}$$

This ratio understood to be proportional to the ratio between the replicated ISRF due to the ghost with respect to $ISRF_{max}$.

The evolution over time of ghost amplitude with respect to $ISRF_{max}$ amplitude is shown below for the 4 IASI pixels.





09-02-16 18:03 IASI PFM-R ROUTINE

CNES DCT/SI/MO

Figure 38 : Ghost amplitude as a function of wave number for different time (Top: pixel 2, bottom: pixel 4)

Maximum values of fraction of $ISRF_{max}$ (@2760 cm^{-1}) are proportional to wavenumber; they are similar for the couples pixel 1-2 and pixel 3-4, due to the position of the beam splitter wrt the FOV.

The ghost has an effect on the radiometric calibration and leads to an imaginary residual because the phase at Zpd of the micro-vibration is random and changes each time the mobile cube corner changes its direction. So the phase added by the ghost is not the same on the black body view and on the cold space view of the line LN, and on the black body view of the line LN+1.

As the ghost is not the only effect included in this variable (for example, there is also the noise), we have to be careful in the interpretation of these plots: it is not the exact amplitude of the ghost.



The compensation device (CD) was permanently stopped on the 7th October 2015. Since this date, there is no more ghost in the data. The imaginary residuals in the plots above have decreased since this date. These residuals are not null because, as mentioned above, the ghost is not the only effect included in this variable. Other indicators of the ghost effect, such as the correlation matrix, have shown that the ghost has disappeared.

4.6.4 Conclusion

All parameters impacting IASI spectral calibration are stable and within specifications.

The ghost effect has disappeared since the compensation device (CD) permanent stop that was performed on the 7th October 2015.

IASI has a fully satisfactory spectral calibration. The L1B processing, consisting in the spectral shift correction, and the L1C processing, consisting in the ISRF removal, are working very well.

		Doc n°: IA-RP-2000-4252-CNE Issue: 1.0 Date: 2017-09-27 Sheet: 51 Of: 67
---	---	---

4.7 GEOMETRIC PERFORMANCES

The geometric calibration is performed on ground (level 1 processing). Most of the analyses of geometric performances require being in external calibration mode.

Specifications are the following: the IIS/AVHRR co-registration has to be better than 0.3AVHRR pixel while the IIS/sounder co-registration has to be better than 0.8mrad.

4.7.1 Sounder / IIS co-registration monitoring

This monitoring is performed one time a year, generally around September for REVEX and march for mid-REVEX.

The sonder/IIS coregistration error is lower than 100 μ rad (eq. 100m on ground).

4.7.2 IIS / AVHRR co-registration

The IIS/AVHRR co-registration is permanently estimated by the L1 processing chain.

Note that AVHRR channels 4 and 5 are within the IIS spectral filter. The spatial resolution of the IIS (0,7km) is close to AVHRR (1km).

The IIS/AVHRR offset guess in the ground segment configuration is used when the algorithm of correlation between IIS and AVHRR does not converge (typically over homogeneous scenes).

The following figures show a comparison of IIS-AVHRR offsets (GiacOffsetIISAvhrr) mean profiles.

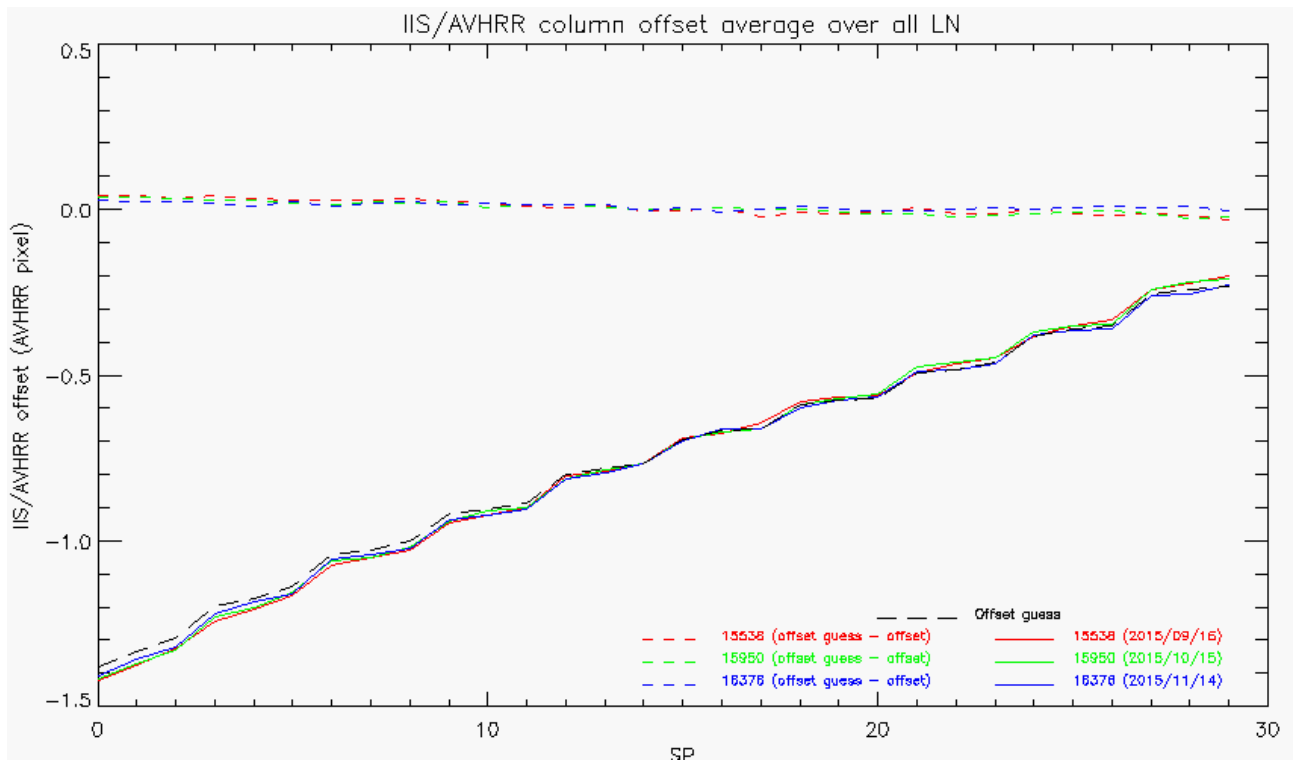


Figure 39 : Column offset (black) guess vs. column offset averaged over all lines (LN) as a function of the scan position (SP=SN), and orbit number

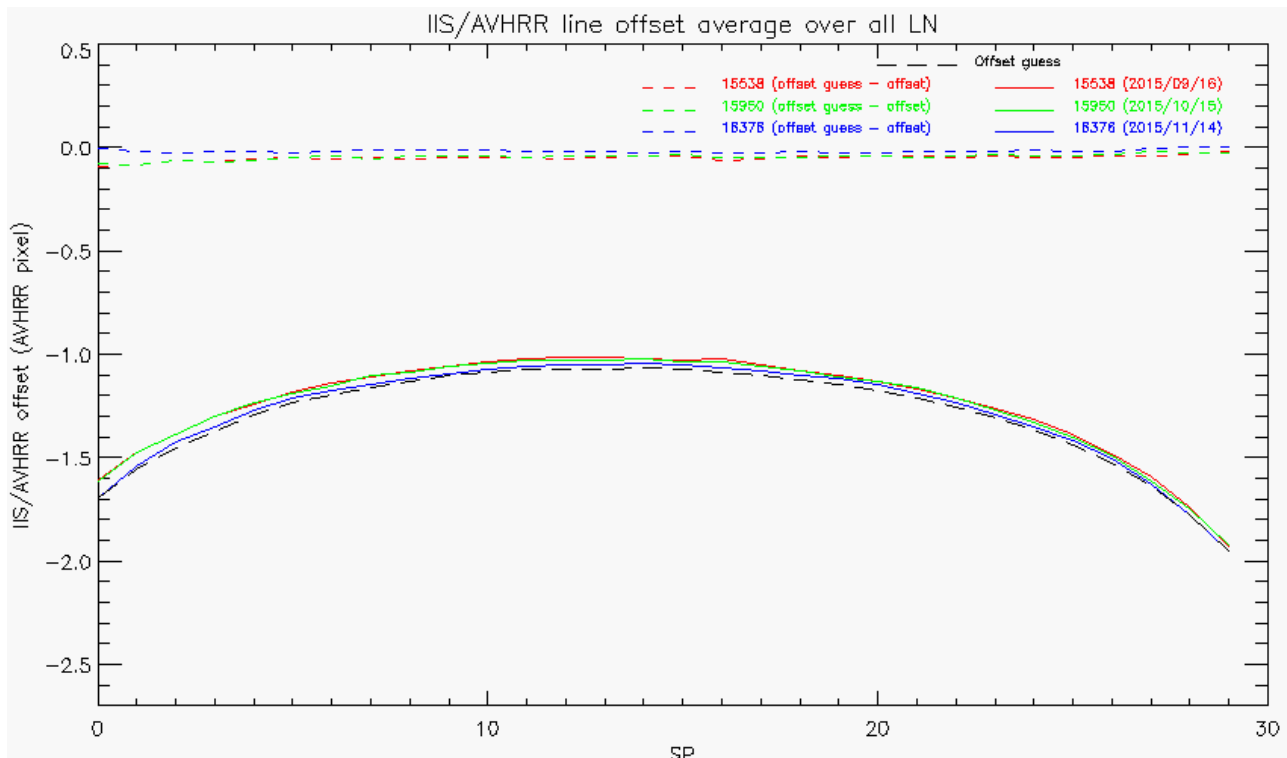


Figure 40 : Line offset guess (black) vs. line offset averaged over all lines (LN) as a function of the scan position (SP=SN), and the orbit number

For both across track and along track, the residuals between measured and IIS/AVHRR offset guess in the ground segment configuration are lower than 0.1 AVHRR pixel for all viewing angles, that is equivalent to 100m on ground.

The values are stable.

4.7.3 Conclusion

The positions of IASI pixel are considered stable and well within specification.

IIS-sounder co-registration is stable at about 100 μ rad which is equivalent to 100m on ground (specification : < 0.8 mrad).



IIS-AVHRR offset is lower than two pixels and stable over time: less than 0.1 AVHRR pixels over three months (specification: < 0.3 AVHRR pixel).

IASI pixel centre location accuracy in AVHRR raster is around 200m. The geolocation of IASI pixels are thus considered stable and well within specification (5 km).

4.8 IASI-B INTER-CALIBRATION WITH IASI-A, CRIS AND AIRS

The objective of the radiometric and spectral inter-calibration between IASI-B, IASI-A, CRIS and AIRS is to perform an external monitoring of the IASI performances and to ensure the consistency of the hyperspectral TIR sensors and in particular the continuity of the IASI mission. We aim here at checking the performance of the radiometric absolute calibration accuracy of 0.5K per IASI channel, and of the spectral absolute calibration accuracy of 2 ppm.

The inter-calibration is performed with the SIC software. The methodology is described in the technical note DA.2. Roughly, the methodology is based on the construction of a database in which each data is the difference IASI-B – IASI-A, IASI-B – CRIS or IASI-B - AIRS over a common observation made by both sounders. “Common” means same place, same time and same viewing conditions so that the only difference is not geophysical but due to a calibration bias. Statistics over this database emphasize the radiometric and spectral biases.

		Doc n°: IA-RP-2000-4252-CNE Issue: 1.0 Date: 2017-09-27 Sheet: 53 Of: 67
--	--	---

4.8.1 IASI-B inter-calibration with IASI-A

For IASI-B / IASI-A, the common observations are the overlapping areas between two consecutive orbits of MetOp-A and MetOp-B. They always exhibit a temporal gap of ~50 min between IASI-A and B (with the two cases “A before B” and “A after B”), and the geometries of the observations are different and generally off-nadir with opposite angles. These two drawbacks are minimized by a pre-filtering performed to only use the most stable and homogeneous scenes, using the geolocation, Cld_AVHRR and ECMWF information. Each scene is then a regional averaging of the soundings. The comparison is performed at native spectral resolution.

Figure 41 gives the mean and standard deviation of $\Delta T @ 280K$ for one year of data. We see that IASI-A and IASI-B are very well cross-calibrated, with biases lower or equal to 0.15K in absolute value. For information, we checked that the distribution of the surface temperature of the scenes in the database covers a large range (from 220K to 280K).

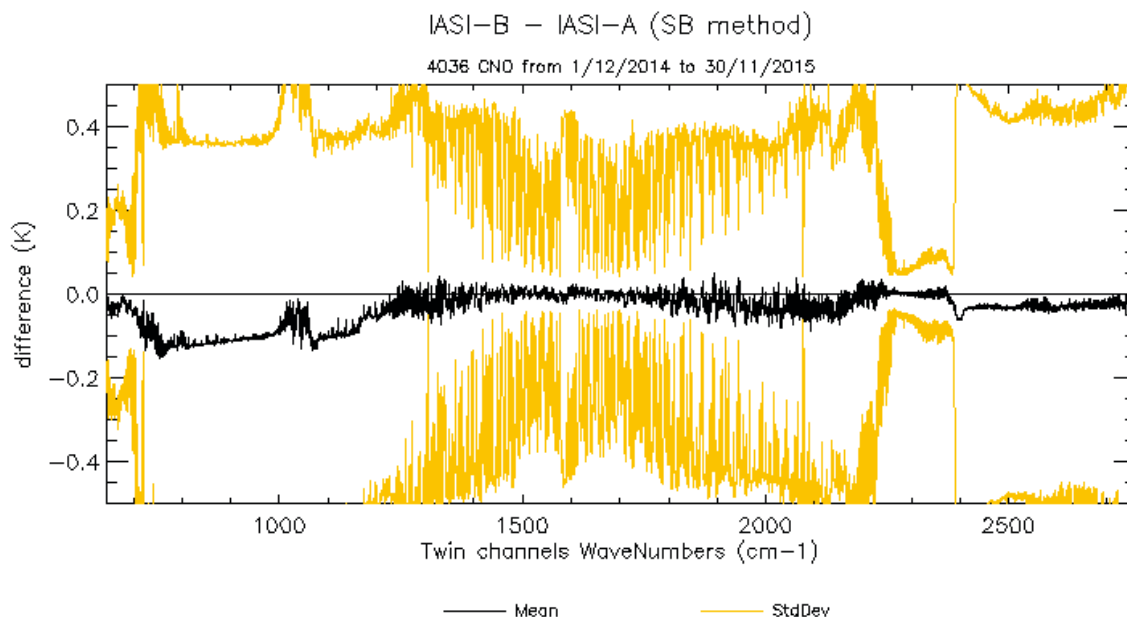
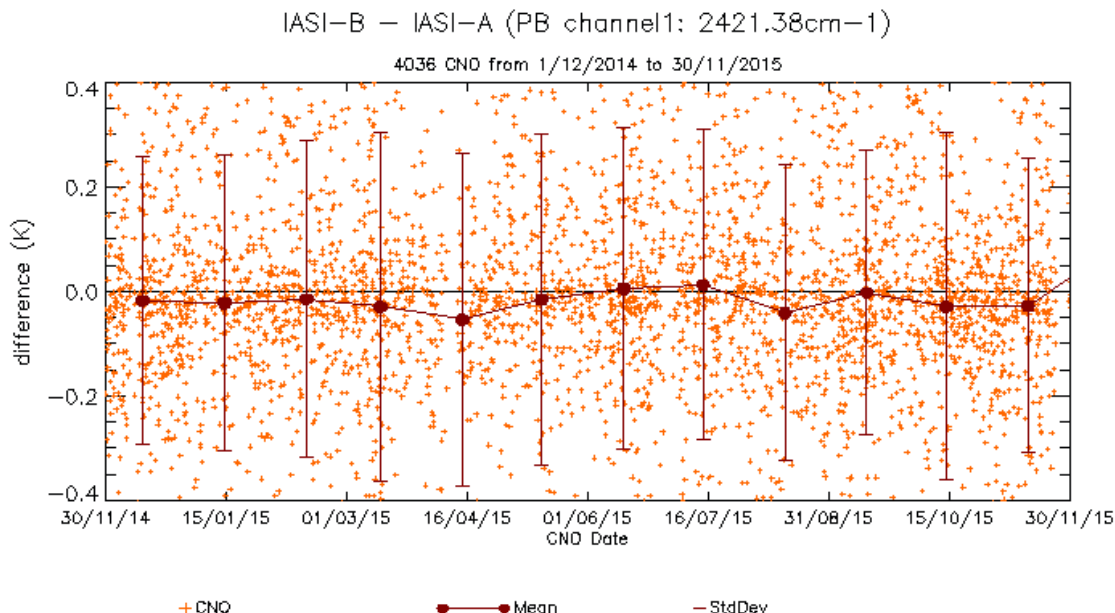


Figure 41 : Mean (black curve) and standard deviation (yellow) of the difference in brightness temperature IASI-B – IASI-A

Figure 42 shows the temporal evolution of three broad pseudo-channels, corresponding approximately to the IASI bands 1, 2 and 3 (more precisely, to their overlapping with the CRIS and AIRS coverage). We see that the difference between IASI-B and IASI-A is stable with time, with slight variations in IASI B1.



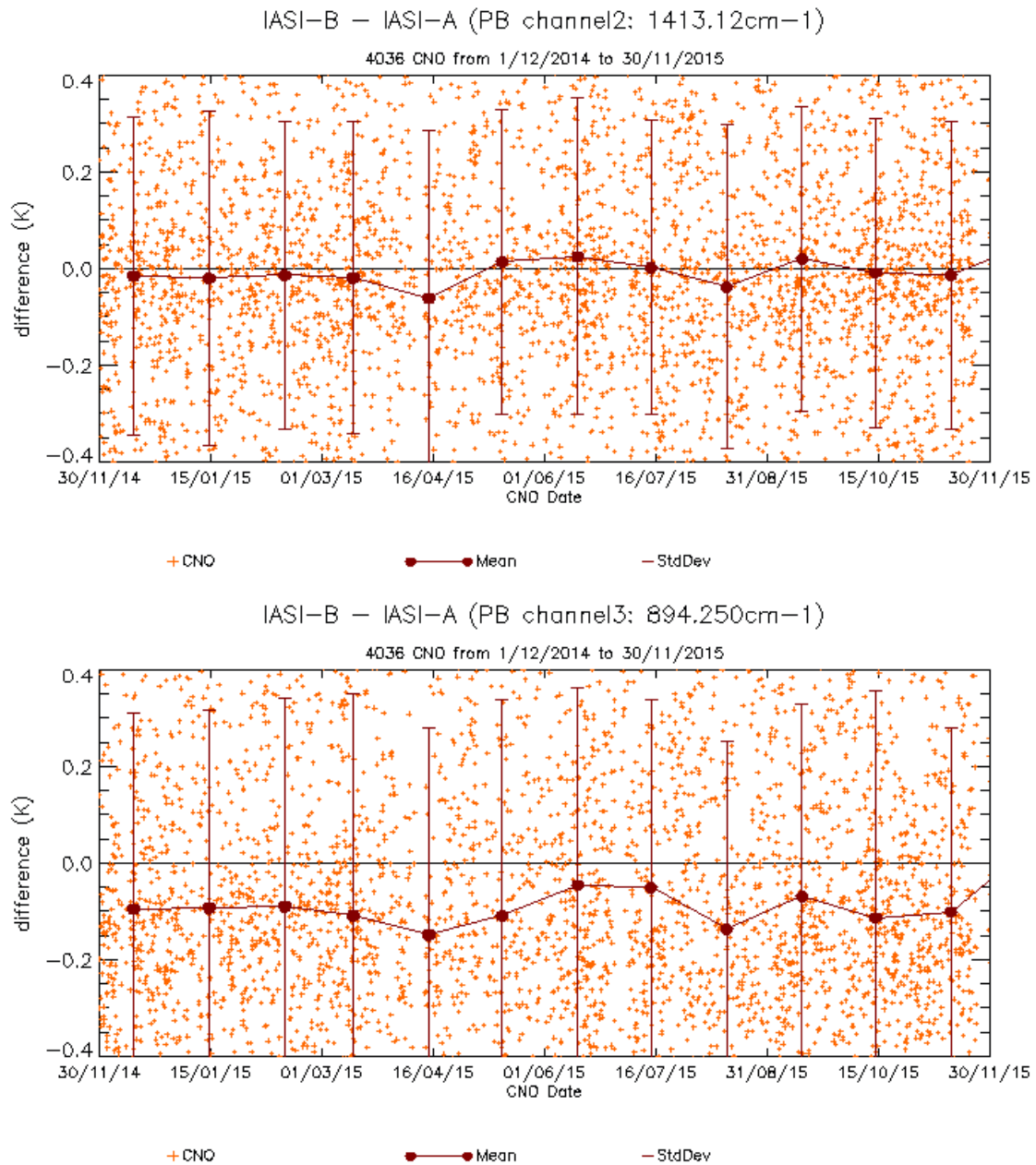


Figure 42 : Temporal evolution of differences IASI-B – IASI-A in brightness temperature spectrally integrated over the approximate three IASI bands

The spectral inter-comparison is performed on the same spectra as the radiometric inter-comparison. For each common observation, a cross-correlation of both spectra is performed in 30 small spectral windows for different spectral shifts. The maximum of correlation gives the actual spectral shifts expressed in $\Delta\nu/\nu$. Figure 43 gives the mean of $\Delta\nu/\nu$ over the complete dataset. We see that the spectral bias between IASI-B and IASI-A is lower than 1 ppm in absolute value, which is compliant with the specification of 2 ppm for most channels. The channels out of specification are due to the perturbation of the cross-correlation by noise.

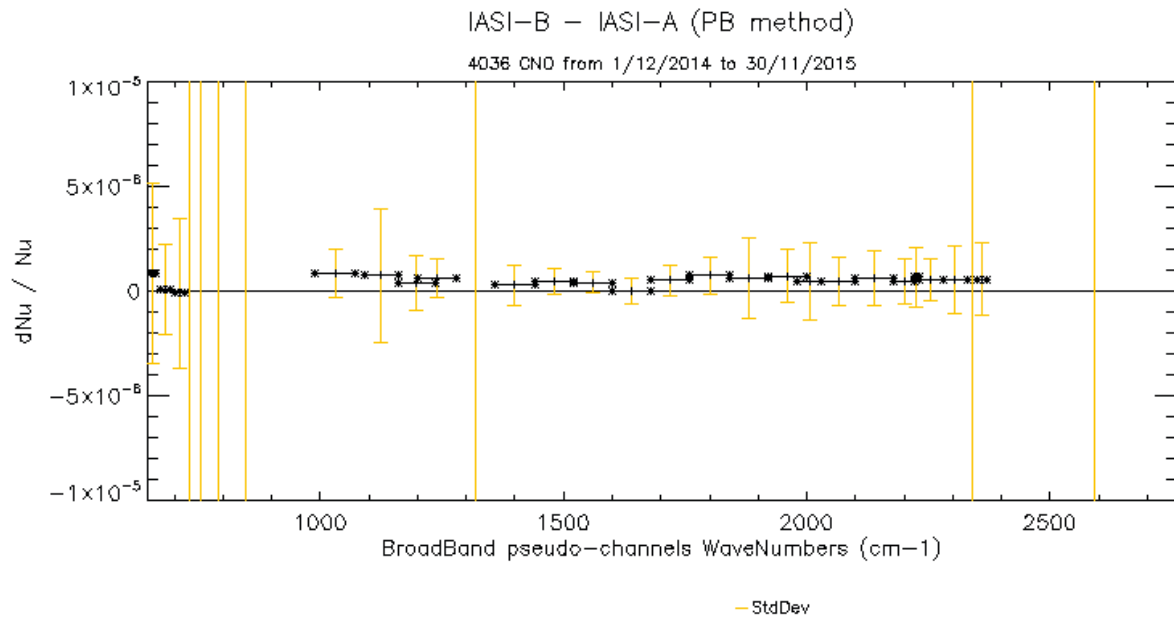


Figure 43 : Mean (black curve) and standard deviation (yellow curve) of the difference spectral calibration $\Delta\nu/\nu$ between IASI-B and A.

Figure 44 shows the temporal evolution of the difference spectral calibration $\Delta\nu/\nu$ between IASI-B and A in the spectral window centered on 2200cm-1. We see that the IASI-A/IASI-B spectral inter-calibration is very stable.

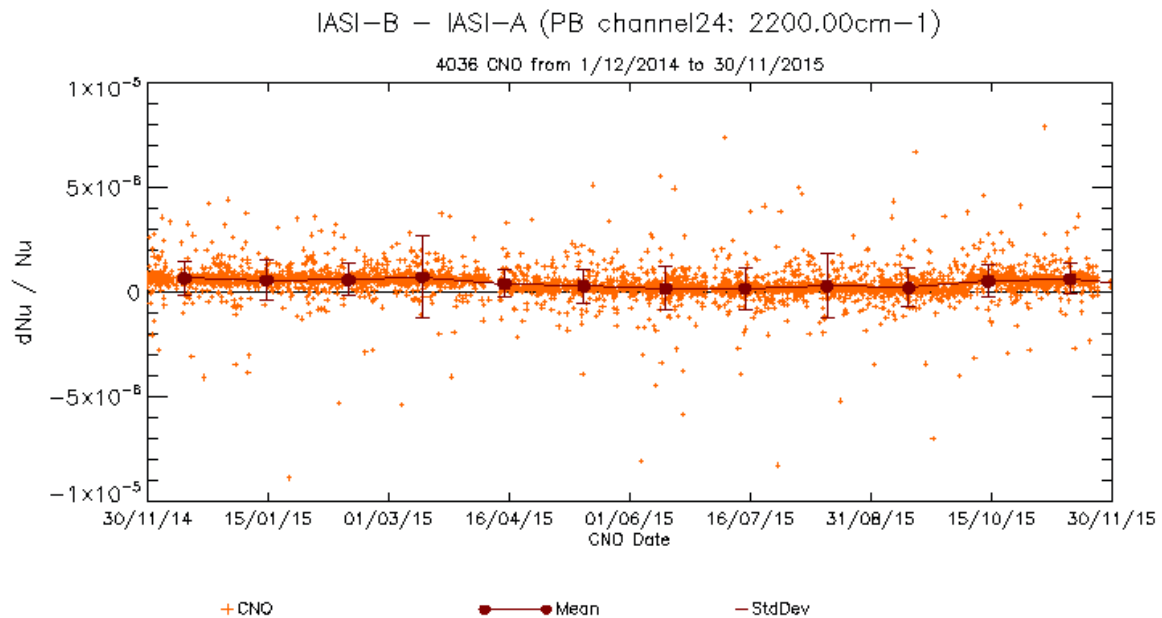


Figure 44 : Temporal evolution of the difference spectral calibration $\Delta\nu/\nu$ between IASI-B and A in the spectral window centered around 2200cm-1.

4.8.2 IASI-B inter-calibration with CRIS

For IASI-B and CRIS, the basis of the algorithm is similar to that IASI-B / IASI-A, but now the database is filled with Simultaneous Nadir Overpasses, occurring at high latitudes (because of the differences in the local time of the orbits). Each scene is a regional averaging of the soundings, with a spectral reduction in broad pseudo-bands. Because of the differences in spectral resolution, no spectral inter-calibration is performed.

Figure 45 shows the mean and standard deviation of IASI-B - CRIS for one year of data. We see that IASI-A and CRIS are very well cross-calibrated, with biases lower or equal to 0.1K in absolute value.

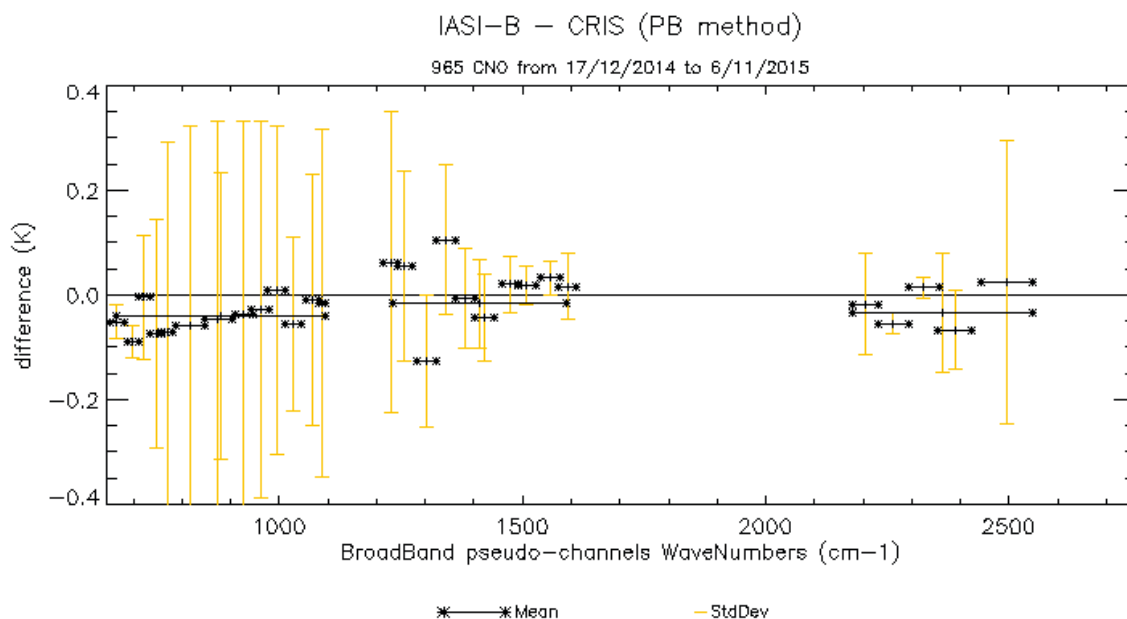
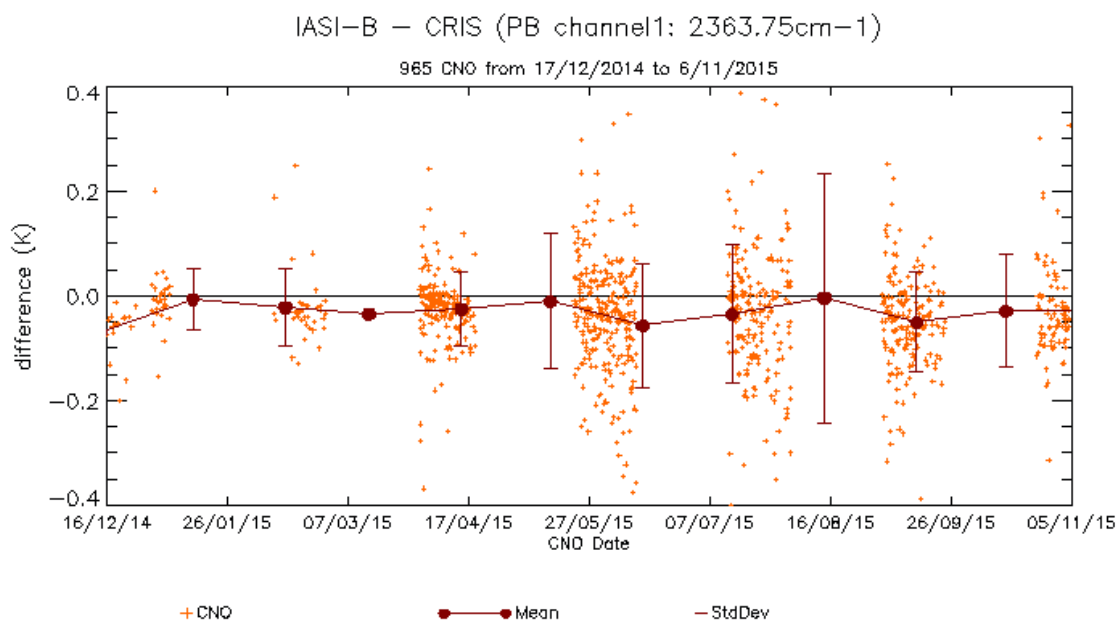


Figure 45 : Mean (black curve) and standard deviation (yellow) of the difference in brightness temperature IASI-B - CRIS

Figure 46 shows the temporal evolution of the three broadest pseudo-channels, corresponding approximately to the IASI bands 1, 2 and 3 (more precisely, to their overlapping with the CRIS coverage). We see that the difference between IASI-B and CRIS is stable with time, with slight variations in IASI B1. Note that some large temporal gaps may be encountered for IASI-B / CRIS, due to the orbital configuration and the tolerance in simultaneity, making some monthly means meaningless.



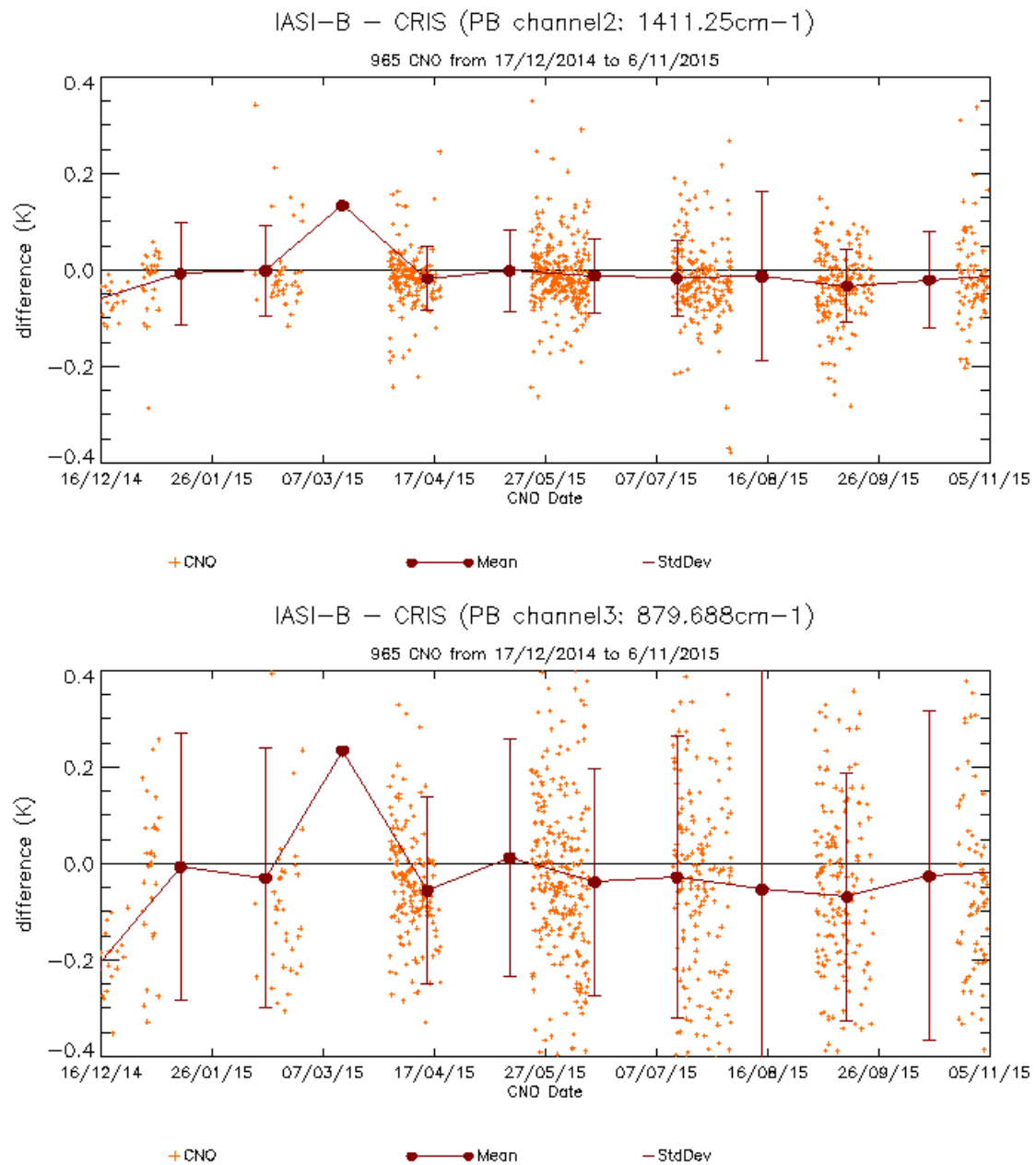




Figure 46 : Temporal evolution of the differences IASI-B – CRIS in brightness temperature over the approximate three IASI bands, with monthly means.

		Doc n°: IA-RP-2000-4252-CNE Issue: 1.0 Date: 2017-09-27 Sheet: 58 Of: 67
--	--	---

4.8.3 IASI-B inter-calibration with AIRS

For IASI-B and AIRS, the algorithm is similar to that IASI-B / CRIS (similar orbital configuration).

Figure 47 shows the mean and standard deviation of IASI-B - AIRS for one year of data. We see that IASI-B and AIRS are very well cross-calibrated, with biases lower or equal to 0.15K in absolute value (except for one pseudo-band).

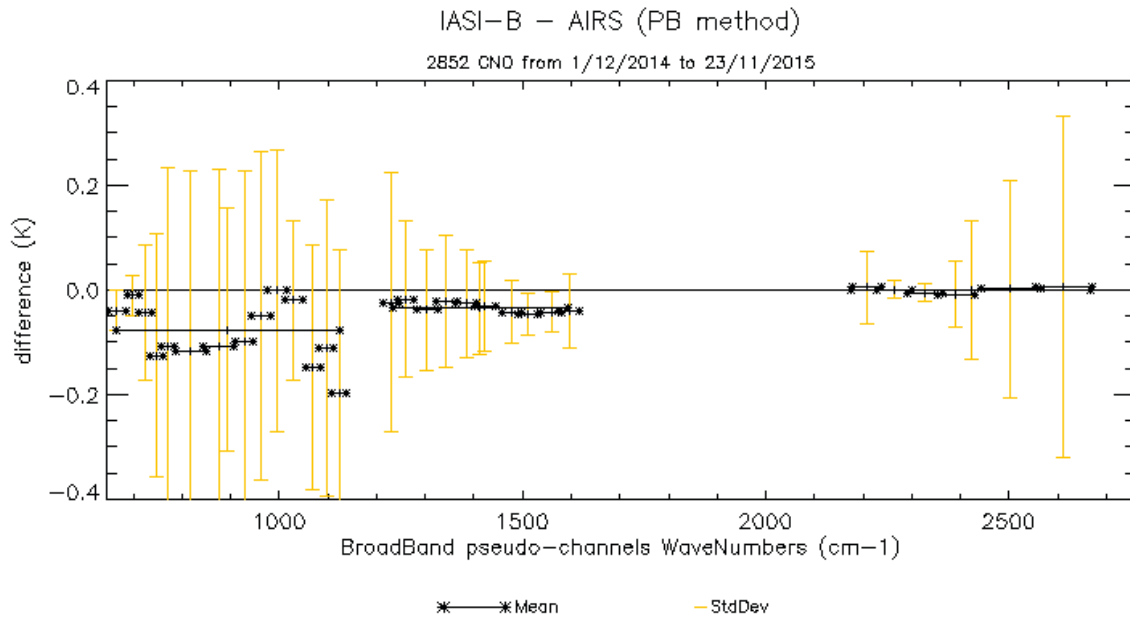
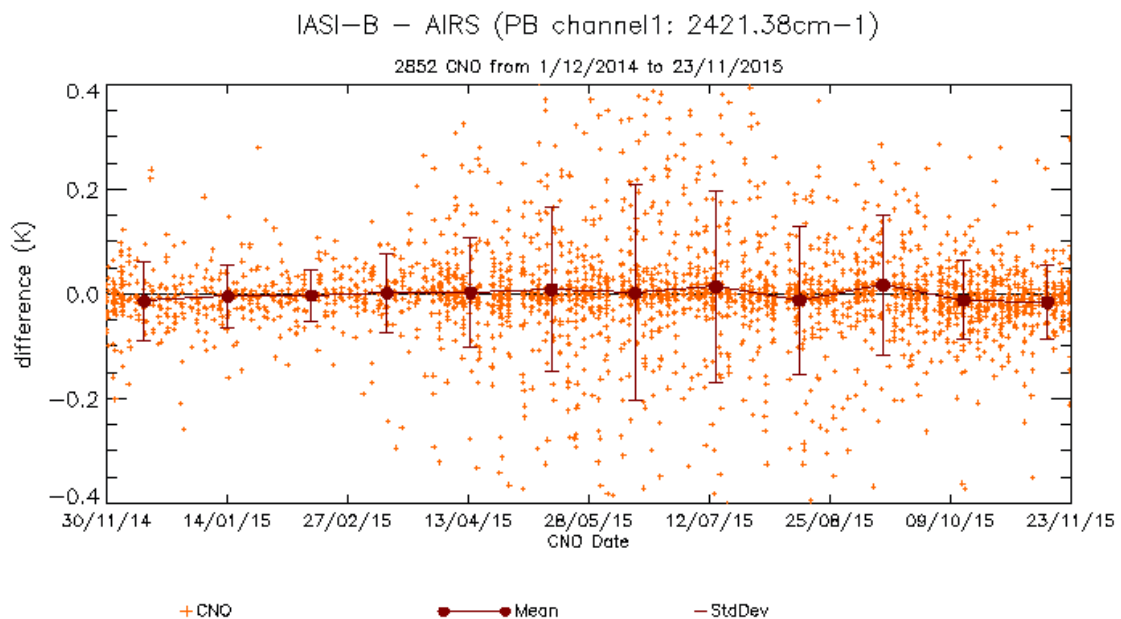


Figure 47 : Mean (black curve) and standard deviation (yellow) of the difference in brightness temperature IASI-B – AIRS.

Figure 48 shows the temporal evolution of the three broadest pseudo-channels, corresponding approximately to the IASI bands 1, 2 and 3 (more precisely, to their overlapping with the AIRS coverage). We see that the difference between IASI-B and AIRS is very stable with time, even more than IASI-B - CRIS. For IASI-B / AIRS no large temporal gaps are observed.



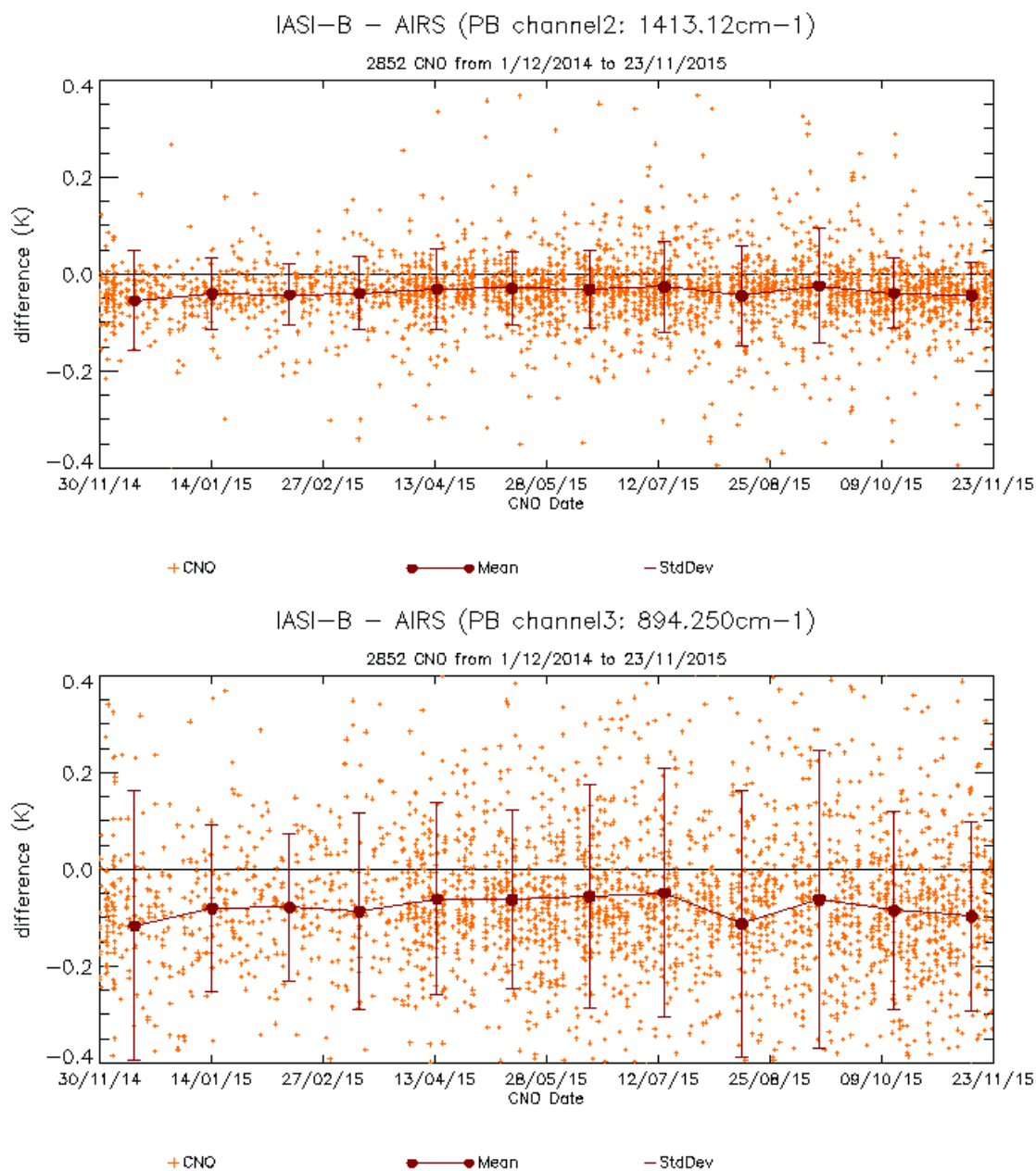


Figure 48 : Temporal evolution of the differences IASI-B – AIRS in brightness temperature over the approximate three IASI bands, with monthly mean.

4.9 IIS RADIOMETRIC PERFORMANCES

The main task of IIS is to insure a good relative positioning of IASI sounder pixels with respect to AVHRR. Its performances are studied each month using routine External Calibration data.

4.9.1 IIS Radiometric Noise Monitoring

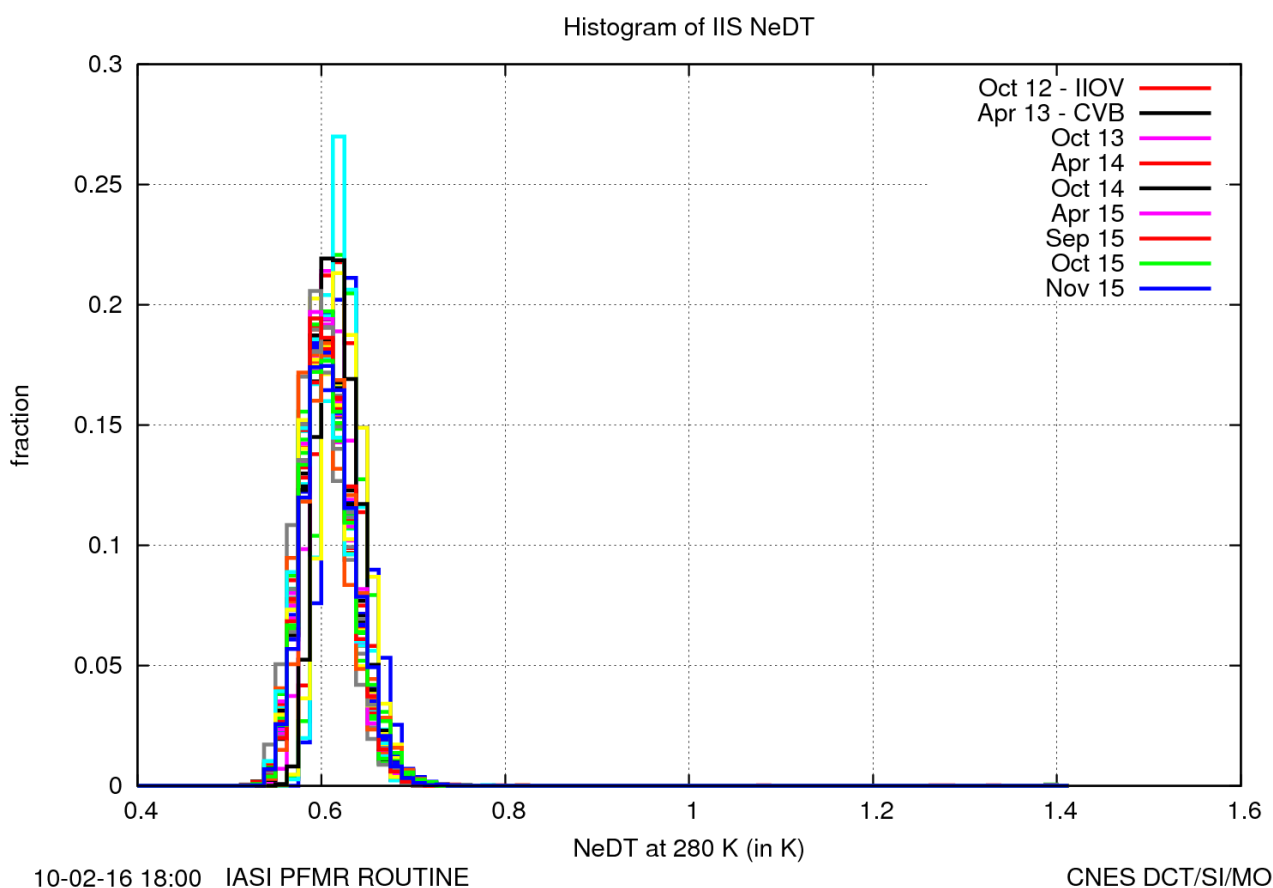




Figure 49 : Temporal evolution of the noise between start and end of the period

Radiometric noise of the IIS is very stable and lower than the specification of 0.8K.

		Doc n°: IA-RP-2000-4252-CNE Issue: 1.0 Date: 2017-09-27 Sheet: 61 Of: 67
--	--	---

4.9.2 IIS Radiometric Calibration Monitoring

In order to assess the stability of IIS radiometric calibration, we follow the time evolution of slope and offset coefficients. Figure 50 shows a comparison of slope and offset coefficients matrix between start and end of the period.

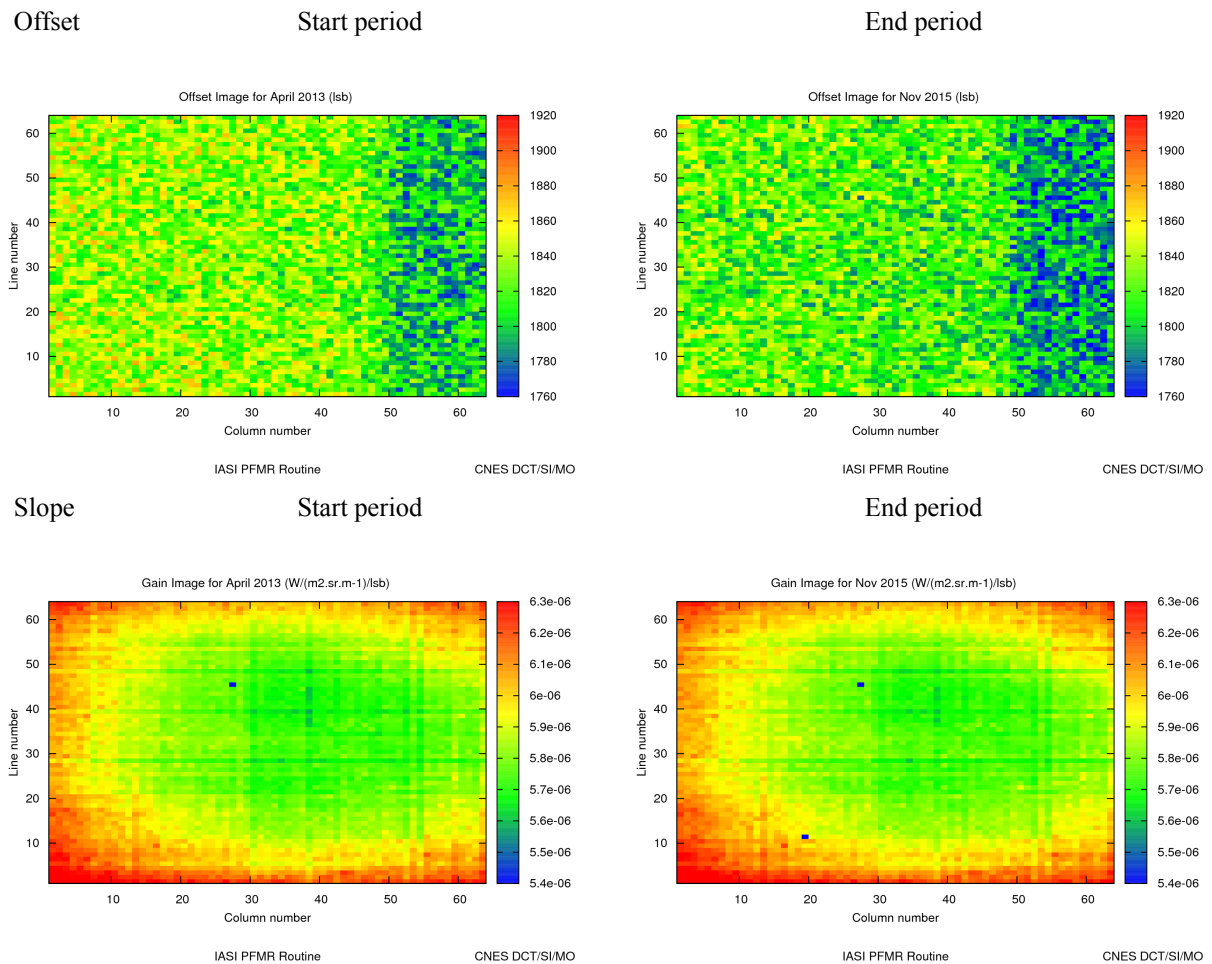
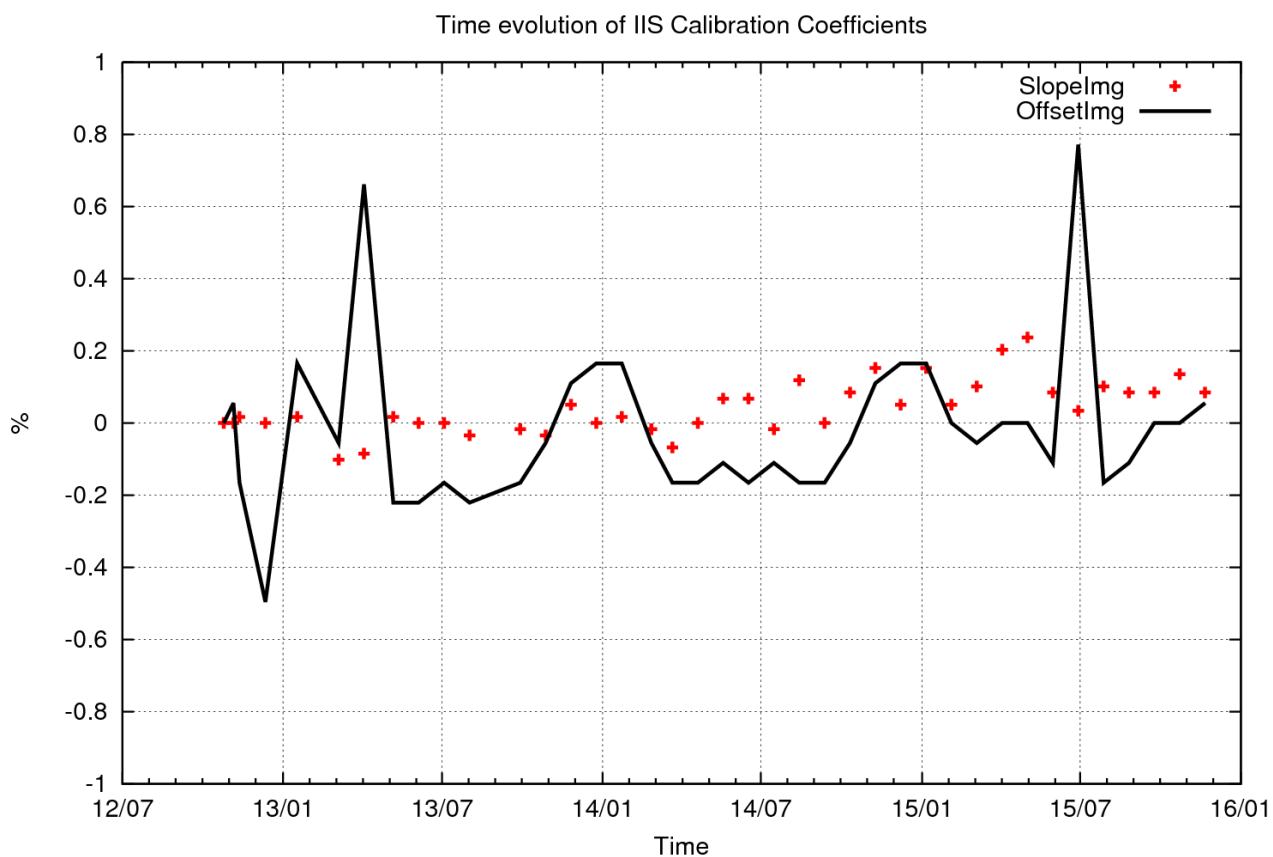


Figure 50 : Slope and offset coefficients matrix

The complete time series of average slope and offset coefficients is given in Figure 51.



10-02-16 18:00 IASI PFMR ROUTINE

CNES DCT/SI/MO

Figure 51 : Relative evolution in % of average of slope (red curve) and offset (black curve) coefficients

The slope coefficient is stable (variations around 0.2%). Small variations of the offset coefficient are observed (between -0.5% and +0.8%).

The performances are nominal.

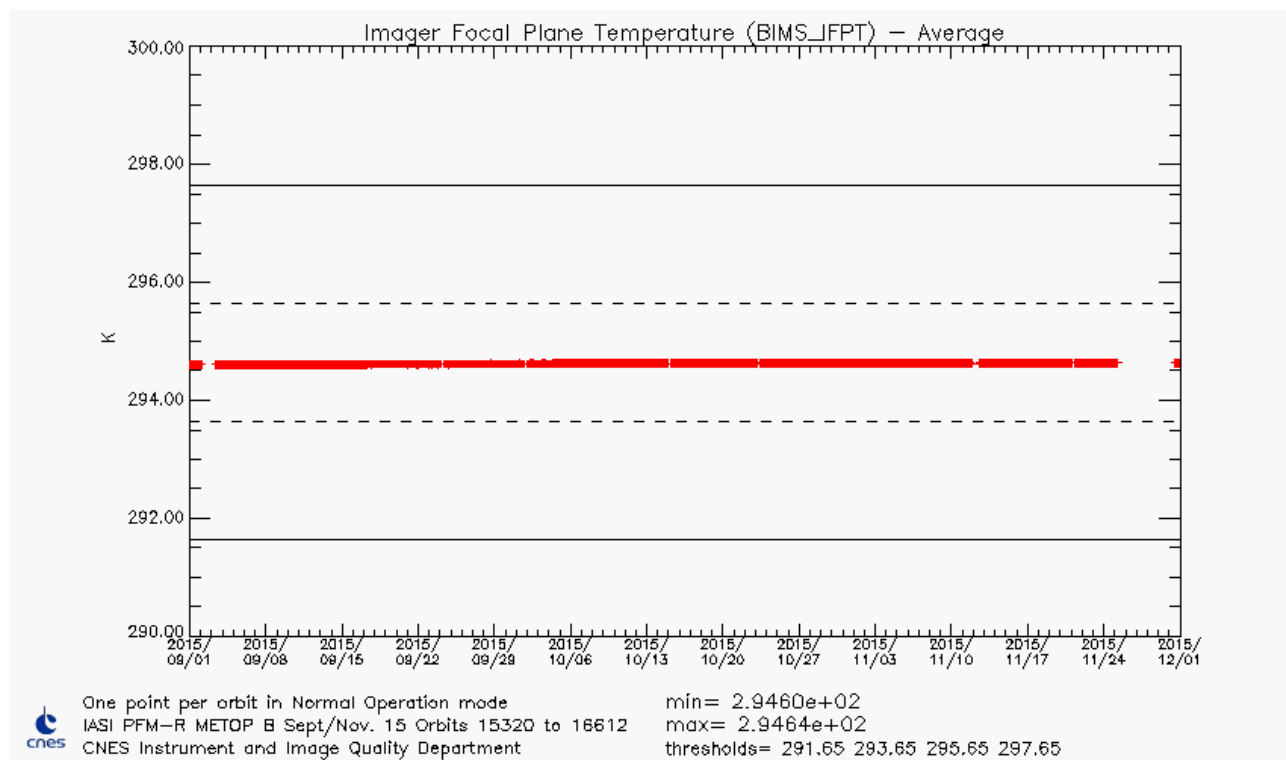




Figure 52 : IIS Focal Plane Temperature

4.9.3 Conclusion

The radiometric performance of IIS is very stable and within specification.

		Doc n°: IA-RP-2000-4252-CNE Issue: 1.0 Date: 2017-09-27 Sheet: 64 Of: 67
--	---	---

5 IASI TEC SOFTWARE AND INTERFACES

5.1 *IASI TEC EVOLUTION*

No evolution within the period.

Table 19 lists previous software evolutions.

IASI TEC software version	implementation	Comments
8.1	06 October 2011	Automatic downloads of L0 products from EUMETSAT FTP
8.2	12 April 2012	New version of product browser (handling IASI L0, L1C products and board configuration).
8.3	22 August 2012	Regularization version before IASI-B CAL/VAL CCAT replaced by CBST in TEC's logs
8.4	19 December 2013	New parameter SP_NV in SLT files Integration of board configuration generation tool (UTOPIE) Integration of LBR products management tool
8.5	19 November 2014	Monitoring of offset voltages from equalization images

Table 19: IASI TEC at CNES Toulouse



5.2 *SIC EVOLUTION*

No evolution within the period

This Table lists the recent evolutions of the software:

SIC software version	implementation	Comments
3.2	04/2014	Add of spectral inter-calibration, synthesis tool processed per days, new methods for CNO pre-selection, add of preselection for IASI/AIRS and IASI/CRIS, intercalibration with convolution method for IASI/CRIS
3.3	04/2015	New functionalities for data transfer. Improvement of CNO prediction and pre-selection. New parameterization for the synthesis tool. Automation of the software installation and deployment, IDL upgrade, correction of NCR

Table 20: SIC at CNES Toulouse



		Doc n°: IA-RP-2000-4252-CNE Issue: 1.0 Date: 2017-09-27 Sheet: 65 Of: 67
--	---	---

5.3 *EUMETCAST INTERFACE*

EUMETCast dissemination is used for Near Real Time data reception by IASI TEC at CNES, Toulouse. Each orbit, L1 ENG, L1 VER, and AVHRR 1B products are received under continuous series of 3 minutes PDU. Full dumps are reconstructed by the EUMETCAST terminal and pushed to a IASI TEC server. Since August 2012, NPP/CrIS PDU are also received to perform inter-comparison with IASI.

In case of failure of the prime EUMETCAST station, products remain available several days on a redundant station.

The behaviour of the EUMETCAST reception is nominal.

		Doc n°: IA-RP-2000-4252-CNE Issue: 1.0 Date: 2017-09-27 Sheet: 66 Of: 67
--	---	---

The following table lists the recent modifications in the EUMETCAST configuration:



Date	EUMETCAST configuration
29/03/2011	End of IASI L0 dissemination via EUMETCAST
03/08/2011	Hardware and software upgrade of the prime station
04/12/2011	Hardware and software upgrade of the back-up station
13/07/2012	Software patch to correct an anomaly concerning AVHRR files (reception of 0 byte files from EUMETCAST)
24/08/2012	Modification of EUMETCAST configuration to receive NPP/CrIS data
03/2013	“PARALLEL_RECONSTRUCTIONS” set to 3 to avoid missing PDU problems
09/2013	“RECONSTRUCTION TIME-OUT” set to 90 to avoid missing PDU problems
09/12/2014	Antenna repointing and update of reception parameters
21/04/2015	New SR1 router
10/08/2015	Replacement of Back-up station HDD

Table 21: EUMETCAST configuration at CNES Toulouse

5.4 FTP INTERFACE

Since March 29th of 2011, IASI L0 full dumps are available in Near Real Time on a EUMETSAT FTP server. The IASI TEC software automatically downloads products from the EUMETSAT FTP server.

The reception of L0 products at IASI TEC is nominal.

		Doc n°: IA-RP-2000-4252-CNE Issue: 1.0 Date: 2017-09-27 Sheet: 67 Of: 67
--	---	---

6 **CONCLUSION AND OPERATIONS FORESEEN**

Please visit <https://iasi.cnes.fr> to get IASI news.

6.1 ***SUMMARY***

The IASI PFM-R instrument is fully operational.

The instrument configuration is the nominal one.

The main events are :

- Moon avoidance on 2-3 September and on 1-2 October 2015
- SEU on DPS equipment on 11 November 2015
- CD stop operations on 7 October 2015
- IIS Equalisation on 14 October 2015
- Decontamination 200K from 25 to 30 November 2015
- New OPS version V7.3 on 29 September 2015

6.2 ***SHORT-TERM EVENTS***

- In Plane manoeuvre on 16 December 2015
- Moon avoidance on 29-30 December 2015

6.3 ***OPERATIONS FORESEEN***

- Update of scan mirror reflectivity and reduced spectra mid 2016
- Next decontamination should happen end of 2017.

End of document